

K_S^0 and Λ production in pp interactions at $\sqrt{s} = 0.9$ and 7 TeV measured with the ATLAS detector at the LHC

G. Aad *et al.**

(The ATLAS Collaboration)

(Dated: August 16, 2018)

The production of K_S^0 and Λ hadrons is studied in pp collision data at $\sqrt{s} = 0.9$ and 7 TeV collected with the ATLAS detector at the LHC using a minimum-bias trigger. The observed distributions of transverse momentum, rapidity, and multiplicity are corrected to hadron level in a model-independent way within well defined phase-space regions. The distribution of the production ratio of $\bar{\Lambda}$ to Λ baryons is also measured. The results are compared with various Monte Carlo simulation models. Although most of these models agree with data to within 15% in the K_S^0 distributions, substantial disagreements are found in the Λ distributions of transverse momentum.

PACS numbers: 13.85.Hd, 13.85.Ni, 14.20.Jn, 14.40.Df

I. INTRODUCTION

Yields and production spectra of hadrons containing strange quarks have been measured previously at the Large Hadron Collider (LHC) and the Tevatron at various center-of-mass energies [1–3]. Measurements of particle production provide insight into the behavior of QCD interactions at low momentum transfer, typically described by models with empirical parameters tuned from experimental data. Accurate modeling of such interactions is also essential for constraining the effects of the underlying event in the high- p_T collisions studied at the LHC. As the strange quark is heavier than the up and down quarks, the production of strange hadrons is suppressed relative to hadrons containing only up and down quarks. However, since the mass of the strange quark is comparable in value to the Λ_{QCD} scale constant, it is not sufficiently heavy for perturbative techniques to be used in modeling the production of strange hadrons and experimental input is required to tune it in Monte Carlo (MC) simulation. Moreover, the ratio of the production of strange antibaryons to strange baryons is related to the transfer of baryon number from the colliding protons to the mid-rapidity region and can be used to constrain “diquark” [4] and “string-junction” [5] models in MC generators. Since the initial state in pp collisions has a net baryon number of two, these models can be tested even at zero rapidity at the LHC.

In this paper, the production of K_S^0 and Λ hadrons is studied using the first $190 \mu\text{b}^{-1}$ collected by the ATLAS experiment at $\sqrt{s} = 7$ TeV and $7 \mu\text{b}^{-1}$ at 900 GeV. In addition, the measurement of the ratio between $\bar{\Lambda}$ and Λ baryon production is presented. Data were collected with a minimum-bias trigger with the same selection as

in the inclusive minimum-bias measurement of charged particles [6]. Strange hadrons are reconstructed in the $K_S^0 \rightarrow \pi^+\pi^-$, $\Lambda \rightarrow p\pi^-$, and $\bar{\Lambda} \rightarrow \bar{p}\pi^+$ decay modes by identifying two tracks originating from a displaced vertex, exploiting the long lifetimes of strange hadrons ($c\tau \approx 2.7$ cm for K_S^0 hadrons and $c\tau \approx 7.9$ cm for Λ hadrons). The measured distributions are

$$\frac{1}{N} \frac{dN}{dp_T}, \frac{1}{N} \frac{dN}{dy}, \frac{1}{N_{\text{ev}}} \frac{dN_{\text{ev}}}{dN}, \quad (1)$$

where N is the number of K_S^0 or Λ hadrons, p_T is the transverse momentum, y is the rapidity [7], and N_{ev} is the number of events with two charged particles satisfying $p_T > 100$ MeV and $|\eta| < 2.5$. The Λ distributions do not include $\bar{\Lambda}$ baryons, while the ratio of $\bar{\Lambda}$ to Λ is presented versus p_T and y as a separate measurement. The kinematic spectra of strange hadrons are extracted from the reconstructed distributions by correcting for detector effects modeled with MC simulation samples that are validated with data. The observed distributions are corrected to the $|\eta| < 2.5$ and $p_T > 100$ MeV phase-space region where tracks can be reconstructed (imposed on the charged decay products) with minimum and maximum flight-length requirements imposed on the K_S^0 and Λ hadrons to avoid model-dependent extrapolations outside of the detector acceptance. A similar approach was used in the ATLAS measurement of charged-hadron production [6].

II. THE ATLAS DETECTOR

The ATLAS detector [8] at the LHC [9] covers almost the whole solid angle around the collision point with layers of tracking detectors, calorimeters and muon chambers. It has been designed to study a wide range of

* Full author list given at the end of the article.

physics topics at LHC energies. For the measurements presented in this paper, the tracking devices and the trigger system are used.

The ATLAS Inner Detector (ID) has full coverage in ϕ and covers the pseudorapidity range $|\eta| < 2.5$. It consists of a silicon pixel detector (Pixel), a silicon microstrip detector (SCT) and a transition radiation tracker (TRT). The sensitive elements of these detectors cover a radial distance from the interaction point of 51-150 mm, 299-560 mm, and 563-1066 mm, respectively, and are immersed in a 2 T axial magnetic field. The ID barrel (end-cap) region consists of 3 (2×3) Pixel layers, 4 (2×9) double-layers of single-sided silicon microstrips with a 40 mrad stereo angle, and 73 (2×160) layers of TRT straws. Typical position resolutions are 10, 17 and 130 μm for the $R - \phi$ coordinate and, in the case of the Pixel and SCT, 115 and 580 μm for the second measured coordinate. A track from a charged particle traversing the barrel detector would typically have 11 silicon hits (3 pixel clusters and 8 strip clusters) and more than 30 straw hits.

The ATLAS detector has a three-level trigger system; data for this measurement were collected with Level 1 signals from the Beam Pickup Timing devices (BPTX) and the Minimum Bias Trigger Scintillators (MBTS). The BPTX stations consist of electrostatic button pickup detectors attached to the beam pipe at ± 175 m from the center of the detector. The coincidence of the BPTX signal between the two sides of the detector is used to determine when beam bunches are colliding in the center of the detector. The MBTS are mounted at each end of the detector in front of the liquid-argon end-cap calorimeter cryostats at $z = \pm 3.56$ m. They are segmented into eight sectors in azimuth and two rings in pseudorapidity ($2.09 < |\eta| < 2.82$ and $2.82 < |\eta| < 3.84$). Data were collected for this analysis using a trigger requiring a BPTX coincidence and MBTS trigger signals. The MBTS trigger used for this paper is configured to require at least one hit above threshold from either side of the detector, referred to as a single-arm trigger.

III. DATA SAMPLES AND EVENT SELECTION

The data used in this analysis consist of about 16 million events recorded by ATLAS in March and April 2010, corresponding to about $190 \mu\text{b}^{-1}$ of proton-proton collisions provided by the LHC at the center-of-mass energy of 7 TeV, as well as 1 million events corresponding to about $7 \mu\text{b}^{-1}$ at $\sqrt{s} = 900$ GeV recorded in December 2009. Data events are required to pass the same data-quality and event requirements as those used in Ref. [6]. These include a primary vertex reconstructed from two or more tracks with $p_{\text{T}} > 100$ MeV and transverse distance of closest approach to the beam-spot position of at most 4 mm. Events containing more than one primary vertex are rejected. After the selection, the fraction of events with more than one interaction in the same bunch crossing in these early LHC data is estimated to be at

the 0.1% level and is neglected.

A sample of 20 million non-diffractive minimum-bias MC events generated with PYTHIA using the early ATLAS MC09 tune [10, 11] and GEANT4 [12] simulation is passed through the same reconstruction as the data sample. The distribution of the longitudinal position of the primary vertex in the simulated sample is re-weighted to make it consistent with data. Samples of single-diffractive and double-diffractive events generated with the same tune are combined with the non-diffractive sample according to their relative total cross sections in the same manner as in Ref. [6]. The distributions of the longitudinal position of the primary vertex are found to be nearly identical in the simulated minimum-bias and diffractive samples. For some systematic studies, a fully simulated sample of events produced with the PHOJET generator [13] is used. To compare the data at particle level with different phenomenological models describing minimum-bias events, the following samples are also used:

- PYTHIA6 using the AMBT2B-CTEQ6L1 tune [14, 15];
- PYTHIA6 using the Perugia2011 tune [16] (CTEQ5L parton distribution functions (PDFs) [17]);
- PYTHIA6 using the Z1 tune [18] (CTEQ5L PDFs);
- PYTHIA8 using the 4C tune [19, 20] (CTEQ6L1 PDFs);
- HERWIG++ 2.5.1 [21, 22], using the UE7-2 underlying-event tune at 7 TeV and the MU900-2 minimum-bias tune at 900 GeV [23] (both with MRST2007LO* PDFs [24]).

IV. V^0 RECONSTRUCTION AND SELECTION

Tracks with $p_{\text{T}} > 50$ MeV are reconstructed within the $|\eta| < 2.5$ acceptance of the ID as described in detail in Refs. [6, 25, 26]. To form K_S^0 candidates, oppositely charged track pairs with $p_{\text{T}} > 100$ MeV and at least two silicon hits are fit to a common vertex, assuming the pion mass for both tracks. The K_S^0 candidates are required to satisfy the following criteria:

- The χ^2 of the two-track vertex fit is required to be less than 15 (with 1 degree of freedom).
- The transverse flight distance, defined by the transverse distance between the secondary vertex (K_S^0 decay point) and the reconstructed primary vertex, is required to be between 4 mm and 450 mm.
- The cosine of the pointing angle in the transverse plane ($\cos \theta_{\text{K}}$) between the K_S^0 momentum vector and the K_S^0 flight direction, defined as the line connecting the reconstructed primary vertex to the decay vertex, is required to be greater than 0.999 (equivalent to an angle of 2.56°).

For Λ and $\bar{\Lambda}$ decays, the track with the higher p_T is assigned the proton mass and the other track is assigned the pion mass. In the simulated sample this identification is correct for 99.8% of the candidates. The Λ and $\bar{\Lambda}$ candidates are required to satisfy the following criteria:

- The χ^2 of the two-track vertex fit is required to be less than 15 (with 1 degree of freedom).
- The transverse flight distance is required to be between 17 mm and 450 mm.
- The cosine of the pointing angle is required to be greater than 0.9998 (equivalent to an angle of 1.15°).
- The p_T of the Λ candidate is required to be greater than 500 MeV

These requirements reduce the combinatorial background. The smaller signal-to-background ratio in the Λ sample with respect to the K_S^0 sample requires a tighter pointing requirement, while the larger value of the flight-distance selection exploits the longer lifetime of the Λ baryon. The minimum p_T cut removes poorly reconstructed candidates. The distributions of the invariant mass of the K_S^0 and Λ candidates in the data and MC samples are shown in Fig. 1.

Figures 2 and 3 show the reconstruction efficiency of K_S^0 , Λ , and $\bar{\Lambda}$ candidates versus the radial position of the decay vertex, p_T , and rapidity. The efficiency is determined from simulation by comparing the number of generated K_S^0 hadrons with the number of reconstructed candidates after all selection criteria are applied. The efficiency turn-on curve versus p_T is mainly an effect of tracking efficiency, while the radial plot clearly shows the drops in efficiency when crossing detector layers, reflecting the lower efficiency of reconstructing and selecting tracks that have fewer hits in the silicon detector. (The effect is most pronounced at the Pixel layers, located roughly at radii of 50, 80, and 120 mm.)

V. EFFICIENCY AND CORRECTION PROCEDURE

The measured K_S^0 and Λ production quantities are distributions versus rapidity and transverse momentum as well as the number of K_S^0 or Λ candidates per event (the ‘‘multiplicity’’). To remove the background from the p_T and rapidity distributions, the reconstructed invariant-mass distribution is fitted for signal and background separately in every bin of p_T and rapidity. The background-subtracted distributions are then corrected through an unfolding algorithm for detector resolution of the p_T and rapidity measurements as well as for the reconstruction efficiency. In the measurement of the production ratio of $\bar{\Lambda}$ to Λ baryons, a separate correction procedure is employed accounting for the difference in the detector response to positively and negatively charged baryons.

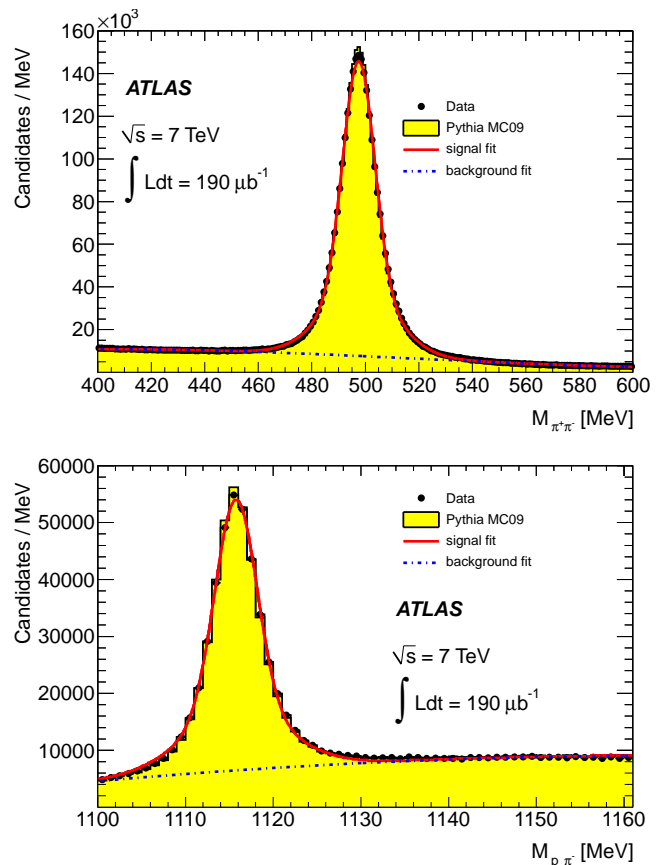


FIG. 1. Comparison of measured and predicted K_S^0 (top) and Λ (bottom) invariant-mass distributions in the 7 TeV samples. The points are data, while the histograms show the MC sample with signal and background components separately normalized to the data. The solid line is the line-shape function fitted to data, while the dot-dashed line shows the component of the fitted function describing the combinatoric background (see Sec. VA 1).

A. Corrections to K_S^0 and Λ distributions

The corrections are evaluated separately for the 7 TeV and 900 GeV samples and are described sequentially below. The final distributions are normalized to unity by dividing by the total number of measured hadrons.

1. Background correction

The number of signal candidates in a given bin of the rapidity and transverse-momentum distributions is determined by fitting the invariant-mass spectrum of the K_S^0 or Λ candidates in that bin. The value and statistical uncertainty on the bin are then determined from the fitted signal yield and its uncertainty. For the K_S^0 candidates the functional form that is found to describe well the shape in data combines the sum of two Gaussians for the signal peak and a third-order polynomial for the com-

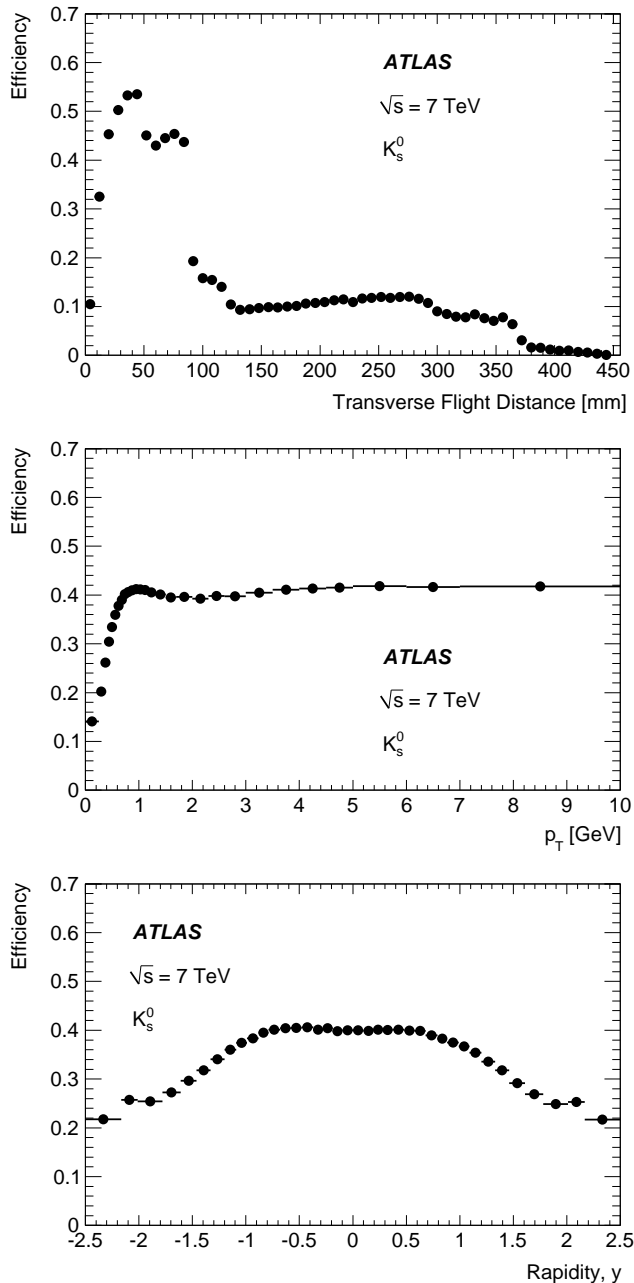


FIG. 2. The reconstruction efficiency of K_S^0 candidates in the 7 TeV MC sample after all selection criteria versus the transverse flight distance (top), p_T (center), and rapidity (bottom).

binatorial background. The means of the two Gaussian components are constrained to be the same, while the widths and relative fractions are determined from the fit. For the Λ candidates a second-order polynomial is used for the background and the following modified Gaussian shape is used for the signal:

$$C \cdot \exp \left[-0.5 \cdot x \left(1 + \frac{1}{1+0.5 \cdot x} \right) \right], \quad x = \left| \frac{m - \mu}{\sigma} \right|, \quad (2)$$

	fit mean [MeV]	world average [MeV]
K_S^0 Data	497.536 ± 0.006	497.614 ± 0.024
K_S^0 MC	497.495 ± 0.006	
Λ Data	1115.75 ± 0.01	1115.683 ± 0.006
Λ MC	1115.72 ± 0.01	
$\bar{\Lambda}$ Data	1115.81 ± 0.01	
$\bar{\Lambda}$ MC	1115.76 ± 0.01	

TABLE I. The position of the mass peak in the fit to the 7 TeV data and simulation samples. The fit uncertainties on the mean are statistical only.

where m is the invariant mass and the fitted parameters are the normalization parameter C , the mean μ , and the width σ . This shape is found to model the invariant mass better than the sum of two Gaussians.

The results of the fits to the entire 7 TeV data and MC samples are summarized in Table I. The means of the mass peaks obtained from the fits in data are in reasonable agreement with simulation and with the world average [27]. The agreement demonstrates the accuracy of the track momentum scale and of the modeling of the Inner Detector's 2T solenoid magnetic field, which has been mapped to a precision of about 0.4 mT [28]. Although the deviation of data from the simulated and world-average values is statistically significant since the uncertainties do not include systematic effects, it is no larger than about 100 keV and does not affect the results presented in this article, as the mean mass position is not directly used in the measurement.

The contamination from secondary K_S^0 and Λ production from long-lived baryon decays or nuclear interactions in the detector material is at the negligible level of 0.1% for K_S^0 decays in simulation and at the 10% level in the Λ case, where it is subtracted from the measured data distributions. The modeling of secondary Λ baryons is evaluated by varying the pointing-angle selection and comparing its efficiency between MC and data. The measured deviations at the level of 2% in the efficiency are assessed as a systematic uncertainty. The effect of Λ contamination in the K_S^0 signal and vice versa is similarly studied and the contamination of less than 1% is included in the evaluation of systematic uncertainties.

2. Resolution correction

The PYTHIA MC09 simulation sample is used to fill a two-dimensional migration matrix, where one dimension is binned in the generated value of the variable of interest (p_T , rapidity, or multiplicity) and the other is binned in the reconstructed value of the same variable. This matrix thus models the effect of the experimental resolution on the true value of p_T or rapidity for reconstructed candidates, which are matched to the generated candidates

using a hit-based matching algorithm [26]. This matrix is then used to unfold the migration across bins in the background-subtracted distributions in data.

3. Efficiency correction

The resolution-corrected p_T and rapidity distributions from the previous step are corrected bin by bin for the reconstruction efficiency, ϵ_i , in a given bin i . The correction factor, $1/\epsilon_i$, is derived from the PYTHIA MC09 sample as the ratio of generated to reconstructed candidates in bin i of the generated distribution. Only the generated K_S^0 and Λ hadrons originating from the primary vertex and decaying within the tracking acceptance are considered: the two pions (the proton and the pion) that the K_S^0 (Λ) hadron decays to are required to have $|\eta| < 2.5$ and $p_T > 100$ MeV, while the K_S^0 or Λ hadron itself is required to satisfy the appropriate minimum flight-distance requirement and a maximum flight-distance requirement of 450 mm, which corresponds to the effective acceptance imposed by the silicon hit-content selection on the tracks. The reconstructed distributions in data are thus corrected to particles produced within the same acceptance, as extrapolating to regions not probed by the Inner Detector would introduce a dependence on the MC generator model in the correction procedure. The efficiency derived from MC is binned in p_T or rapidity and the effectiveness of the entire correction procedure is evaluated through pseudo-experiments where the PHOJET MC sample is unfolded using migration matrices filled from the PYTHIA MC09 sample. (See Section VI.)

B. Corrections to the $\bar{\Lambda}/\Lambda$ production ratio

The background in the $\bar{\Lambda}$ and Λ distributions is subtracted in the same manner as the K_S^0 background but with the modified Gaussian shape for the signal component. As most systematic tracking effects cancel in the production ratio, the ratio is corrected only for the difference in reconstruction efficiency between Λ and $\bar{\Lambda}$ decays. This difference is mainly a consequence of the difference in tracking efficiency between protons (for Λ candidates) and antiprotons (for $\bar{\Lambda}$ candidates) caused by different interactions with detector material. The correction is estimated from the MC sample in bins of p_T and rapidity by comparing the reconstruction efficiency for Λ and $\bar{\Lambda}$ decays, which is shown in Fig. 3. The ALICE experiment has reported that the nuclear-interaction cross section of antiprotons used by GEANT4 is over-estimated [1, 29], resulting in an over-estimated efficiency difference between Λ and $\bar{\Lambda}$ reconstruction as shown in Fig. 3. Validation and correction of the model of detector material and the GEANT modeling of material-interaction cross sections and the associated systematic uncertainties are described in Section VI.

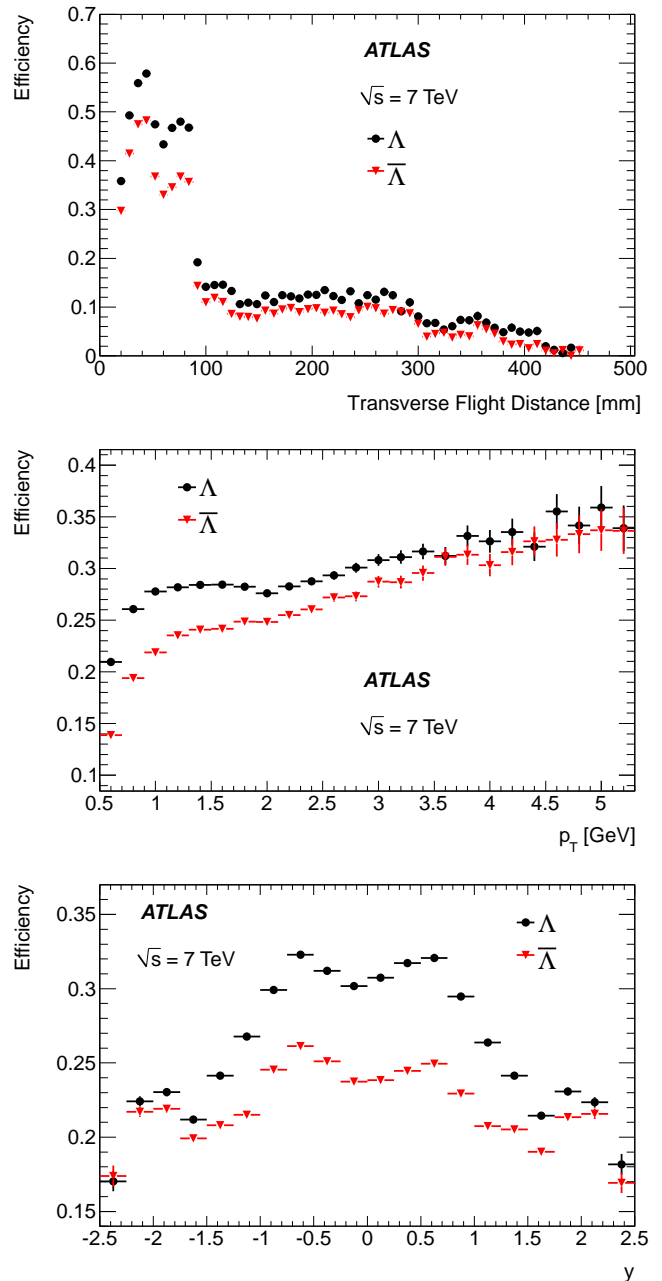


FIG. 3. The efficiency in 7 TeV MC for reconstructing $\bar{\Lambda}$ and Λ candidates after all selection criteria versus the transverse flight distance (top), p_T (middle) and rapidity (bottom). The uncertainties are statistical only.

VI. SYSTEMATIC UNCERTAINTIES

The systematic uncertainties are evaluated separately for the measurement of the K_S^0 and Λ distributions and for the measurement of the $\bar{\Lambda}/\Lambda$ production ratio. For the K_S^0 and Λ distributions, systematic uncertainties are evaluated for the reconstruction efficiency, the background-subtraction procedure, the method of cor-

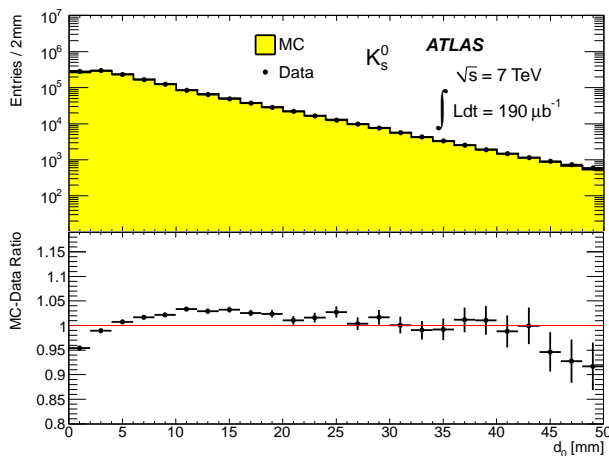


FIG. 4. The distribution of the reconstructed transverse impact parameter in 7 TeV data and MC for pions originating in K_S^0 decays after all selection criteria are imposed.

recting for the resolution and efficiency, and the event selection. For the measurement of the $\bar{\Lambda}/\Lambda$ production ratio, the modeling of proton and antiproton reconstruction, the effect of Λ baryons interacting with the detector material before decaying, and the production of secondary Λ baryons are considered.

A. Reconstruction efficiency

The systematic uncertainty on the efficiency is evaluated by comparing impact-parameter distributions between the MC and data samples. This uncertainty is then cross-checked by comparing decay-time distributions with the lifetime of K_S^0 mesons and comparing the selection efficiencies between MC and data.

1. Impact-parameter distributions

The systematic uncertainty on the tracking efficiency is evaluated using the transverse impact parameter, d_0 , of the tracks produced in the K_S^0 or Λ decay. The d_0 measurement is sensitive to different orientations of tracks with respect to the primary vertex and it is correlated with the measured flight distance of the K_S^0 candidate through the vertexing of the decay point. Figures 4 and 5 show a comparison of the reconstructed d_0 distributions in the data and MC samples.

In a given two-dimensional p_T -rapidity bin, the d_0 distribution in the MC sample is normalized to data. The absolute values of the deviations between data and MC for all d_0 bins are summed, corrected for the expected value from statistical fluctuations, and divided by the integral of the distribution. This summed relative difference is then assigned as the relative systematic uncertainty on the efficiency in that p_T -rapidity bin. The

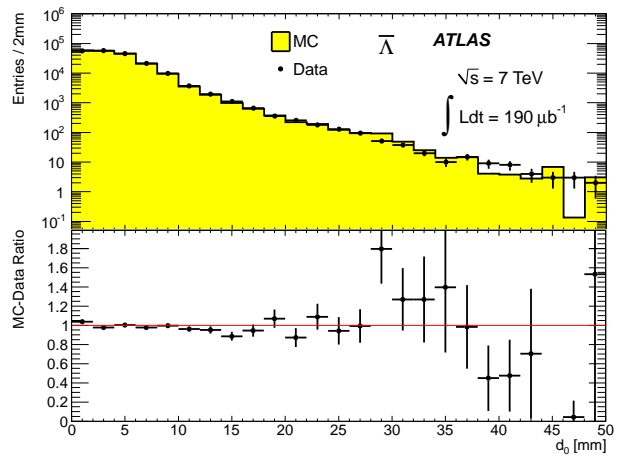
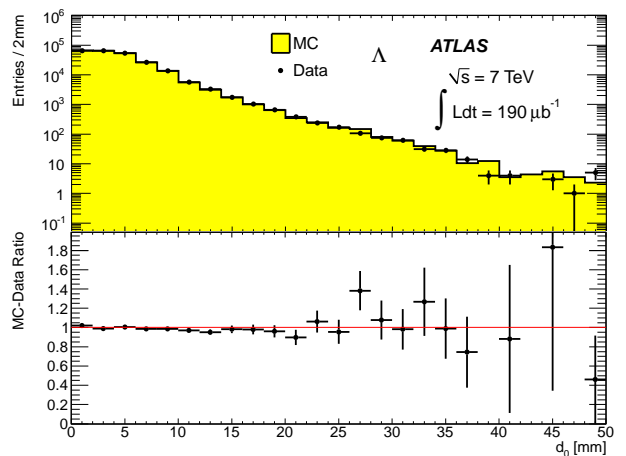


FIG. 5. The distribution of the reconstructed transverse impact parameter in 7 TeV data and MC for protons and antiprotons originating in Λ (top) and $\bar{\Lambda}$ decays (bottom) with $p_T > 500$ MeV after all selection criteria are imposed.

two-dimensional p_T -rapidity uncertainty map is then projected onto each axis to determine the one-dimensional uncertainty on the efficiency versus either p_T or rapidity. The uncertainty for the K_S^0 efficiency is at the 1% level or less in the p_T projection except at high- p_T , where the deviation increases to 5%, and at around 200 MeV, where it rises to 3%. When evaluated versus rapidity, the typical uncertainty is 1%. The corresponding uncertainty versus rapidity for the Λ candidates is at 2%, with larger uncertainties at low p_T . The effect of the uncertainty in the detector material on the d_0 distribution in the simulation is also studied and verified to be consistent with the results of previous studies of detector material in minimum-bias events [6].

2. Decay-time distributions

The distribution of the K_S^0 proper decay time is used to cross-check the modeling of the reconstruction efficiency in MC simulation. This method is sensitive to the vari-

ation of efficiency versus flight distance and p_T , as both are correlated with the decay time. The background-subtracted decay-time distribution in data is unfolded in the same manner as the p_T and rapidity distributions, accounting for bin migration and efficiency separately according to the MC corrections. The unfolded distribution in data is then fitted with an exponential shape and the lifetime compared with the world-average value. The fitted value of the lifetime, 89.37 ± 0.13 ps, is consistent with the world-average value of 89.58 ps to better than 0.3%, indicating excellent modeling of the variation of tracking efficiency versus flight distance.

3. Selection requirements

Although the previous two methods already include systematic uncertainties due to the flight-distance and kinematic selection criteria, the separate systematic effect of the selection requirements is studied as an additional cross-check on the reconstruction efficiency; the result of this study is not included in the total uncertainty. The signal efficiency of each criterion is evaluated by fitting the invariant-mass distribution before and after the selection is imposed in the same manner as in the background subtraction, with all other selection criteria already applied. The difference between the data and MC samples in the value of this efficiency is taken as a measure of how accurately the selection is modeled in the MC sample. The deviation is evaluated in bins of p_T and rapidity, with the finest granularity allowed by the stability and precision of the fitting procedure. For the silicon hit-content, flight-distance, track-momentum, and χ^2 requirements, the deviation is at the 1% level in most bins and under 2% in all bins. For the pointing-angle requirement, the deviation is at the 2% level in most regions, but can reach higher levels in a few bins in regions of large material and at low p_T . These systematic effects due to the selection requirements are consistent with the quoted systematic uncertainties obtained from the impact-parameter study.

B. Background

The systematic uncertainty on the background subtraction is evaluated by comparing the signal yield from the fit to the invariant-mass distribution with the number obtained by simple sideband subtraction. The deviation for the K_S^0 candidates is at the 1% level in the barrel rapidity region and rises to roughly 4% in the forward rapidity region, as can be seen in Fig. 6. The uncertainty for the Λ candidates is roughly twice as large, as can be seen in Fig. 7, reflecting the smaller signal-to-background levels. The 2% uncertainty due to secondary Λ production is also included in Fig. 7.

C. Correction procedure for resolution and efficiency

To test the accuracy of the unfolding procedure, the reconstructed p_T and rapidity distributions in the PHOJET MC sample are unfolded using the corrections derived from the PYTHIA MC sample. As the difference between the PHOJET and PYTHIA distributions is larger than the difference between the PYTHIA and data distributions, this is a conservative test of any model dependence in the unfolding procedure. To remove the effect of statistical fluctuations, the reconstructed distribution in the PHOJET sample is used to generate 10000 pseudo-experiments by Poisson variation of each bin. The pseudo-experiments are then unfolded and the residual distribution for each p_T or rapidity bin with respect to the particle-level distribution in the PHOJET sample is fitted to a Gaussian shape. The fitted residual mean is an indication of the bias due to the unfolding procedure in the bin, while the width is an estimate of the statistical uncertainty on the unfolding. The bias is at the 3% level or less in most K_S^0 rapidity bins and at the 5% level in the p_T bins with most of the K_S^0 candidates. For the Λ candidates, the bias is at the 8% level in most rapidity bins and at the 5% level in the p_T bins with most of the candidates. These biases are assigned as the systematic uncertainty on the unfolding procedure. The bias due to unfolding the multiplicity distribution is evaluated in a similar manner, with the resulting uncertainty rising with multiplicity and reaching the 20% level in the three-candidate bin in the K_S^0 case and 40% in the Λ case.

The statistical uncertainty on the corrected distributions in data is evaluated from the spread in the residual distribution when unfolding 10000 pseudo-experiments generated from the reconstructed data distributions. These uncertainties include both the fluctuations in the reconstructed distribution itself and any statistical spread from the correction procedure.

D. Event selection

As the data sample and event selection requirements in this measurement are identical to those used in Ref. [6], the systematic uncertainties on the event selection are taken directly from that analysis. These include uncertainties on the presence of beam backgrounds, the trigger efficiency, the efficiency of primary vertexing, and the presence of additional primary vertices from pile-up collisions. The total systematic uncertainty on the number of K_S^0 and Λ hadrons due to the event selection is 0.1%.

E. Total uncertainty on K_S^0 and Λ production

All the systematic and statistical uncertainties on the K_S^0 distributions in 7 TeV data are summarized in Fig. 6.

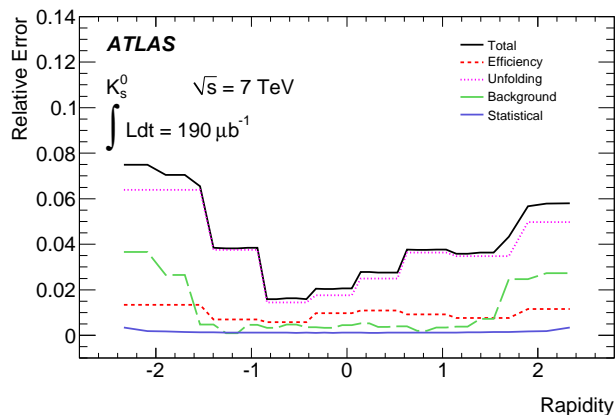
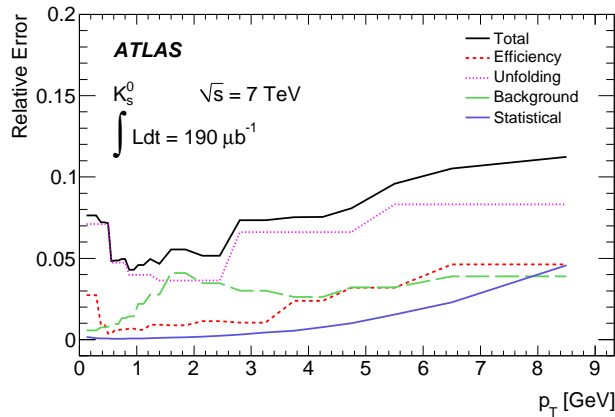


FIG. 6. The systematic, statistical, and total uncertainties versus p_T (top) and rapidity (bottom) of the K_S^0 candidate in 7 TeV data.

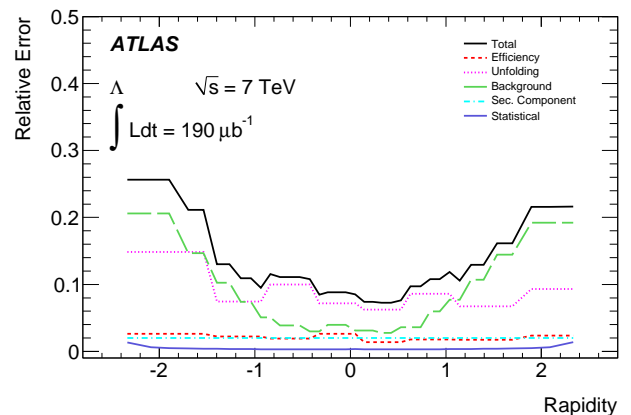
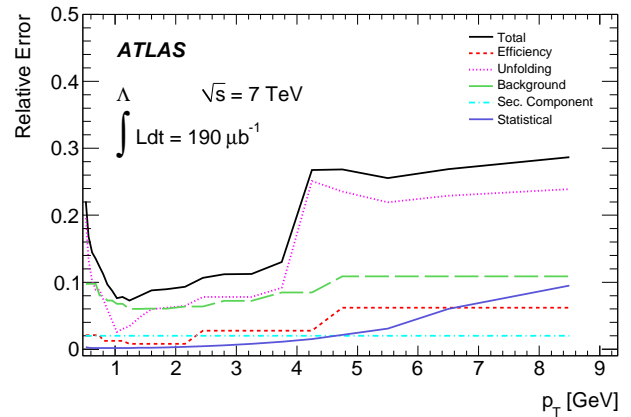


FIG. 7. The systematic, statistical, and total uncertainties versus p_T (top) and rapidity (bottom) of the Λ candidate in 7 TeV data.

The total uncertainty, which is dominated by the systematic component, is at the 5% level in the peak of the p_T distribution and rises to 10% at higher p_T . In the rapidity distribution, the uncertainty is at 4% in the central region and rises to 6 – 8% in the forward region. Figure 7 summarizes the systematic and statistical uncertainties on the Λ distributions, which are larger everywhere but show qualitatively similar behavior.

F. Systematic uncertainty on the $\bar{\Lambda}/\Lambda$ ratio

Several systematic effects on the $\bar{\Lambda}/\Lambda$ production ratio are considered:

- The modeling of the interaction cross section for antiprotons in detector material and its difference from the corresponding cross section for protons;
- The interactions of Λ and $\bar{\Lambda}$ baryons in the detector material before decaying;
- Contamination from secondary Λ and $\bar{\Lambda}$ baryons.

1. Modeling of proton and antiproton reconstruction

The cross sections used by the GEANT4 simulation to model the nuclear interactions of antiprotons with material have been found to be over-estimated by the ALICE experiment [1, 29]. Any such overestimate biases the correction to the $\bar{\Lambda}/\Lambda$ ratio described in Section VB. To constrain the accuracy of the GEANT4 model, patterns of hits on tracks in the outermost two layers of the SCT are compared between data and MC. For tracks that have hits in the three Pixel layers and the first two SCT layers, the fraction that do not have hits in the outer two layers is a measure of the inefficiency due to material interactions in those layers. This inefficiency is compared between data and MC for protons (antiprotons) coming from the selected Λ ($\bar{\Lambda}$) candidates and corrected for background contributions using the invariant-mass sidebands. While the data and MC are consistent for proton tracks, the efficiency for antiprotons is significantly lower in MC than in data, consistent with the expectation that the interaction cross section for antiprotons is overestimated in GEANT4. Comparing the ratio of antiproton-to-proton efficiency in the outer two layers between data and MC, a multiplicative correction factor to the $\bar{\Lambda}/\Lambda$ ratio is extracted as a function of p_T of the Λ candidate. This factor

ranges from 0.9 at $p_T = 500$ MeV to 0.99 at $p_T = 2$ GeV. (Λ candidates below 500 MeV are rejected as not enough proton candidates are reconstructed at low p_T to reliably evaluate the correction factor for these candidates.) As several correction factors can be formed from various combinations of hit patterns in the outer two layers, the largest variation among them is taken as a systematic uncertainty on this correction. This uncertainty ranges from 5% at $p_T = 500$ MeV to about 1% at $p_T = 2$ GeV. As an additional cross-check, a sample of protons is selected using the specific energy loss dE/dx measurement in the Pixel detector [30] and similar data-MC correction factors are calculated using the efficiency to extend the Pixel tracks to the SCT. The results of the dE/dx method are consistent with the hit-pattern study.

2. Interactions with material before decay and secondary Λ production

When evaluated versus the radial position of the decay vertex, the reconstructed $\bar{\Lambda}/\Lambda$ ratio shows sharp discrete changes of up to 10% at the detector layers. In the MC sample, the dominant cause of this effect is the asymmetric interaction of Λ and $\bar{\Lambda}$ baryons with the detector material before decay, since such interactions preclude the reconstruction of the final state of interest. In addition, roughly 15% of the effect is caused by secondary baryons asymmetrically produced at the detector layers by nuclear interactions of other particles. To constrain the modeling of these effects in the MC sample, the difference between data and MC in the change of the ratio at the detector layers is evaluated. The data/MC differences at every layer of the tracker are added together and the sum is assessed as a systematic uncertainty. Although the value varies in different regions of the detector due to detector geometry, the largest value of 2.6% (obtained in the central region) is conservatively assigned to the entire measured tracking acceptance. Other evaluations of possible effects of interactions with material in the MC sample yield an additional 1.5% uncertainty, for a total uncertainty of 3%. Although the radial study already includes the effect of secondary Λ baryons produced at the detector layers, an additional uncertainty of 1.5% evaluated from the MC sample is assessed to account for the effect of Λ baryons produced in the decay of heavier strange baryons.

3. Total uncertainty on Λ production ratio

The systematic uncertainties are summarized in Table II. The uncertainty is largest at low p_T , where it is at the 4.5% level, and approaches the 3.5% level at higher p_T , where the effect of the proton and antiproton modeling in GEANT4 is smallest.

	Systematic uncertainty
Antiproton cross section (p_T -dependent)	± 1.0 -2.8 %
Interaction with material	± 3.0 %
Secondary production	± 1.5 %
Total	± 3.5 -4.4 %

TABLE II. Summary of all systematic uncertainties on the $\bar{\Lambda}/\Lambda$ production ratio, in %.

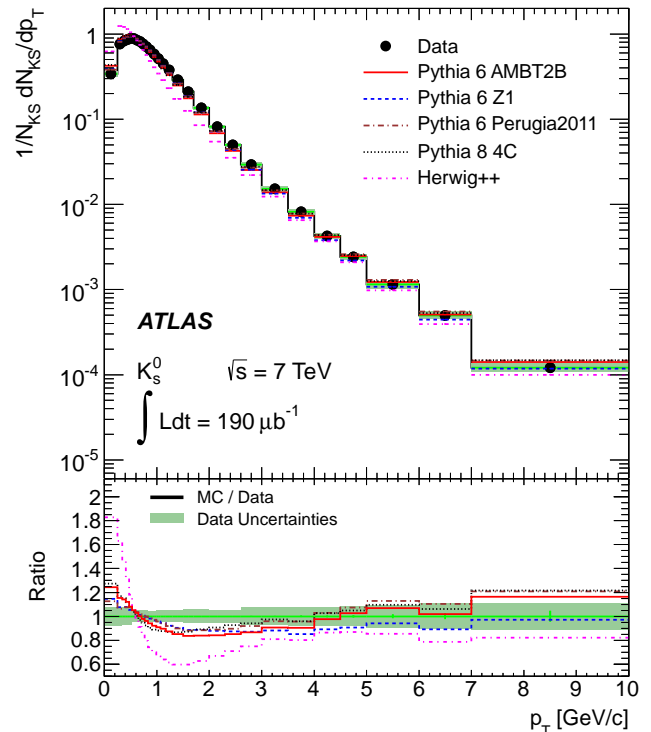


FIG. 8. The corrected p_T distribution of K_S^0 mesons in 7 TeV data compared with the hadron-level distributions in the MC samples for a variety of tunes, normalized to unity. The bottom part of the plot shows the ratio of the MC and data distributions, with the shaded band showing the statistical and systematic uncertainties on the data sample added in quadrature.

VII. RESULTS

In all corrected distributions, K_S^0 mesons are required to have a flight distance between 4 mm and 450 mm and to decay to two charged pions with $|\eta| < 2.5$ and $p_T > 100$ MeV, while Λ and $\bar{\Lambda}$ baryons are required to have $p_T > 500$ MeV, flight distance between 17 mm and 450 mm, and to decay to a proton and a pion with $|\eta| < 2.5$ and $p_T > 100$ MeV. Only K_S^0 and Λ hadrons consistent with originating from the primary vertex are considered. The p_T and rapidity distributions

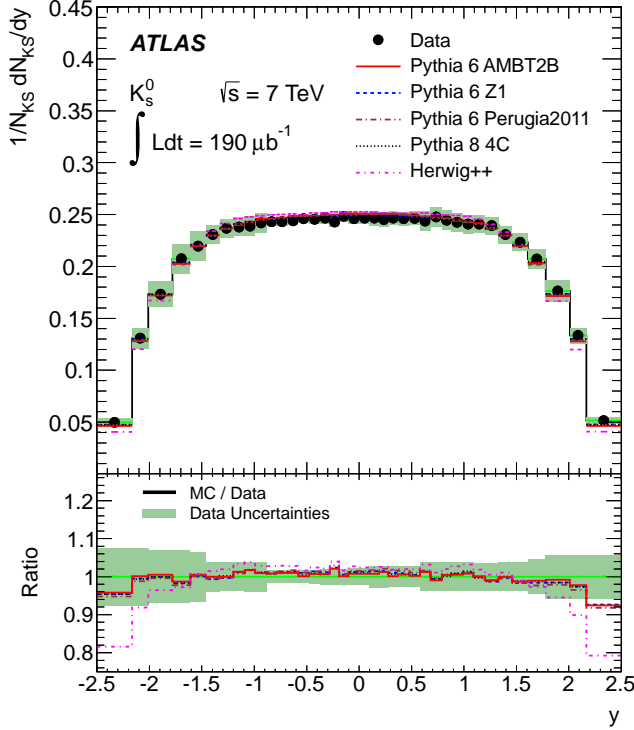


FIG. 9. The corrected rapidity distribution of K_S^0 mesons in 7 TeV data compared with the hadron-level distributions in the MC samples for a variety of tunes, normalized to unity. The bottom part of the plot shows the ratio of the MC and data distributions, with the shaded band showing the statistical and systematic uncertainties on the data sample added in quadrature.

are normalized to the number of K_S^0 or Λ hadrons, while the multiplicity distributions are normalized to the total number of events with two charged particles satisfying $p_T > 100$ MeV and $|\eta| < 2.5$. The multiplicity distributions are corrected for branching fractions to the measured final states using world-average values [27]. Predictions from several MC generators are shown with the same acceptance requirements.

Figures 8 and 9 show the corrected production distributions of K_S^0 mesons versus transverse momentum and rapidity, respectively, in 7 TeV data. Figure 10 shows the distribution of K_S^0 multiplicity in 7 TeV data. Figures 11 and 12 show the corrected production distributions of K_S^0 mesons versus transverse momentum and rapidity, respectively, in 900 GeV data, while Fig. 13 shows the distribution of K_S^0 multiplicity in 900 GeV data. Figures 14 and 15 show the corrected production distributions of Λ baryons versus transverse momentum and rapidity, respectively, in 7 TeV data, while Fig. 16 shows the distribution of Λ multiplicity in 7 TeV data. Figures 17 and 18 show the corrected production distributions of Λ baryons versus transverse momentum and rapidity, respectively, in 900 GeV data, while Fig. 19 shows the distribution of

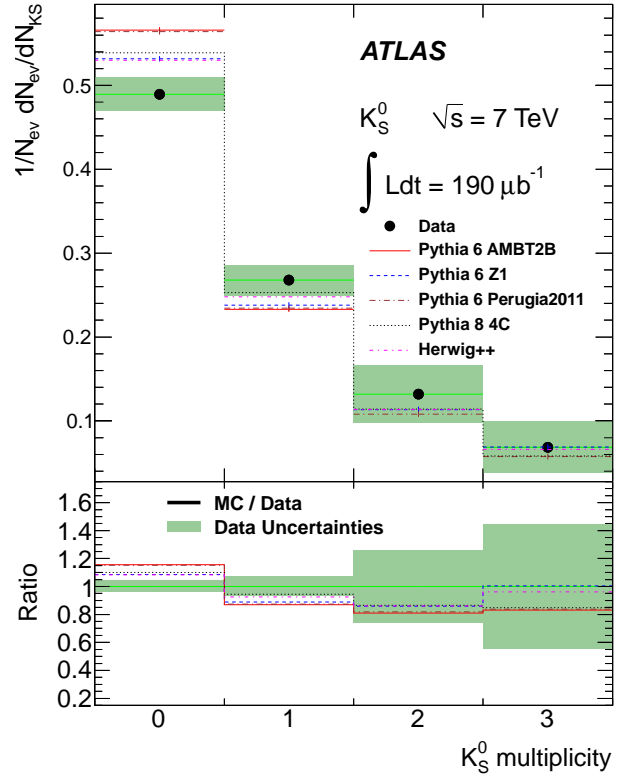


FIG. 10. The corrected multiplicity distribution of K_S^0 mesons in 7 TeV data compared with the hadron-level distributions in the MC samples for a variety of tunes, normalized to unity. The bottom part of the plot shows the ratio of the MC and data distributions, with the shaded band showing the statistical and systematic uncertainties on the data sample added in quadrature.

Λ multiplicity in 900 GeV data.

The fully corrected $\bar{\Lambda}/\Lambda$ production ratio is shown in Fig. 20 versus the absolute value of rapidity and in Fig. 21 versus p_T , along with predictions from several MC models. The ratio is shown only for candidates with $p_T > 500$ MeV. The corrected ratio is consistent with unity everywhere, while the uncertainties within the barrel, transition, and endcap regions in rapidity are highly correlated due to common detector corrections and systematic effects. The measurement is statistically limited at higher p_T , while at lower p_T the systematic effects of the modeling of antiproton reconstruction in simulation dominate the uncertainty. Figs. 22 and 23 show the $\bar{\Lambda}/\Lambda$ production ratio in 900 GeV data.

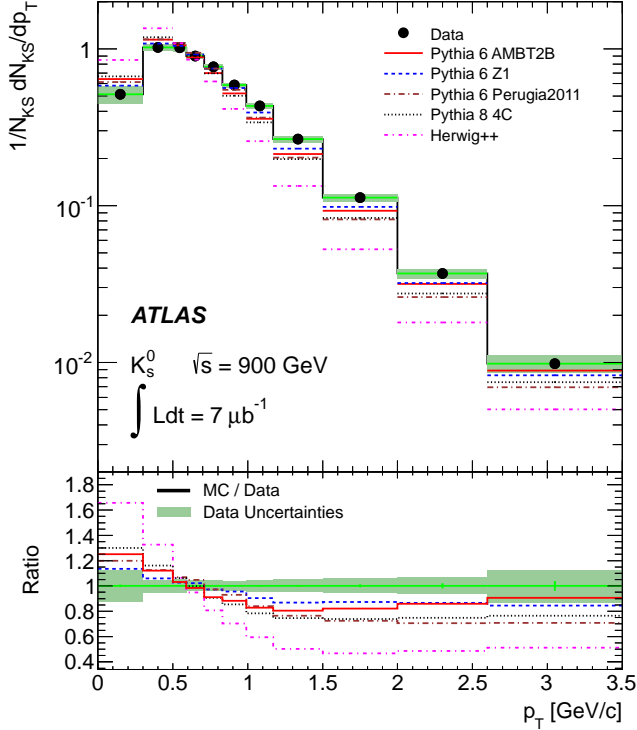


FIG. 11. The corrected p_T distribution of K_S^0 mesons in 900 GeV data compared with the hadron-level distributions in the MC samples for a variety of tunes, normalized to unity. The bottom part of the plot shows the ratio of the MC and data distributions, with the shaded band showing the statistical and systematic uncertainties on the data sample added in quadrature.

VIII. DISCUSSION AND CONCLUSIONS

While the shape of the rapidity distribution for K_S^0 mesons in 7 TeV data agrees with the hadron-level PYTHIA distributions to 5% (Fig. 9), the PYTHIA tunes fall more slowly than data versus p_T above 2 GeV (Fig. 8), although the deviations are within 15% everywhere except at the lowest p_T bin. This shape discrepancy is much improved from the earlier generation of tunes used in ATLAS, as the current models have been tuned using minimum-bias data from the LHC experiments. The best agreement is observed in the PYTHIA6 Z1 tune, but the variation among the PYTHIA tunes is small. Although the shape of the HERWIG++ distribution (UE7-2 tune) agrees with data above 3 GeV, it does a poor job at lower momenta. All of the MC models underestimate the number of K_S^0 mesons per minimum-bias event (Fig. 10), but the experimental uncertainties preclude drawing a significant conclusion about the shape of the multiplicity distribution.

In the case of Λ baryons at 7 TeV, all of the tunes disagree with data at high- p_T and to a greater degree than in the K_S^0 case (Fig. 14). The worst agreement

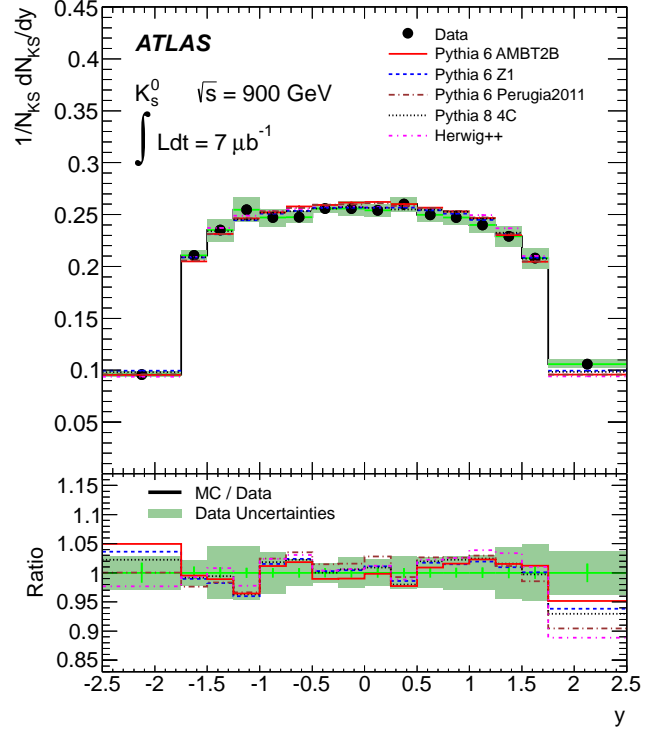


FIG. 12. The corrected rapidity distribution of K_S^0 mesons in 900 GeV data compared with the hadron-level distributions in the MC samples for a variety of tunes, normalized to unity. The bottom part of the plot shows the ratio of the MC and data distributions, with the shaded band showing the statistical and systematic uncertainties on the data sample added in quadrature.

is for PYTHIA8, which deviates from data by a factor of about 2.5 at the highest measured momenta. The Perugia2011 and Z1 tunes also significantly overestimate the production of Λ baryons per event at both energies (Fig. 16).

The AMBT2B tune agrees with 900 GeV data for K_S^0 mesons to better than about 25% across the whole p_T range (Fig. 11), while HERWIG++ (MU900-2 tune) disagrees with data more strongly than in the 7 TeV case (UE7-2 tune). The number of K_S^0 mesons per event (Fig. 13) is underestimated as in the 7 TeV data. In the Λ p_T distribution (Fig. 17) all tunes agree with data better at 900 GeV than at 7 TeV.

The $\bar{\Lambda}/\Lambda$ production ratio at both energies is consistent with unity everywhere and does not show a significant variation with either rapidity or p_T within our total uncertainties. HERWIG++ (MU900-2 tune) shows a decrease in the ratio versus both p_T and rapidity at 900 GeV that is not reproduced by the data (Fig. 22). The measurement is consistent with other antibaryon-baryon ratio measurements from the ALICE, LHCb, and STAR experiments [1, 29, 31, 32]. Measurements from several other experiments are shown in Fig. 24 in terms of the difference between the rapidity of the observed baryons

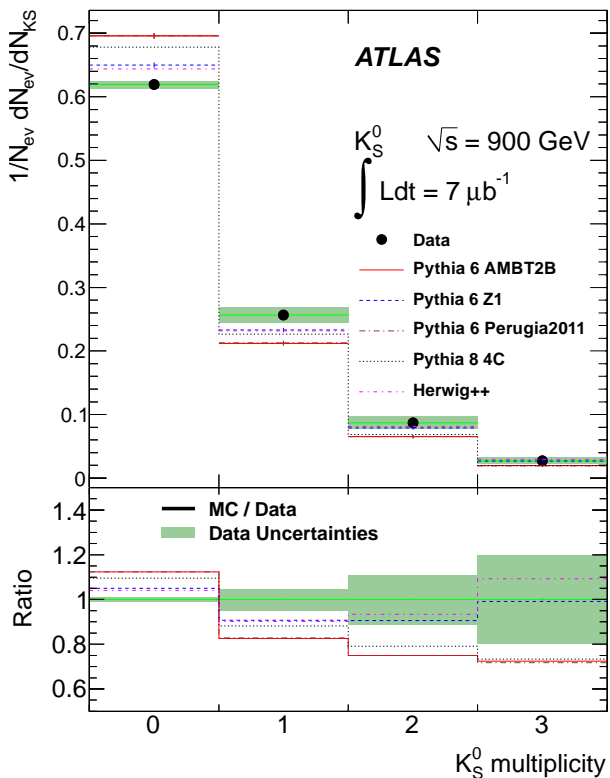


FIG. 13. The corrected multiplicity distribution of K_S^0 mesons in 900 GeV data compared with the hadron-level distributions in the MC samples for a variety of tunes, normalized to unity. The bottom part of the plot shows the ratio of the MC and data distributions, with the shaded band showing the statistical and systematic uncertainties on the data sample added in quadrature.

and the rapidity of the proton beam ($y_{\text{beam}} \approx 8.9$ and 6.9 at 7 TeV and 900 GeV, respectively), along with a combined fit to the following functional form [29] that has been found empirically to describe the data at several energies:

$$\frac{1}{\text{ratio}} = 1 + C \times e^{(\alpha_J - \alpha_P)\Delta y}, \quad (3)$$

where α_J and α_P are related to the string-junction and Pomeron models, respectively. Following Ref. [29], the parameters are fixed to $\alpha_J = 0.5$ and $\alpha_P = 1.2$ and the value $C = 4.6 \pm 0.5$ is obtained from the fit, assuming that the uncertainties are uncorrelated among the measurements.

In summary, measurements are presented of the p_T , rapidity, and multiplicity distributions of K_S^0 and Λ production in pp collisions at $\sqrt{s} = 0.9$ and 7 TeV with the ATLAS detector, as well as the $\bar{\Lambda}/\Lambda$ production ratio. The data results are compared with several recent PYTHIA MC models that were tuned on early LHC data and are found to describe the data significantly better

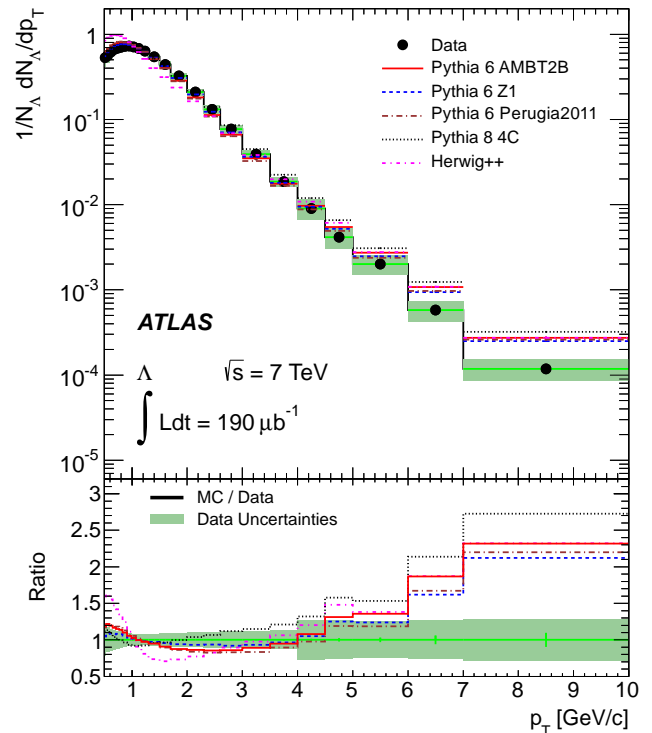


FIG. 14. The corrected p_T distribution of Λ baryons in 7 TeV data compared with the hadron-level distributions in the MC samples for a variety of tunes, normalized to unity. The bottom part of the plot shows the ratio of the MC and data distributions, with the shaded band showing the statistical and systematic uncertainties on the data sample added in quadrature.

than the previous generation of tunes. All PYTHIA tunes underestimate the production of K_S^0 mesons per event and overestimate the production of Λ baryons per event. The HERWIG++ tunes significantly disagree with data in both p_T and multiplicity at the respective energies. Despite the general improvement in the agreement with data, no considered model agrees in both the p_T and multiplicity quantities simultaneously, indicating the need for further model development. The $\bar{\Lambda}/\Lambda$ ratio is consistent with unity in data, indicating that no significant transport of baryon number to mid-rapidities is present, in accordance with SM predictions and measurements from other experiments.

IX. ACKNOWLEDGEMENTS

We thank CERN for the very successful operation of the LHC, as well as the support staff from our institutions without whom ATLAS could not be operated efficiently.

We acknowledge the support of ANPCyT, Argentina; YerPhI, Armenia; ARC, Australia; BMWF, Austria; ANAS, Azerbaijan; SSTC, Belarus; CNPq and FAPESP, Brazil; NSERC, NRC and CFI, Canada; CERN; CON-

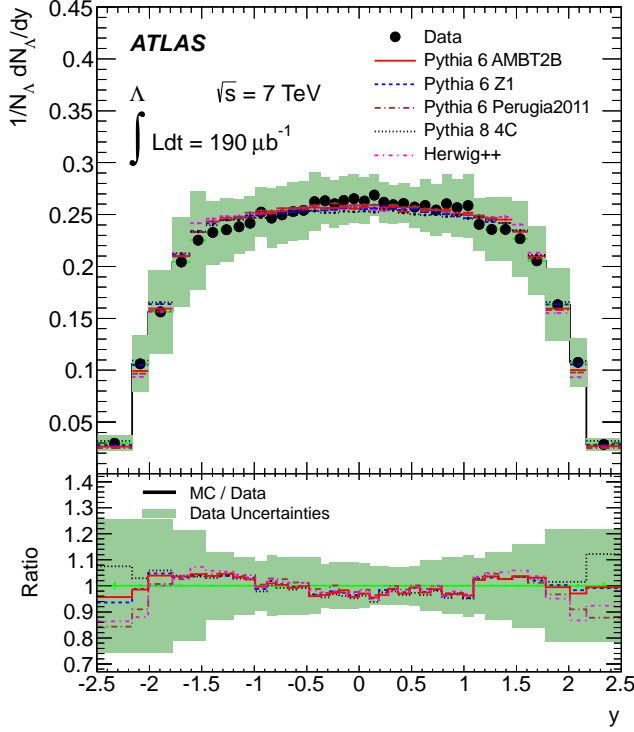


FIG. 15. The corrected rapidity distribution of Λ baryons in 7 TeV data compared with the hadron-level distributions in the MC samples for a variety of tunes, normalized to unity. The bottom part of the plot shows the ratio of the MC and data distributions, with the shaded band showing the statistical and systematic uncertainties on the data sample added in quadrature.

ICYT, Chile; CAS, MOST and NSFC, China; COLCIENCIAS, Colombia; MSMT CR, MPO CR and VSC CR, Czech Republic; DNRf, DNSRC and Lundbeck Foundation, Denmark; ARTEMIS, European Union; IN2P3-CNRS, CEA-DSM/IRFU, France; GNAS, Georgia; BMBF, DFG, HGF, MPG and AvH Foundation, Germany; GSRT, Greece; ISF, MINERVA, GIF, DIP and Benozziyo Center, Israel; INFN, Italy; MEXT and JSPS, Japan; CNRST, Morocco; FOM and NWO, Netherlands; RCN, Norway; MNiSW, Poland; GRICES and FCT, Portugal; MERYs (MECTS), Romania; MES of Russia and ROSATOM, Russian Federation; JINR; MSTd, Serbia; MSSR, Slovakia; ARRS and MVZT, Slovenia; DST/NRF, South Africa; MICINN, Spain; SRC and Wallenberg Foundation, Sweden; SER, SNSF and Cantons of Bern and Geneva, Switzerland; NSC, Taiwan;

TAEK, Turkey; STFC, the Royal Society and Leverhulme Trust, United Kingdom; DOE and NSF, United States of America.

The crucial computing support from all WLCG partners is acknowledged gratefully, in particular from CERN and the ATLAS Tier-1 facilities at TRIUMF (Canada), NDGF (Denmark, Norway, Sweden), CC-IN2P3 (France), KIT/GridKA (Germany), INFN-CNAF (Italy), NL-T1 (Netherlands), PIC (Spain), ASGC (Taiwan), RAL (UK) and BNL (USA) and in the Tier-2 facilities worldwide.

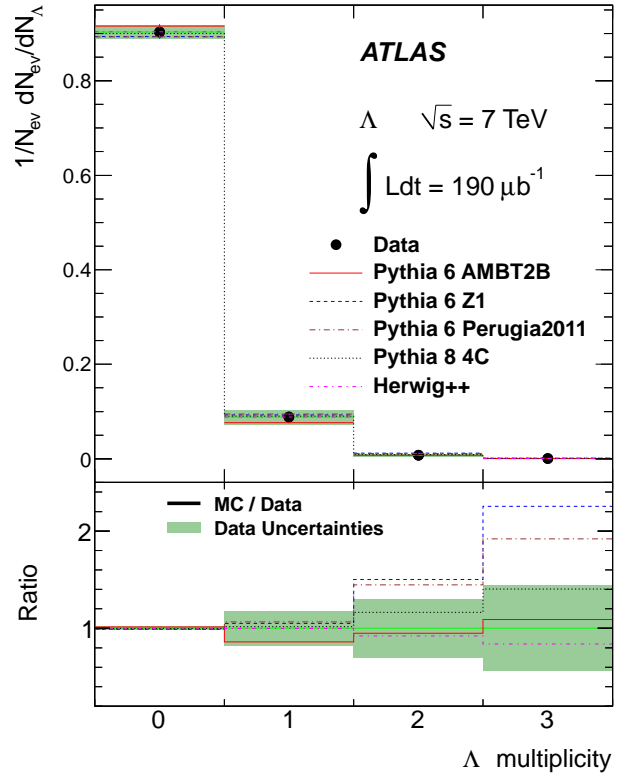


FIG. 16. The corrected multiplicity distribution of Λ baryons in 7 TeV data compared with the hadron-level distributions in the MC samples for a variety of tunes, which are normalized to unity. The bottom part of the plot shows the ratio of the MC and data distributions, with the shaded band showing the statistical and systematic uncertainties on the data sample added in quadrature.

[1] ALICE Collaboration, Eur. Phys. J. C 71, 1594 (2011).
 [2] CMS Collaboration, JHEP 05 (2011) 064.
 [3] CDF Collaboration, Phys. Rev. D 72, 052001 (2005).
 [4] A. Capella et al., Phys. Rep. 236, 225 (1994); A.B.

Kaidalov and K.A. Ter-Martirosyan, Sov. J. Nucl. Phys. 39, 1545 (1984).
 [5] G.C. Rossi and G. Veneziano, Nucl. Phys. B123, (1977) 507; X. Artru, Nucl. Phys. B85, 442 (1975); M. Imachi, S.

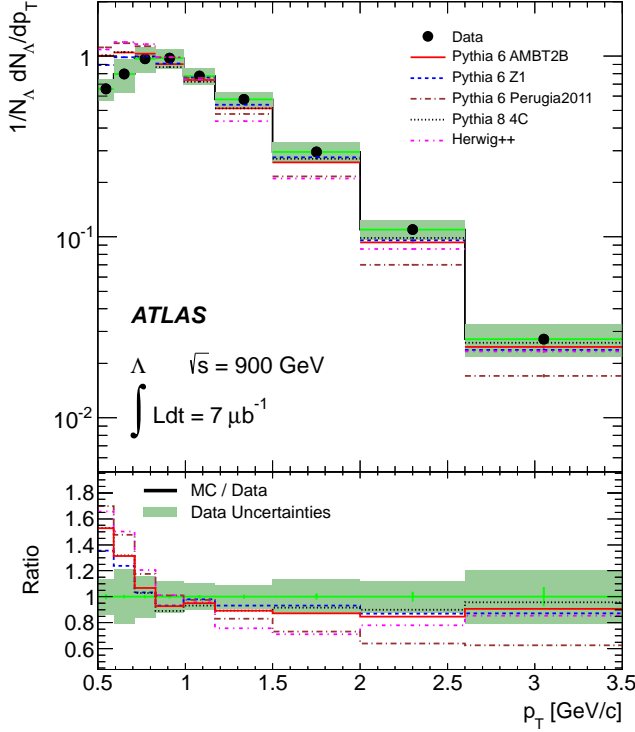


FIG. 17. The corrected p_T distribution of Λ baryons in 900 GeV data compared with the hadron-level distributions in the MC samples for a variety of tunes, normalized to unity. The bottom part of the plot shows the ratio of the MC and data distributions, with the shaded band showing the statistical and systematic uncertainties on the data sample added in quadrature.

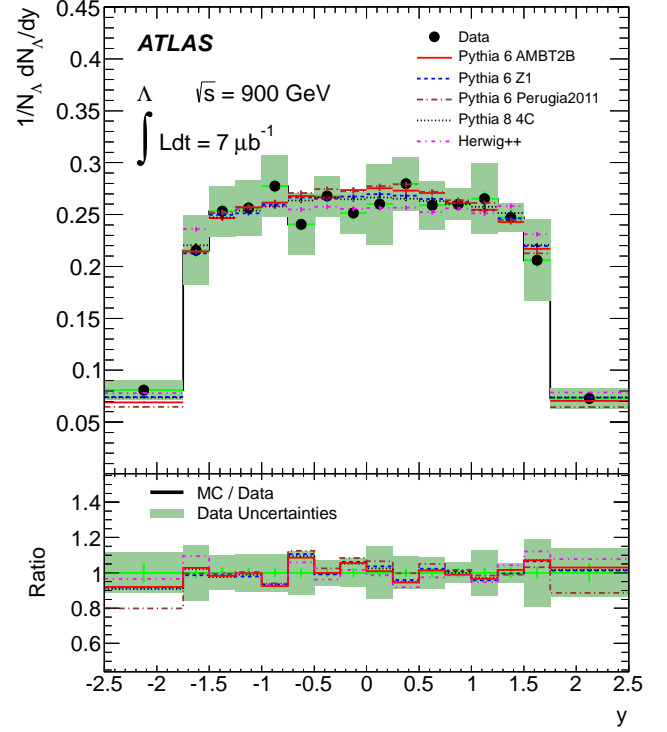


FIG. 18. The corrected rapidity distribution of Λ baryons in 900 GeV data compared with the hadron-level distributions in the MC samples for a variety of tunes, normalized to unity. The bottom part of the plot shows the ratio of the MC and data distributions, with the shaded band showing the statistical and systematic uncertainties on the data sample added in quadrature.

Otsuki and F. Toyoda, Prog. Theor. Phys. 52, 341 (1974); Prog. Theor. Phys. 54, 280 (1975); B.Z. Kopeliovich, Sov. J. Nucl. Phys. 45, 1078 (1987); B.Z. Kopeliovich, B. Povh, Z. Phys. C75, 693 (1997); B.Z. Kopeliovich, B. Povh, Phys. Lett. B446, 321 (1999); D. Kharzeev, Phys. Lett. B378, 238 (1996); C. Merino et al., Eur.Phys.J. C54 577 (2008); C. Merino, M.M. Ryzhinskiy, Yu.M. Shabelski, arXiv:0906.2659; S. E. Vance and M. Gyulassy, Phys. Rev. Lett. 83, 1735 (1999).

[6] ATLAS Collaboration, New J. Phys. 13 (2011) 053033.

[7] The ATLAS reference system is a Cartesian right-handed coordinate system, with the nominal collision point at the origin. The counter-clockwise beam direction defines the positive z -direction, while the positive x -direction is defined as pointing from the collision point to the center of the LHC ring and the positive y -axis points upwards. The azimuthal angle ϕ is measured around the beam axis and the polar angle θ is measured with respect to the z -axis. The pseudorapidity is defined as $\eta = -\ln[\tan(\theta/2)]$, while the rapidity is defined as $y = \frac{1}{2} \ln \frac{E+p_L}{E-p_L}$, where E is the particle energy and p_L is the particle momentum along the z -axis.

[8] ATLAS Collaboration, JINST 3 (2008) S08003.

[9] L. Evans, (ed.) and P. Bryant, (ed.), JINST 3 (2008) S08001.

[10] T. Sjostrand, S. Mrenna, and P. Skands, JHEP 05 (2006)

026.

[11] ATLAS Collaboration, ATLAS Monte Carlo Tunes for MC09, ATL-PHYS-PUB-2010-002.

[12] GEANT4 Collaboration, S. Agostinelli et al., Nucl. Instr. Meth. A506 (2003) 250303.

[13] R. Engel, Z. Phys. C66 (1995) 203-214.

[14] ATLAS Collaboration, ATLAS tunes of PYTHIA6 and PYTHIA8 for MC11, ATL-PHYS-PUB-2011-009.

[15] J. Pumplin et al., JHEP 07 (2002), 012.

[16] P. Skands, Phys. Rev. D 82, 074018 (2010).

[17] CTEQ Collaboration, Eur. Phys. J. C 12 (2000) 375.

[18] R. Field, Early LHC Underlying Event Data - Findings and Surprises (2010), arXiv:1010.3558.

[19] T. Sjostrand, S. Mrenna, and P. Skands, Comput. Phys. Comm. 178 (2008).

[20] R. Corke and T. Sjostrand, JHEP 03 (2011) 032.

[21] M. Bahr et al., Eur. Phys. J. C 58 (2008), 639-707.

[22] S. Gieseke, et al., HERWIG++ 2.5 Release Note (2011), arXiv:1102.1672.

[23] http://projects.hepforge.org/herwig/trac/wiki/MB_UE_tunes.

[24] A. Sherstnev and R. S. Thorne, Eur. Phys. J. C 55 (2008), 553-575.

[25] ATLAS Collaboration, Performance of the ATLAS Silicon Pattern Recognition Algorithm in Data and Simulation at $\sqrt{s} = 7$ TeV, ATLAS-CONF-2010-072.

[26] ATLAS Collaboration, Tracking Results and Comparison

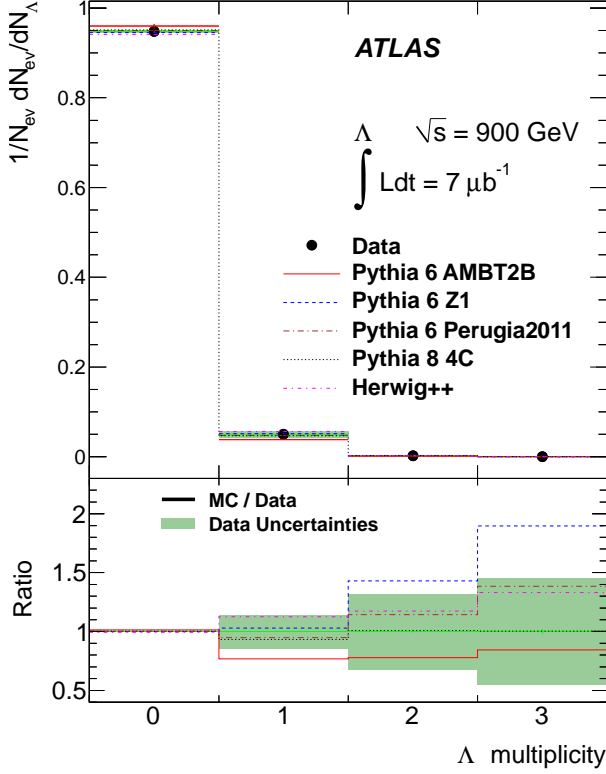


FIG. 19. The corrected multiplicity distribution of Λ baryons in 900 GeV data compared with the hadron-level distributions in the MC samples for a variety of tunes, which are normalized to unity. The bottom part of the plot shows the ratio of the MC and data distributions, with the shaded band showing the statistical and systematic uncertainties on the data sample added in quadrature.

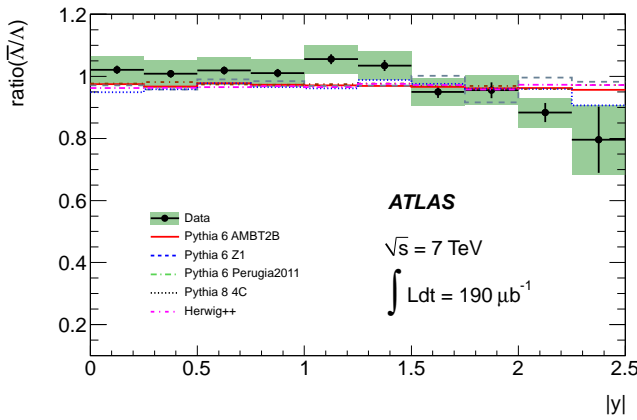


FIG. 20. The production ratio between $\bar{\Lambda}$ and Λ baryons in 7 TeV data versus the absolute value of the rapidity. The error bars show the statistical uncertainties while the band shows statistical and systematic uncertainties added in quadrature.

- to Monte Carlo simulation at $\sqrt{s} = 900$ GeV, ATLAS-CONF-2010-011.
- [27] K. Nakamura et al. (Particle Data Group), J. Phys. G 37, 075021 (2010).
- [28] ATLAS Collaboration, JINST 3 (2008) P04003.
- [29] ALICE Collaboration, Phys. Rev. Lett. 105, 072002 (2010).
- [30] ATLAS Collaboration, dE/dx measurement in the ATLAS Pixel Detector and its use for particle identification, ATLAS-CONF-2011-16.
- [31] LHCb Collaboration, Measurement of V^0 production ratios in pp collisions at $\sqrt{s} = 0.9$ and 7 TeV, arXiv:1107.0882.
- [32] STAR Collaboration, Phys. Rev. C 75, 064901 (2007).

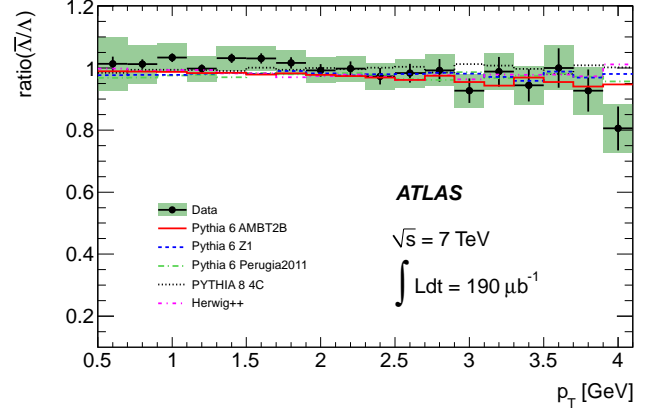


FIG. 21. The production ratio between $\bar{\Lambda}$ and Λ baryons in 7 TeV data versus p_T . The error bars show the statistical uncertainties while the band shows statistical and systematic uncertainties added in quadrature.

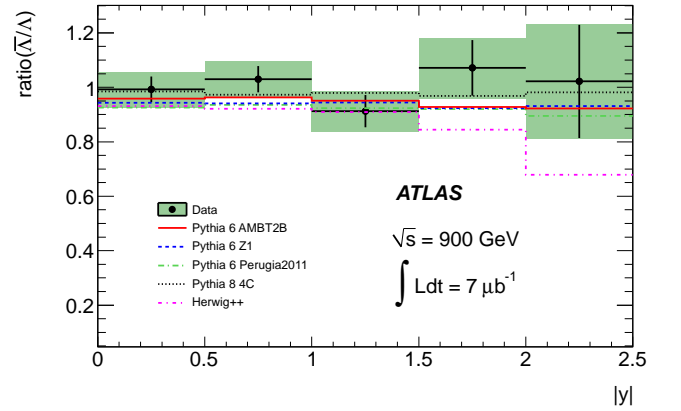


FIG. 22. The production ratio between $\bar{\Lambda}$ and Λ baryons in 900 GeV data versus the absolute value of the rapidity. The error bars show the statistical uncertainties while the band shows statistical and systematic uncertainties added in quadrature.

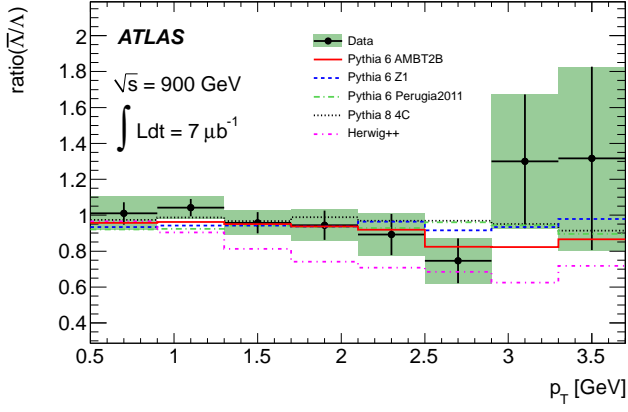


FIG. 23. The production ratio between $\bar{\Lambda}$ and Λ baryons in 900 GeV data versus p_T . The error bars show the statistical uncertainties while the band shows statistical and systematic uncertainties added in quadrature.

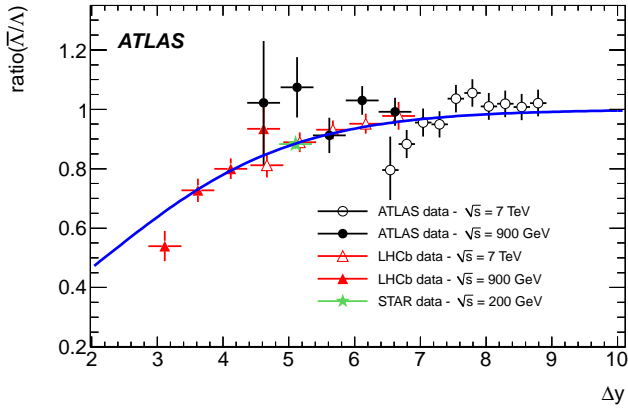


FIG. 24. The production ratio between $\bar{\Lambda}$ and Λ baryons measured by ATLAS and other experiments versus the rapidity difference with respect to the beam. The error bars on the ATLAS data show statistical and systematic uncertainties added in quadrature. The solid line shows the fit to all data points described in the text.

The ATLAS Collaboration

G. Aad⁴⁸, B. Abbott¹¹¹, J. Abdallah¹¹,
A.A. Abdelalim⁴⁹, A. Abdesselam¹¹⁸, O. Abdinov¹⁰,
B. Abi¹¹², M. Abolins⁸⁸, H. Abramowicz¹⁵³,
H. Abreu¹¹⁵, E. Acerbi^{89a,89b}, B.S. Acharya^{164a,164b},
D.L. Adams²⁴, T.N. Addy⁵⁶, J. Adelman¹⁷⁵,
M. Aderholz⁹⁹, S. Adomeit⁹⁸, P. Adragna⁷⁵,
T. Adye¹²⁹, S. Aefsky²², J.A. Aguilar-Saavedra^{124b,a},
M. Aharrouche⁸¹, S.P. Ahlen²¹, F. Ahles⁴⁸,
A. Ahmad¹⁴⁸, M. Ahsan⁴⁰, G. Aielli^{133a,133b},
T. Akdogan^{18a}, T.P.A. Åkesson⁷⁹, G. Akimoto¹⁵⁵,
A.V. Akimov⁹⁴, A. Akiyama⁶⁷, M.S. Alam¹,
M.A. Alam⁷⁶, J. Albert¹⁶⁹, S. Albrand⁵⁵, M. Aleksa²⁹,
I.N. Aleksandrov⁶⁵, F. Alessandria^{89a}, C. Alexa^{25a},
G. Alexander¹⁵³, G. Alexandre⁴⁹, T. Alexopoulos⁹,
M. Alhroob²⁰, M. Aliev¹⁵, G. Alimonti^{89a}, J. Alison¹²⁰,
M. Aliyev¹⁰, P.P. Allport⁷³, S.E. Allwood-Spiers⁵³,
J. Almond⁸², A. Aloisio^{102a,102b}, R. Alon¹⁷¹,
A. Alonso⁷⁹, B. Alvarez Gonzalez⁸⁸,
M.G. Alvigi^{102a,102b}, K. Amako⁶⁶, P. Amaral²⁹,
C. Amelung²², V.V. Ammosov¹²⁸, A. Amorim^{124a,b},
G. Amorós¹⁶⁷, N. Amram¹⁵³, C. Anastopoulos²⁹,
L.S. Ancu¹⁶, N. Andari¹¹⁵, T. Andeen³⁴, C.F. Anders²⁰,
G. Anders^{58a}, K.J. Anderson³⁰, A. Andreazza^{89a,89b},
V. Andrei^{58a}, M.-L. Andrieux⁵⁵, X.S. Anduaga⁷⁰,
A. Angerami³⁴, F. Anghinolfi²⁹, N. Anjos^{124a},
A. Annovi⁴⁷, A. Antonaki⁸, M. Antonelli⁴⁷,
A. Antonov⁹⁶, J. Antos^{144b}, F. Anulli^{132a}, S. Aoun⁸³,
L. Aperio Bella⁴, R. Apolle^{118,c}, G. Arabidze⁸⁸,
I. Aracena¹⁴³, Y. Arai⁶⁶, A.T.H. Arce⁴⁴,
J.P. Archambault²⁸, S. Arfaoui⁸³, J.-F. Arguin¹⁴,
E. Arik^{18a,*}, M. Arik^{18a}, A.J. Armbruster⁸⁷,
O. Arnaez⁸¹, A. Artamonov⁹⁵, G. Artoni^{132a,132b},
D. Arutinov²⁰, S. Asai¹⁵⁵, R. Asfandiyarov¹⁷², S. Ask²⁷,
B. Åsman^{146a,146b}, L. Asquith⁵, K. Assamagan²⁴,
A. Astbury¹⁶⁹, A. Astvatsatourov⁵², G. Atoian¹⁷⁵,
B. Aubert⁴, E. Auge¹¹⁵, K. Augsten¹²⁷,
M. Aurousseau^{145a}, G. Avolio¹⁶³, R. Avramidou⁹,
D. Axen¹⁶⁸, C. Ay⁵⁴, G. Azuelos^{93,d}, Y. Azuma¹⁵⁵,
M.A. Baak²⁹, G. Baccaglioni^{89a}, C. Bacci^{134a,134b},
A.M. Bach¹⁴, H. Bachacou¹³⁶, K. Bachas²⁹, G. Bachy²⁹,
M. Backes⁴⁹, M. Backhaus²⁰, E. Badescu^{25a},
P. Bagnaia^{132a,132b}, S. Bahinipati², Y. Bai^{32a},
D.C. Bailey¹⁵⁸, T. Bain¹⁵⁸, J.T. Baines¹²⁹,
O.K. Baker¹⁷⁵, M.D. Baker²⁴, S. Baker⁷⁷, E. Banas³⁸,
P. Banerjee⁹³, Sw. Banerjee¹⁷², D. Banfi²⁹,
A. Bangert¹³⁷, V. Bansal¹⁶⁹, H.S. Bansil¹⁷, L. Barak¹⁷¹,
S.P. Baranov⁹⁴, A. Barashkou⁶⁵, A. Barbaro Galtieri¹⁴,
T. Barber²⁷, E.L. Barberio⁸⁶, D. Barberis^{50a,50b},
M. Barbero²⁰, D.Y. Bardin⁶⁵, T. Barillari⁹⁹,
M. Barisonzi¹⁷⁴, T. Barklow¹⁴³, N. Barlow²⁷,
B.M. Barnett¹²⁹, R.M. Barnett¹⁴, A. Baroncelli^{134a},
G. Barone⁴⁹, A.J. Barr¹¹⁸, F. Barreiro⁸⁰, J. Barreiro
Guimarães da Costa⁵⁷, R. Bartoldus¹⁴³, A.E. Barton⁷¹,
V. Bartsch¹⁴⁹, R.L. Bates⁵³, L. Batkova^{144a},
J.R. Batley²⁷, A. Battaglia¹⁶, M. Battistin²⁹,
G. Battistoni^{89a}, F. Bauer¹³⁶, H.S. Bawa^{143,e},
B. Beare¹⁵⁸, T. Beau⁷⁸, P.H. Beauchemin¹⁶¹,
R. Beccherle^{50a}, P. Bechtler⁴¹, H.P. Beck¹⁶, S. Becker⁹⁸,
M. Beckingham¹³⁸, K.H. Becks¹⁷⁴, A.J. Beddall^{18c},
A. Beddall^{18c}, S. Bedikian¹⁷⁵, V.A. Bednyakov⁶⁵,
C.P. Bee⁸³, M. Begel²⁴, S. Behar Harpaz¹⁵²,
P.K. Behera⁶³, M. Beimforde⁹⁹,
C. Belanger-Champagne⁸⁵, P.J. Bell⁴⁹, W.H. Bell⁴⁹,
G. Bella¹⁵³, L. Bellagamba^{19a}, F. Bellina²⁹,
M. Bellomo²⁹, A. Belloni⁵⁷, O. Beloborodova¹⁰⁷,
K. Belotskiy⁹⁶, O. Beltramello²⁹, S. Ben Ami¹⁵²,
O. Benary¹⁵³, D. Benchechroun^{135a}, C. Benchouk⁸³,
M. Bendel⁸¹, N. Benekos¹⁶⁵, Y. Benhammou¹⁵³,
D.P. Benjamin⁴⁴, M. Benoit¹¹⁵, J.R. Bensinger²²,
K. Benslama¹³⁰, S. Bentvelsen¹⁰⁵, D. Berge²⁹,
E. Bergeaas Kuutmann⁴¹, N. Berger⁴, F. Berghaus¹⁶⁹,
E. Berglund⁴⁹, J. Beringer¹⁴, P. Bernat⁷⁷,
R. Bernhard⁴⁸, C. Bernius²⁴, T. Berry⁷⁶,
A. Bertin^{19a,19b}, F. Bertinelli²⁹, F. Bertolucci^{122a,122b},
M.I. Besana^{89a,89b}, N. Besson¹³⁶, S. Bethke⁹⁹,
W. Bhimji⁴⁵, R.M. Bianchi²⁹, M. Bianco^{72a,72b},
O. Biebel⁹⁸, S.P. Bieniek⁷⁷, K. Bierwagen⁵⁴,
J. Biesiada¹⁴, M. Biglietti^{134a,134b}, H. Bilokon⁴⁷,
M. Bindi^{19a,19b}, S. Binet¹¹⁵, A. Bingul^{18c},
C. Bini^{132a,132b}, C. Biscarat¹⁷⁷, U. Bitenc⁴⁸,
K.M. Black²¹, R.E. Blair⁵, J.-B. Blanchard¹¹⁵,
G. Blanchot²⁹, T. Blazek^{144a}, C. Blocker²², J. Blocki³⁸,
A. Blondel⁴⁹, W. Blum⁸¹, U. Blumenschein⁵⁴,
G.J. Bobbink¹⁰⁵, V.B. Bobrovnikov¹⁰⁷,
S.S. Bocchetta⁷⁹, A. Bocci⁴⁴, C.R. Boddy¹¹⁸,
M. Boehler⁴¹, J. Boek¹⁷⁴, N. Boelaert³⁵, S. Böser⁷⁷,
J.A. Bogaerts²⁹, A. Bogdanchikov¹⁰⁷, A. Bogouch^{90,*},
C. Bohm^{146a}, V. Boisvert⁷⁶, T. Bold³⁷, V. Boldea^{25a},
N.M. Bolnet¹³⁶, M. Bona⁷⁵, V.G. Bondarenko⁹⁶,
M. Bondioli¹⁶³, M. Boonekamp¹³⁶, G. Boorman⁷⁶,
C.N. Booth¹³⁹, S. Bordoni⁷⁸, C. Borer¹⁶, A. Borisov¹²⁸,
G. Borissov⁷¹, I. Borjanovic^{12a}, S. Borroni⁸⁷, K. Bos¹⁰⁵,
D. Boscherini^{19a}, M. Bosman¹¹, H. Boterenbrood¹⁰⁵,
D. Botterill¹²⁹, J. Bouchami⁹³, J. Boudreau¹²³,
E.V. Bouhova-Thacker⁷¹, C. Bourdarios¹¹⁵,
N. Bousson⁸³, A. Boveia³⁰, J. Boyd²⁹, I.R. Boyko⁶⁵,
N.I. Bozhko¹²⁸, I. Bozovic-Jelisavcic^{12b}, J. Bracinik¹⁷,
A. Braem²⁹, P. Branchini^{134a}, G.W. Brandenburg⁵⁷,
A. Brandt⁷, G. Brandt¹⁵, O. Brandt⁵⁴, U. Bratzler¹⁵⁶,
B. Brau⁸⁴, J.E. Brau¹¹⁴, H.M. Braun¹⁷⁴, B. Brelier¹⁵⁸,
J. Bremer²⁹, R. Brenner¹⁶⁶, S. Bressler¹⁵²,
D. Breton¹¹⁵, D. Britton⁵³, F.M. Brochu²⁷, I. Brock²⁰,
R. Brock⁸⁸, T.J. Brodbeck⁷¹, E. Brodet¹⁵³,
F. Broggi^{89a}, C. Bromberg⁸⁸, G. Brooijmans³⁴,
W.K. Brooks^{31b}, G. Brown⁸², H. Brown⁷,
P.A. Bruckman de Renstrom³⁸, D. Bruncko^{144b},
R. Bruneliere⁴⁸, S. Brunet⁶¹, A. Bruni^{19a}, G. Bruni^{19a},
M. Bruschi^{19a}, T. Buanes¹³, F. Bucci⁴⁹, J. Buchanan¹¹⁸,
N.J. Buchanan², P. Buchholz¹⁴¹, R.M. Buckingham¹¹⁸,
A.G. Buckley⁴⁵, S.I. Buda^{25a}, I.A. Budagov⁶⁵,
B. Budick¹⁰⁸, V. Büscher⁸¹, L. Bugge¹¹⁷,
D. Buirra-Clark¹¹⁸, O. Bulekov⁹⁶, M. Bunse⁴²,
T. Buran¹¹⁷, H. Burckhart²⁹, S. Burdin⁷³, T. Burgess¹³,
S. Burke¹²⁹, E. Busato³³, P. Bussey⁵³, C.P. Buszello¹⁶⁶,

- F. Butin²⁹, B. Butler¹⁴³, J.M. Butler²¹, C.M. Buttar⁵³, J.M. Butterworth⁷⁷, W. Buttinger²⁷, S. Cabrera Urbán¹⁶⁷, D. Caforio^{19a,19b}, O. Cakir^{3a}, P. Calafiura¹⁴, G. Calderini⁷⁸, P. Calfayan⁹⁸, R. Calkins¹⁰⁶, L.P. Caloba^{23a}, R. Caloi^{132a,132b}, D. Calvet³³, S. Calvet³³, R. Camacho Toro³³, P. Camarri^{133a,133b}, M. Cambiaghi^{119a,119b}, D. Cameron¹¹⁷, L.M. Caminada¹⁴, S. Campana²⁹, M. Campanelli⁷⁷, V. Canale^{102a,102b}, F. Canelli^{30,f}, A. Canepa^{159a}, J. Cantero⁸⁰, L. Capasso^{102a,102b}, M.D.M. Capeans Garrido²⁹, I. Caprini^{25a}, M. Caprini^{25a}, D. Capriotti⁹⁹, M. Capua^{36a,36b}, R. Caputo¹⁴⁸, R. Cardarelli^{133a}, T. Carli²⁹, G. Carlino^{102a}, L. Carminati^{89a,89b}, B. Caron^{159a}, S. Caron⁴⁸, G.D. Carrillo Montoya¹⁷², A.A. Carter⁷⁵, J.R. Carter²⁷, J. Carvalho^{124a,g}, D. Casadei¹⁰⁸, M.P. Casado¹¹, M. Cascella^{122a,122b}, C. Caso^{50a,50b,*}, A.M. Castaneda Hernandez¹⁷², E. Castaneda-Miranda¹⁷², V. Castillo Gimenez¹⁶⁷, N.F. Castro^{124a}, G. Cataldi^{72a}, F. Cataneo²⁹, A. Catinaccio²⁹, J.R. Catmore⁷¹, A. Cattai²⁹, G. Cattani^{133a,133b}, S. Caughron⁸⁸, D. Caut^{164a,164c}, P. Cavalleri⁷⁸, D. Cavalli^{89a}, M. Cavalli-Sforza¹¹, V. Cavasinni^{122a,122b}, F. Ceradini^{134a,134b}, A.S. Cerqueira^{23b}, A. Cerri²⁹, L. Cerrito⁷⁵, F. Cerutti⁴⁷, S.A. Cetin^{18b}, F. Cevenini^{102a,102b}, A. Chafaq^{135a}, D. Chakraborty¹⁰⁶, K. Chan², B. Chapleau⁸⁵, J.D. Chapman²⁷, J.W. Chapman⁸⁷, E. Chareyre⁷⁸, D.G. Charlton¹⁷, V. Chavda⁸², C.A. Chavez Barajas²⁹, S. Cheatham⁸⁵, S. Chekanov⁵, S.V. Chekulaev^{159a}, G.A. Chelkov⁶⁵, M.A. Chelstowska¹⁰⁴, C. Chen⁶⁴, H. Chen²⁴, S. Chen^{32c}, T. Chen^{32c}, X. Chen¹⁷², S. Cheng^{32a}, A. Cheplakov⁶⁵, V.F. Chepurinov⁶⁵, R. Cherkaoui El Moursli^{135e}, V. Chernyatin²⁴, E. Cheu⁶, S.L. Cheung¹⁵⁸, L. Chevalier¹³⁶, G. Chiefari^{102a,102b}, L. Chikovani^{51a}, J.T. Childers^{58a}, A. Chilingarov⁷¹, G. Chiodini^{72a}, M.V. Chizhov⁶⁵, G. Choudalakis³⁰, S. Chouridou¹³⁷, I.A. Christidi⁷⁷, A. Christov⁴⁸, D. Chromek-Burckhart²⁹, M.L. Chu¹⁵¹, J. Chudoba¹²⁵, G. Ciapetti^{132a,132b}, K. Ciba³⁷, A.K. Ciftci^{3a}, R. Ciftci^{3a}, D. Cinca³³, V. Cindro⁷⁴, M.D. Ciobotaru¹⁶³, C. Ciocca^{19a}, A. Ciocio¹⁴, M. Cirilli⁸⁷, M. Ciubancan^{25a}, A. Clark⁴⁹, P.J. Clark⁴⁵, W. Cleland¹²³, J.C. Clemens⁸³, B. Clement⁵⁵, C. Clement^{146a,146b}, R.W. Clift¹²⁹, Y. Coadou⁸³, M. Cobal^{164a,164c}, A. Coccaro^{50a,50b}, J. Cochran⁶⁴, P. Coe¹¹⁸, J.G. Cogan¹⁴³, J. Coggeshall¹⁶⁵, E. Cogneras¹⁷⁷, C.D. Cojocar²⁸, J. Colas⁴, A.P. Colijn¹⁰⁵, C. Collard¹¹⁵, N.J. Collins¹⁷, C. Collins-Tooth⁵³, J. Collot⁵⁵, G. Colon⁸⁴, P. Conde Muiño^{124a}, E. Coniavitis¹¹⁸, M.C. Conidi¹¹, M. Consonni¹⁰⁴, V. Consorti⁴⁸, S. Constantinescu^{25a}, C. Conta^{119a,119b}, F. Conventi^{102a,h}, J. Cook²⁹, M. Cooke¹⁴, B.D. Cooper⁷⁷, A.M. Cooper-Sarkar¹¹⁸, K. Copic¹⁴, T. Cornelissen¹⁷⁴, M. Corradi^{19a}, F. Corriveau^{85,i}, A. Cortes-Gonzalez¹⁶⁵, G. Cortiana⁹⁹, G. Costa^{89a}, M.J. Costa¹⁶⁷, D. Costanzo¹³⁹, T. Costin³⁰, D. Côté²⁹, L. Courneyea¹⁶⁹, G. Cowan⁷⁶, C. Cowden²⁷, B.E. Cox⁸², K. Cranmer¹⁰⁸, F. Crescioli^{122a,122b}, M. Cristinziani²⁰, G. Crosetti^{36a,36b}, R. Crupi^{72a,72b}, S. Crépé-Renaudin⁵⁵, C.-M. Cuciuc^{25a}, C. Cuenca Almenar¹⁷⁵, T. Cuhadar Donszelmann¹³⁹, M. Curatolo⁴⁷, C.J. Curtis¹⁷, P. Cwetanski⁶¹, H. Czirr¹⁴¹, Z. Czyczula¹⁷⁵, S. D'Auria⁵³, M. D'Onofrio⁷³, A. D'Orazio^{132a,132b}, P.V.M. Da Silva^{23a}, C. Da Via⁸², W. Dabrowski³⁷, T. Dai⁸⁷, C. Dallapiccola⁸⁴, M. Dam³⁵, M. Dameri^{50a,50b}, D.S. Damiani¹³⁷, H.O. Danielsson²⁹, D. Dannheim⁹⁹, V. Dao⁴⁹, G. Darbo^{50a}, G.L. Darlea^{25b}, C. Daum¹⁰⁵, W. Davey²⁰, T. Davidek¹²⁶, N. Davidson⁸⁶, R. Davidson⁷¹, E. Davies^{118,c}, M. Davies⁹³, A.R. Davison⁷⁷, Y. Davygora^{58a}, E. Dawe¹⁴², I. Dawson¹³⁹, J.W. Dawson^{5,*}, R.K. Daya³⁹, K. De⁷, R. de Asmundis^{102a}, S. De Castro^{19a,19b}, P.E. De Castro Faria Salgado²⁴, S. De Cecco⁷⁸, J. de Graat⁹⁸, N. De Groot¹⁰⁴, P. de Jong¹⁰⁵, C. De La Taille¹¹⁵, H. De la Torre⁸⁰, B. De Lotto^{164a,164c}, L. De Mora⁷¹, L. De Nooij¹⁰⁵, D. De Pedis^{132a}, A. De Salvo^{132a}, U. De Sanctis^{164a,164c}, A. De Santo¹⁴⁹, J.B. De Vivie De Regie¹¹⁵, S. Dean⁷⁷, R. Debbé²⁴, C. Debenedetti⁴⁵, D.V. Dedovich⁶⁵, J. Degenhardt¹²⁰, M. Dehchar¹¹⁸, C. Del Papa^{164a,164c}, J. Del Peso⁸⁰, T. Del Prete^{122a,122b}, T. Delemontex⁵⁵, M. Deliyergiyev⁷⁴, A. Dell'Acqua²⁹, L. Dell'Asta²¹, M. Della Pietra^{102a,h}, D. della Volpe^{102a,102b}, M. Delmastro²⁹, N. Delruelle²⁹, P.A. Delsart⁵⁵, C. Deluca¹⁴⁸, S. Demers¹⁷⁵, M. Demichev⁶⁵, B. Demirkoz^{11,j}, J. Deng¹⁶³, S.P. Denisov¹²⁸, D. Derendarz³⁸, J.E. Derkaoui^{135d}, F. Derue⁷⁸, P. Dervan⁷³, K. Desch²⁰, E. Devetak¹⁴⁸, P.O. Deviveiros¹⁵⁸, A. Dewhurst¹²⁹, B. DeWilde¹⁴⁸, S. Dhaliwal¹⁵⁸, R. Dhullipudi^{24,k}, A. Di Ciaccio^{133a,133b}, L. Di Ciaccio⁴, A. Di Girolamo²⁹, B. Di Girolamo²⁹, S. Di Luise^{134a,134b}, A. Di Mattia¹⁷², B. Di Micco²⁹, R. Di Nardo⁴⁷, A. Di Simone^{133a,133b}, R. Di Sipio^{19a,19b}, M.A. Diaz^{31a}, F. Diblen^{18c}, E.B. Diehl⁸⁷, J. Dietrich⁴¹, T.A. Dietzsch^{58a}, K. Dindar Yagci³⁹, J. Dingfelder²⁰, C. Dionisi^{132a,132b}, P. Dita^{25a}, S. Dita^{25a}, F. Dittus²⁹, F. Djama⁸³, T. Djobava^{51b}, M.A.B. do Vale^{23a}, A. Do Valle Wemans^{124a}, T.K.O. Doan⁴, M. Dobbs⁸⁵, R. Dobinson^{29,*}, D. Dobos²⁹, E. Dobson²⁹, M. Dobson¹⁶³, J. Dodd³⁴, C. Doglioni¹¹⁸, T. Doherty⁵³, Y. Doi^{66,*}, J. Dolejsi¹²⁶, I. Dolenc⁷⁴, Z. Dolezal¹²⁶, B.A. Dolgoshein^{96,*}, T. Dohmae¹⁵⁵, M. Donadelli^{23d}, M. Donega¹²⁰, J. Donini⁵⁵, J. Dopke²⁹, A. Doria^{102a}, A. Dos Anjos¹⁷², M. Dosil¹¹, A. Dotti^{122a,122b}, M.T. Dova⁷⁰, J.D. Dowell¹⁷, A.D. Doxiadis¹⁰⁵, A.T. Doyle⁵³, Z. Drasal¹²⁶, J. Drees¹⁷⁴, N. Dressnandt¹²⁰, H. Drevermann²⁹, C. Driouichi³⁵, M. Dris⁹, J. Dubbert⁹⁹, S. Dube¹⁴, E. Duchovni¹⁷¹, G. Duckeck⁹⁸, A. Dudarev²⁹, F. Dudziak⁶⁴, M. Dührssen²⁹, I.P. Duerdoth⁸², L. Duflot¹¹⁵, M.-A. Dufour⁸⁵, M. Dunford²⁹, H. Duran Yildiz^{3b}, R. Duxfield¹³⁹, M. Dwuznik³⁷, F. Dydak²⁹, M. Düren⁵², W.L. Ebenstein⁴⁴, J. Ebke⁹⁸

- S. Eckweiler⁸¹, K. Edmonds⁸¹, C.A. Edwards⁷⁶, N.C. Edwards⁵³, W. Ehrenfeld⁴¹, T. Ehrich⁹⁹, T. Eifert²⁹, G. Eigen¹³, K. Einsweiler¹⁴, E. Eisenhandler⁷⁵, T. Ekelof¹⁶⁶, M. El Kacimi^{135c}, M. Ellert¹⁶⁶, S. Elles⁴, F. Ellinghaus⁸¹, K. Ellis⁷⁵, N. Ellis²⁹, J. Elmsheuser⁹⁸, M. Elsing²⁹, D. Emeliyanov¹²⁹, R. Engelmann¹⁴⁸, A. Engl⁹⁸, B. Epp⁶², A. Eppig⁸⁷, J. Erdmann⁵⁴, A. Ereditato¹⁶, D. Eriksson^{146a}, J. Ernst¹, M. Ernst²⁴, J. Ernwein¹³⁶, D. Errede¹⁶⁵, S. Errede¹⁶⁵, E. Ertel⁸¹, M. Escalier¹¹⁵, C. Escobar¹²³, X. Espinal Curull¹¹, B. Esposito⁴⁷, F. Etienne⁸³, A.I. Etievre¹³⁶, E. Etzion¹⁵³, D. Evangelakou⁵⁴, H. Evans⁶¹, L. Fabbri^{19a,19b}, C. Fabre²⁹, R.M. Fakhruddinov¹²⁸, S. Falciano^{132a}, Y. Fang¹⁷², M. Fanti^{89a,89b}, A. Farbin⁷, A. Farilla^{134a}, J. Farley¹⁴⁸, T. Farooque¹⁵⁸, S.M. Farrington¹¹⁸, P. Farthouat²⁹, P. Fassnacht²⁹, D. Fassouliotis⁸, B. Fatholahzadeh¹⁵⁸, A. Favareto^{89a,89b}, L. Fayard¹¹⁵, S. Fazio^{36a,36b}, R. Febbraro³³, P. Federic^{144a}, O.L. Fedin¹²¹, W. Fedorko⁸⁸, M. Fehling-Kaschek⁴⁸, L. Felgioni⁸³, C. Feng^{32d}, E.J. Feng³⁰, A.B. Fenyuk¹²⁸, J. Ferencei^{144b}, J. Ferland⁹³, W. Fernando¹⁰⁹, S. Ferrag⁵³, J. Ferrando⁵³, V. Ferrara⁴¹, A. Ferrari¹⁶⁶, P. Ferrari¹⁰⁵, R. Ferrari^{119a}, A. Ferrer¹⁶⁷, M.L. Ferrer⁴⁷, D. Ferrere⁴⁹, C. Ferretti⁸⁷, A. Ferretto Parodi^{50a,50b}, M. Fiascaris³⁰, F. Fiedler⁸¹, A. Filipčić⁷⁴, A. Filippas⁹, F. Filthaut¹⁰⁴, M. Fincke-Keeler¹⁶⁹, M.C.N. Fiolhais^{124a,g}, L. Fiorini¹⁶⁷, A. Firan³⁹, G. Fischer⁴¹, P. Fischer²⁰, M.J. Fisher¹⁰⁹, M. Flechl⁴⁸, I. Fleck¹⁴¹, J. Fleckner⁸¹, P. Fleischmann¹⁷³, S. Fleischmann¹⁷⁴, T. Flick¹⁷⁴, L.R. Flores Castillo¹⁷², M.J. Flowerdew⁹⁹, M. Fokitis⁹, T. Fonseca Martin¹⁶, D.A. Forbush¹³⁸, A. Formica¹³⁶, A. Forti⁸², D. Fortin^{159a}, J.M. Foster⁸², D. Fournier¹¹⁵, A. Foussat²⁹, A.J. Fowler⁴⁴, K. Fowler¹³⁷, H. Fox⁷¹, P. Francavilla^{122a,122b}, S. Franchino^{119a,119b}, D. Francis²⁹, T. Frank¹⁷¹, M. Franklin⁵⁷, S. Franz²⁹, M. Fraternali^{119a,119b}, S. Fratina¹²⁰, S.T. French²⁷, F. Friedrich⁴³, R. Froeschl²⁹, D. Froidevaux²⁹, J.A. Frost²⁷, C. Fukunaga¹⁵⁶, E. Fullana Torregrosa²⁹, J. Fuster¹⁶⁷, C. Gabaldon²⁹, O. Gabizon¹⁷¹, T. Gadfort²⁴, S. Gadomski⁴⁹, G. Gagliardi^{50a,50b}, P. Gagnon⁶¹, C. Galea⁹⁸, E.J. Gallas¹¹⁸, V. Gallo¹⁶, B.J. Gallop¹²⁹, P. Gallus¹²⁵, K.K. Gan¹⁰⁹, Y.S. Gao^{143,e}, V.A. Gapienko¹²⁸, A. Gaponenko¹⁴, F. Garberson¹⁷⁵, M. Garcia-Sciveres¹⁴, C. García¹⁶⁷, J.E. García Navarro⁴⁹, R.W. Gardner³⁰, N. Garelli²⁹, H. Garitaonandia¹⁰⁵, V. Garonne²⁹, J. Garvey¹⁷, C. Gatti⁴⁷, G. Gaudio^{119a}, O. Gaumer⁴⁹, B. Gaur¹⁴¹, L. Gauthier¹³⁶, I.L. Gavrilenko⁹⁴, C. Gay¹⁶⁸, G. Gaycken²⁰, J.-C. Gayde²⁹, E.N. Gazis⁹, P. Ge^{32d}, C.N.P. Gee¹²⁹, D.A.A. Geerts¹⁰⁵, Ch. Geich-Gimbel²⁰, K. Gellerstedt^{146a,146b}, C. Gemme^{50a}, A. Gemmell⁵³, M.H. Genest⁹⁸, S. Gentile^{132a,132b}, M. George⁵⁴, S. George⁷⁶, P. Gerlach¹⁷⁴, A. Gershon¹⁵³, C. Geweniger^{58a}, H. Ghazlane^{135b}, P. Ghez⁴, N. Ghodbane³³, B. Giacobbe^{19a}, S. Giagu^{132a,132b}, V. Giakoumopoulou⁸, V. Giangiobbe^{122a,122b}, F. Gianotti²⁹, B. Gibbard²⁴, A. Gibson¹⁵⁸, S.M. Gibson²⁹, L.M. Gilbert¹¹⁸, V. Gilevsky⁹¹, D. Gillberg²⁸, A.R. Gillman¹²⁹, D.M. Gingrich^{2,d}, J. Ginzburg¹⁵³, N. Giokaris⁸, M.P. Giordani^{164c}, R. Giordano^{102a,102b}, F.M. Giorgi¹⁵, P. Giovannini⁹⁹, P.F. Giraud¹³⁶, D. Giugni^{89a}, M. Giunta⁹³, P. Giusti^{19a}, B.K. Gjelsten¹¹⁷, L.K. Gladilin⁹⁷, C. Glasman⁸⁰, J. Glatzer⁴⁸, A. Glazov⁴¹, K.W. Glitza¹⁷⁴, G.L. Glonti⁶⁵, J. Godfrey¹⁴², J. Godlewski²⁹, M. Goebel⁴¹, T. Göpfert⁴³, C. Goeringer⁸¹, C. Gössling⁴², T. Göttfert⁹⁹, S. Goldfarb⁸⁷, T. Golling¹⁷⁵, S.N. Golovnia¹²⁸, A. Gomes^{124a,b}, L.S. Gomez Fajardo⁴¹, R. Gonçalo⁷⁶, J. Goncalves Pinto Firmino Da Costa⁴¹, L. Gonella²⁰, A. Gonidec²⁹, S. Gonzalez¹⁷², S. González de la Hoz¹⁶⁷, G. Gonzalez Parra¹¹, M.L. Gonzalez Silva²⁶, S. Gonzalez-Sevilla⁴⁹, J.J. Goodson¹⁴⁸, L. Goossens²⁹, P.A. Gorbounov⁹⁵, H.A. Gordon²⁴, I. Gorelov¹⁰³, G. Gorfine¹⁷⁴, B. Gorini²⁹, E. Gorini^{72a,72b}, A. Gorišek⁷⁴, E. Gornicki³⁸, S.A. Gorokhov¹²⁸, V.N. Goryachev¹²⁸, B. Gosdzik⁴¹, M. Gosselink¹⁰⁵, M.I. Gostkin⁶⁵, I. Gough Eschrich¹⁶³, M. Gouighri^{135a}, D. Goujdami^{135c}, M.P. Goulette⁴⁹, A.G. Goussiou¹³⁸, C. Goy⁴, S. Gozpinar²², I. Grabowska-Bold³⁷, P. Grafström²⁹, K.-J. Grah⁴¹, F. Grancagnolo^{72a}, S. Grancagnolo¹⁵, V. Grassi¹⁴⁸, V. Gratchev¹²¹, N. Grau³⁴, H.M. Gray²⁹, J.A. Gray¹⁴⁸, E. Graziani^{134a}, O.G. Grebenyuk¹²¹, T. Greenshaw⁷³, Z.D. Greenwood^{24,k}, K. Gregersen³⁵, I.M. Gregor⁴¹, P. Grenier¹⁴³, J. Griffiths¹³⁸, N. Grigalashvili⁶⁵, A.A. Grillo¹³⁷, S. Grinstein¹¹, Y.V. Grishkevich⁹⁷, J.-F. Grivaz¹¹⁵, M. Groh⁹⁹, E. Gross¹⁷¹, J. Grosse-Knetter⁵⁴, J. Groth-Jensen¹⁷¹, K. Grybel¹⁴¹, V.J. Guarino⁵, D. Guest¹⁷⁵, C. Guicheney³³, A. Guida^{72a,72b}, T. Guillemin⁴, S. Guindon⁵⁴, H. Guler^{85,l}, J. Gunther¹²⁵, B. Guo¹⁵⁸, J. Guo³⁴, A. Gupta³⁰, Y. Gusakov⁶⁵, V.N. Gushchin¹²⁸, A. Gutierrez⁹³, P. Gutierrez¹¹¹, N. Guttman¹⁵³, O. Gutzwiller¹⁷², C. Guyot¹³⁶, C. Gwenlan¹¹⁸, C.B. Gwilliam⁷³, A. Haas¹⁴³, S. Haas²⁹, C. Haber¹⁴, R. Hackenburg²⁴, H.K. Hadavand³⁹, D.R. Hadley¹⁷, P. Haefner⁹⁹, F. Hahn²⁹, S. Haider²⁹, Z. Hajduk³⁸, H. Hakobyan¹⁷⁶, J. Haller⁵⁴, K. Hamacher¹⁷⁴, P. Hamal¹¹³, M. Hamer⁵⁴, A. Hamilton⁴⁹, S. Hamilton¹⁶¹, H. Han^{32a}, L. Han^{32b}, K. Hanagaki¹¹⁶, K. Hanawa¹⁶⁰, M. Hance¹⁴, C. Handel⁸¹, P. Hanke^{58a}, J.R. Hansen³⁵, J.B. Hansen³⁵, J.D. Hansen³⁵, P.H. Hansen³⁵, P. Hansson¹⁴³, K. Hara¹⁶⁰, G.A. Hare¹³⁷, T. Harenberg¹⁷⁴, S. Harkusha⁹⁰, D. Harper⁸⁷, R.D. Harrington⁴⁵, O.M. Harris¹³⁸, K. Harrison¹⁷, J. Hartert⁴⁸, F. Hartjes¹⁰⁵, T. Haruyama⁶⁶, A. Harvey⁵⁶, S. Hasegawa¹⁰¹, Y. Hasegawa¹⁴⁰, S. Hassani¹³⁶, M. Hatch²⁹, D. Hauff⁹⁹, S. Haug¹⁶, M. Hauschild²⁹, R. Hauser⁸⁸, M. Havranek²⁰, B.M. Hawes¹¹⁸, C.M. Hawkes¹⁷, R.J. Hawkings²⁹, D. Hawkins¹⁶³, T. Hayakawa⁶⁷, T. Hayashi¹⁶⁰, D. Hayden⁷⁶, H.S. Hayward⁷³, S.J. Haywood¹²⁹, E. Hazen²¹, M. He^{32d}, S.J. Head¹⁷,

- V. Hedberg⁷⁹, L. Heelan⁷, S. Heim⁸⁸, B. Heinemann¹⁴,
 S. Heisterkamp³⁵, L. Helary⁴, S. Hellman^{146a,146b},
 D. Hellmich²⁰, C. Helsens¹¹, R.C.W. Henderson⁷¹,
 M. Henke^{58a}, A. Henrichs⁵⁴, A.M. Henriques Correia²⁹,
 S. Henrot-Versille¹¹⁵, F. Henry-Couannier⁸³,
 C. Hensel⁵⁴, T. Henß¹⁷⁴, C.M. Hernandez⁷,
 Y. Hernández Jiménez¹⁶⁷, R. Herrberg¹⁵,
 A.D. Hershenhorn¹⁵², G. Herten⁴⁸, R. Hertenberger⁹⁸,
 L. Hervas²⁹, N.P. Hessey¹⁰⁵, E. Higón-Rodríguez¹⁶⁷,
 D. Hill^{5,*}, J.C. Hill²⁷, N. Hill⁵, K.H. Hiller⁴¹,
 S. Hillert²⁰, S.J. Hillier¹⁷, I. Hinchliffe¹⁴, E. Hines¹²⁰,
 M. Hirose¹¹⁶, F. Hirsch⁴², D. Hirschbuehl¹⁷⁴,
 J. Hobbs¹⁴⁸, N. Hod¹⁵³, M.C. Hodgkinson¹³⁹,
 P. Hodgson¹³⁹, A. Hoecker²⁹, M.R. Hoferkamp¹⁰³,
 J. Hoffman³⁹, D. Hoffmann⁸³, M. Hohlfeld⁸¹,
 M. Holder¹⁴¹, S.O. Holmgren^{146a}, T. Holy¹²⁷,
 J.L. Holzbauer⁸⁸, Y. Homma⁶⁷, T.M. Hong¹²⁰,
 L. Hoof van Huysduynen¹⁰⁸, T. Horazdovsky¹²⁷,
 C. Horn¹⁴³, S. Horner⁴⁸, K. Horton¹¹⁸, J-Y. Hostachy⁵⁵,
 S. Hou¹⁵¹, M.A. Houlden⁷³, A. Hoummada^{135a},
 J. Howarth⁸², D.F. Howell¹¹⁸, I. Hristova¹⁵,
 J. Hrivnac¹¹⁵, I. Hruska¹²⁵, T. Hryn'ova⁴, P.J. Hsu⁸¹,
 S.-C. Hsu¹⁴, G.S. Huang¹¹¹, Z. Hubacek¹²⁷,
 F. Hubaut⁸³, F. Huegging²⁰, T.B. Huffman¹¹⁸,
 E.W. Hughes³⁴, G. Hughes⁷¹, R.E. Hughes-Jones⁸²,
 M. Huhtinen²⁹, P. Hurst⁵⁷, M. Hurwitz¹⁴,
 U. Husemann⁴¹, N. Huseynov^{65,m}, J. Huston⁸⁸,
 J. Huth⁵⁷, G. Iacobucci⁴⁹, G. Iakovidis⁹, M. Ibbotson⁸²,
 I. Ibragimov¹⁴¹, R. Ichimiya⁶⁷,
 L. Iconomidou-Fayard¹¹⁵, J. Idarraga¹¹⁵,
 P. Iengo^{102a,102b}, O. Igonkina¹⁰⁵, Y. Ikegami⁶⁶,
 M. Ikeno⁶⁶, Y. Ilchenko³⁹, D. Iliadis¹⁵⁴, D. Imbault⁷⁸,
 M. Imori¹⁵⁵, T. Ince²⁰, J. Inigo-Golfín²⁹, P. Ioannou⁸,
 M. Iodice^{134a}, A. Irls Quiles¹⁶⁷, C. Isaksson¹⁶⁶,
 A. Ishikawa⁶⁷, M. Ishino⁶⁸, R. Ishmukhametov³⁹,
 C. Issever¹¹⁸, S. Istin^{18a}, A.V. Ivashin¹²⁸, W. Iwanski³⁸,
 H. Iwasaki⁶⁶, J.M. Izen⁴⁰, V. Izzo^{102a}, B. Jackson¹²⁰,
 J.N. Jackson⁷³, P. Jackson¹⁴³, M.R. Jaekel²⁹, V. Jain⁶¹,
 K. Jakobs⁴⁸, S. Jakobsen³⁵, J. Jakubek¹²⁷,
 D.K. Jana¹¹¹, E. Jankowski¹⁵⁸, E. Jansen⁷⁷,
 A. Jantsch⁹⁹, M. Janus²⁰, G. Jarlskog⁷⁹, L. Jeanty⁵⁷,
 K. Jelen³⁷, I. Jen-La Plante³⁰, P. Jenni²⁹, A. Jeremie⁴,
 P. Jež³⁵, S. Jézéquel⁴, M.K. Jha^{19a}, H. Ji¹⁷², W. Ji⁸¹,
 J. Jia¹⁴⁸, Y. Jiang^{32b}, M. Jimenez Belenguer⁴¹,
 G. Jin^{32b}, S. Jin^{32a}, O. Jinnouchi¹⁵⁷,
 M.D. Joergensen³⁵, D. Joffe³⁹, L.G. Johansen¹³,
 M. Johansen^{146a,146b}, K.E. Johansson^{146a},
 P. Johansson¹³⁹, S. Johnert⁴¹, K.A. Johns⁶,
 K. Jon-And^{146a,146b}, G. Jones⁸², R.W.L. Jones⁷¹,
 T.W. Jones⁷⁷, T.J. Jones⁷³, O. Jonsson²⁹, C. Joram²⁹,
 P.M. Jorge^{124a,b}, J. Joseph¹⁴, T. Jovin^{12b}, X. Ju¹³⁰,
 C.A. Jung⁴², V. Juranek¹²⁵, P. Jussel⁶²,
 A. Juste Rozas¹¹, V.V. Kabachenko¹²⁸, S. Kabana¹⁶,
 M. Kaci¹⁶⁷, A. Kaczmarek³⁸, P. Kadlecik³⁵,
 M. Kado¹¹⁵, H. Kagan¹⁰⁹, M. Kagan⁵⁷, S. Kaiser⁹⁹,
 E. Kajomovitz¹⁵², S. Kalinin¹⁷⁴, L.V. Kalinovskaya⁶⁵,
 S. Kama³⁹, N. Kanaya¹⁵⁵, M. Kaneda²⁹, T. Kanno¹⁵⁷,
 V.A. Kantserov⁹⁶, J. Kanzaki⁶⁶, B. Kaplan¹⁷⁵,
 A. Kapliy³⁰, J. Kaplon²⁹, D. Kar⁴³, M. Karagoz¹¹⁸,
 M. Karnevskiy⁴¹, K. Karr⁵, V. Kartvelishvili⁷¹,
 A.N. Karyukhin¹²⁸, L. Kashif¹⁷², G. Kasieczka^{58b},
 A. Kasmi³⁹, R.D. Kass¹⁰⁹, A. Kastanas¹³, M. Kataoka⁴,
 Y. Kataoka¹⁵⁵, E. Katsoufis⁹, J. Katzy⁴¹, V. Kaushik⁶,
 K. Kawagoe⁶⁷, T. Kawamoto¹⁵⁵, G. Kawamura⁸¹,
 M.S. Kayl¹⁰⁵, V.A. Kazanin¹⁰⁷, M.Y. Kazarinov⁶⁵,
 J.R. Keates⁸², R. Keeler¹⁶⁹, R. Kehoe³⁹, M. Keil⁵⁴,
 G.D. Kekelidze⁶⁵, J. Kennedy⁹⁸, C.J. Kenney¹⁴³,
 M. Kenyon⁵³, O. Kepka¹²⁵, N. Kerschen²⁹,
 B.P. Kerševan⁷⁴, S. Kersten¹⁷⁴, K. Kessoku¹⁵⁵,
 J. Keung¹⁵⁸, M. Khakzad²⁸, F. Khalil-zada¹⁰,
 H. Khandanyan¹⁶⁵, A. Khanov¹¹², D. Kharchenko⁶⁵,
 A. Khodinov⁹⁶, A.G. Kholodenko¹²⁸, A. Khomich^{58a},
 T.J. Khoo²⁷, G. Khoriali²⁰, A. Khoroshilov¹⁷⁴,
 N. Khovanskiy⁶⁵, V. Khovanskiy⁹⁵, E. Khramov⁶⁵,
 J. Khubua^{51b}, H. Kim⁷, M.S. Kim², P.C. Kim¹⁴³,
 S.H. Kim¹⁶⁰, N. Kimura¹⁷⁰, O. Kind¹⁵, B.T. King⁷³,
 M. King⁶⁷, R.S.B. King¹¹⁸, J. Kirk¹²⁹, L.E. Kirsch²²,
 A.E. Kiryunin⁹⁹, T. Kishimoto⁶⁷, D. Kisielewska³⁷,
 T. Kittelmann¹²³, A.M. Kiver¹²⁸, E. Kladiva^{144b},
 J. Klaiber-Lodewigs⁴², M. Klein⁷³, U. Klein⁷³,
 K. Kleinknecht⁸¹, M. Klemetti⁸⁵, A. Klier¹⁷¹,
 A. Klimentov²⁴, R. Klingenberg⁴², E.B. Klinkby³⁵,
 T. Klioutchnikova²⁹, P.F. Klok¹⁰⁴, S. Klous¹⁰⁵,
 E.-E. Kluge^{58a}, T. Kluge⁷³, P. Kluit¹⁰⁵, S. Kluth⁹⁹,
 N.S. Knecht¹⁵⁸, E. Kneringer⁶², J. Knobloch²⁹,
 E.B.F.G. Knoops⁸³, A. Knue⁵⁴, B.R. Ko⁴⁴,
 T. Kobayashi¹⁵⁵, M. Kobel⁴³, M. Kocian¹⁴³,
 P. Kodys¹²⁶, K. Köneke²⁹, A.C. König¹⁰⁴, S. Koenig⁸¹,
 L. Köpke⁸¹, F. Koetsveld¹⁰⁴, P. Koevesarki²⁰,
 T. Koffas²⁸, E. Koffeman¹⁰⁵, F. Kohn⁵⁴, Z. Kohout¹²⁷,
 T. Kohriki⁶⁶, T. Koi¹⁴³, T. Kokott²⁰, G.M. Kolachev¹⁰⁷,
 H. Kolanoski¹⁵, V. Kolesnikov⁶⁵, I. Koletsou^{89a},
 J. Koll⁸⁸, D. Kollar²⁹, M. Kollerfrath⁴⁸, S.D. Kolya⁸²,
 A.A. Komar⁹⁴, Y. Komori¹⁵⁵, T. Kondo⁶⁶, T. Kono^{41,n},
 A.I. Kononov⁴⁸, R. Konoplich^{108,o}, N. Konstantinidis⁷⁷,
 A. Kootz¹⁷⁴, S. Koperny³⁷, S.V. Kopikov¹²⁸,
 K. Korcyl³⁸, K. Kordas¹⁵⁴, V. Koreshev¹²⁸, A. Korn¹¹⁸,
 A. Korol¹⁰⁷, I. Korolkov¹¹, E.V. Korolkova¹³⁹,
 V.A. Korotkov¹²⁸, O. Kortner⁹⁹, S. Kortner⁹⁹,
 V.V. Kostyukhin²⁰, M.J. Kotamäki²⁹, S. Kotov⁹⁹,
 V.M. Kotov⁶⁵, A. Kotwal⁴⁴, C. Kourkoumelis⁸,
 V. Kouskoura¹⁵⁴, A. Koutsman^{159a}, R. Kowalewski¹⁶⁹,
 T.Z. Kowalski³⁷, W. Kozanecki¹³⁶, A.S. Kozhin¹²⁸,
 V. Kral¹²⁷, V.A. Kramarenko⁹⁷, G. Kramberger⁷⁴,
 M.W. Krasny⁷⁸, A. Krasznahorkay¹⁰⁸, J. Kraus⁸⁸,
 J.K. Kraus²⁰, A. Kreisel¹⁵³, F. Krejci¹²⁷,
 J. Kretschmar⁷³, N. Krieger⁵⁴, P. Krieger¹⁵⁸,
 K. Kroeninger⁵⁴, H. Kroha⁹⁹, J. Kroll¹²⁰,
 J. Kroseberg²⁰, J. Krstic^{12a}, U. Kruchonak⁶⁵,
 H. Krüger²⁰, T. Kruker¹⁶, N. Krumnack⁶⁴,
 Z.V. Krumshteyn⁶⁵, A. Kruth²⁰, T. Kubota⁸⁶,
 S. Kuehn⁴⁸, A. Kugel^{58c}, T. Kuhl⁴¹, D. Kuhn⁶²,
 V. Kukhtin⁶⁵, Y. Kulchitsky⁹⁰, S. Kuleshov^{31b},
 C. Kummer⁹⁸, M. Kuna⁷⁸, N. Kundu¹¹⁸, J. Kunkle¹²⁰,
 A. Kupco¹²⁵, H. Kurashige⁶⁷, M. Kurata¹⁶⁰,
 Y.A. Kurochkin⁹⁰, V. Kus¹²⁵, M. Kuze¹⁵⁷, J. Kvita²⁹,

- R. Kwee¹⁵, A. La Rosa⁴⁹, L. La Rotonda^{36a,36b},
L. Labarga⁸⁰, J. Labbe⁴, S. Lablak^{135a}, C. Lacasta¹⁶⁷,
F. Lacava^{132a,132b}, H. Lacker¹⁵, D. Lacour⁷⁸,
V.R. Lacuesta¹⁶⁷, E. Ladygin⁶⁵, R. Lafaye⁴,
B. Laforge⁷⁸, T. Lagouri⁸⁰, S. Lai⁴⁸, E. Laisne⁵⁵,
M. Lamanna²⁹, C.L. Lampen⁶, W. Lamp¹⁶,
E. Lancon¹³⁶, U. Landgraf⁴⁸, M.P.J. Landon⁷⁵,
H. Landsman¹⁵², J.L. Lane⁸², C. Lange⁴¹,
A.J. Lankford¹⁶³, F. Lanni²⁴, K. Lantzschi¹⁷⁴,
S. Laplace⁷⁸, C. Lapoire²⁰, J.F. Laporte¹³⁶, T. Lari^{89a},
A.V. Larionov¹²⁸, A. Lerner¹¹⁸, C. Lasseur²⁹,
M. Lassnig²⁹, P. Laurelli⁴⁷, W. Lavrijsen¹⁴,
P. Laycock⁷³, A.B. Lazarev⁶⁵, O. Le Dortz⁷⁸,
E. Le Guirrec⁸³, C. Le Maner¹⁵⁸, E. Le Menedeu¹³⁶,
C. Lebel⁹³, T. LeCompte⁵, F. Ledroit-Guillon⁵⁵,
H. Lee¹⁰⁵, J.S.H. Lee¹¹⁶, S.C. Lee¹⁵¹, L. Lee¹⁷⁵,
M. Lefebvre¹⁶⁹, M. Legendre¹³⁶, A. Leger⁴⁹,
B.C. LeGeyt¹²⁰, F. Legger⁹⁸, C. Leggett¹⁴,
M. Lehmacher²⁰, G. Lehmann Miotto²⁹, X. Lei⁶,
M.A.L. Leite^{23d}, R. Leitner¹²⁶, D. Lellouch¹⁷¹,
M. Leltchouk³⁴, B. Lemmer⁵⁴, V. Lendermann^{58a},
K.J.C. Leney^{145b}, T. Lenz¹⁰⁵, G. Lenzen¹⁷⁴, B. Lenzi²⁹,
K. Leonhardt⁴³, S. Leontsinis⁹, C. Leroy⁹³,
J.-R. Lessard¹⁶⁹, J. Lesser^{146a}, C.G. Lester²⁷,
A. Leung Fook Cheong¹⁷², J. Levêque⁴, D. Levin⁸⁷,
L.J. Levinson¹⁷¹, M.S. Levitski¹²⁸, A. Lewis¹¹⁸,
G.H. Lewis¹⁰⁸, A.M. Leyko²⁰, M. Leyton¹⁵, B. Li⁸³,
H. Li¹⁷², S. Li^{32b,p}, X. Li⁸⁷, Z. Liang³⁹, Z. Liang^{118,q},
H. Liao³³, B. Liberti^{133a}, P. Lichard²⁹,
M. Lichtnecker⁹⁸, K. Lie¹⁶⁵, W. Liebig¹³, R. Lifshitz¹⁵²,
J.N. Lilley¹⁷, C. Limbach²⁰, A. Limosani⁸⁶,
M. Limper⁶³, S.C. Lin^{151,r}, F. Linde¹⁰⁵,
J.T. Linnemann⁸⁸, E. Lipeles¹²⁰, L. Lipinsky¹²⁵,
A. Lipniacka¹³, T.M. Liss¹⁶⁵, D. Lissauer²⁴, A. Lister⁴⁹,
A.M. Litke¹³⁷, C. Liu²⁸, D. Liu^{151,s}, H. Liu⁸⁷,
J.B. Liu⁸⁷, M. Liu^{32b}, S. Liu², Y. Liu^{32b},
M. Livan^{119a,119b}, S.S.A. Livermore¹¹⁸, A. Lleres⁵⁵,
J. Llorente Merino⁸⁰, S.L. Lloyd⁷⁵, E. Lobodzinska⁴¹,
P. Loch⁶, W.S. Lockman¹³⁷, T. Loddenkoetter²⁰,
F.K. Loebinger⁸², A. Loginov¹⁷⁵, C.W. Loh¹⁶⁸,
T. Lohse¹⁵, K. Lohwasser⁴⁸, M. Lokajicek¹²⁵,
J. Loken¹¹⁸, V.P. Lombardo⁴, R.E. Long⁷¹,
L. Lopes^{124a,b}, D. Lopez Mateos⁵⁷, M. Losada¹⁶²,
P. Loscutoff¹⁴, F. Lo Sterzo^{132a,132b}, M.J. Losty^{159a},
X. Lou⁴⁰, A. Lounis¹¹⁵, K.F. Loureiro¹⁶², J. Love²¹,
P.A. Love⁷¹, A.J. Lowe^{143,e}, F. Lu^{32a}, H.J. Lubatti¹³⁸,
C. Luci^{132a,132b}, A. Lucotte⁵⁵, A. Ludwig⁴³,
D. Ludwig⁴¹, I. Ludwig⁴⁸, J. Ludwig⁴⁸, F. Luehring⁶¹,
G. Luijckx¹⁰⁵, D. Lumb⁴⁸, L. Luminari^{132a}, E. Lund¹¹⁷,
B. Lund-Jensen¹⁴⁷, B. Lundberg⁷⁹,
J. Lundberg^{146a,146b}, J. Lundquist³⁵, M. Lungwitz⁸¹,
G. Lutz⁹⁹, D. Lynn²⁴, J. Lys¹⁴, E. Lytken⁷⁹, H. Ma²⁴,
L.L. Ma¹⁷², J.A. Macana Goia⁹³, G. Maccarrone⁴⁷,
A. Macchiolo⁹⁹, B. Maček⁷⁴, J. Machado Miguens^{124a},
R. Mackeprang³⁵, R.J. Madaras¹⁴, W.F. Mader⁴³,
R. Maenner^{58c}, T. Maeno²⁴, P. Mättig¹⁷⁴, S. Mättig⁴¹,
L. Magnoni²⁹, E. Magradze⁵⁴, Y. Mahalalel¹⁵³,
K. Mahboubi⁴⁸, G. Mahout¹⁷, C. Maiani^{132a,132b},
C. Maidantchik^{23a}, A. Maio^{124a,b}, S. Majewski²⁴,
Y. Makida⁶⁶, N. Makovec¹¹⁵, P. Mal¹³⁶, Pa. Malecki³⁸,
P. Malecki³⁸, V.P. Maleev¹²¹, F. Malek⁵⁵, U. Mallik⁶³,
D. Malon⁵, C. Malone¹⁴³, S. Maltezos⁹, V. Malyshev¹⁰⁷,
S. Malyukov²⁹, R. Mameghani⁹⁸, J. Mamuzic^{12b},
A. Manabe⁶⁶, L. Mandelli^{89a}, I. Mandić⁷⁴,
R. Mandrysch¹⁵, J. Maneira^{124a}, P.S. Mangeard⁸⁸,
I.D. Manjavidze⁶⁵, A. Mann⁵⁴, P.M. Manning¹³⁷,
A. Manousakis-Katsikakis⁸, B. Mansoulie¹³⁶,
A. Manz⁹⁹, A. Mapelli²⁹, L. Mapelli²⁹, L. March⁸⁰,
J.F. Marchand²⁹, F. Marchese^{133a,133b}, G. Marchiori⁷⁸,
M. Marcisovsky¹²⁵, A. Marin^{21,*}, C.P. Marino¹⁶⁹,
F. Marroquim^{23a}, R. Marshall⁸², Z. Marshall²⁹,
F.K. Martens¹⁵⁸, S. Marti-Garcia¹⁶⁷, A.J. Martin¹⁷⁵,
B. Martin²⁹, B. Martin⁸⁸, F.F. Martin¹²⁰,
J.P. Martin⁹³, Ph. Martin⁵⁵, T.A. Martin¹⁷,
V.J. Martin⁴⁵, B. Martin dit Latour⁴⁹,
S. Martin-Haugh¹⁴⁹, M. Martinez¹¹,
V. Martinez Outschoorn⁵⁷, A.C. Martyniuk⁸²,
M. Marx⁸², F. Marzano^{132a}, A. Marzin¹¹¹, L. Masetti⁸¹,
T. Mashimo¹⁵⁵, R. Mashinistov⁹⁴, J. Masik⁸²,
A.L. Maslennikov¹⁰⁷, I. Massa^{19a,19b}, G. Massaro¹⁰⁵,
N. Massol⁴, P. Mastrandrea^{132a,132b},
A. Mastroberardino^{36a,36b}, T. Masubuchi¹⁵⁵,
M. Mathes²⁰, H. Matsumoto¹⁵⁵, H. Matsunaga¹⁵⁵,
T. Matsushita⁶⁷, C. Mattravers^{118,c}, J.M. Maugain²⁹,
J. Maurer⁸³, S.J. Maxfield⁷³, D.A. Maximov¹⁰⁷,
E.N. May⁵, A. Mayne¹³⁹, R. Mazini¹⁵¹, M. Mazur²⁰,
M. Mazzanti^{89a}, E. Mazzoni^{122a,122b}, S.P. Mc Kee⁸⁷,
A. McCarn¹⁶⁵, R.L. McCarthy¹⁴⁸, T.G. McCarthy²⁸,
N.A. McCubbin¹²⁹, K.W. McFarlane⁵⁶,
J.A. Mcfayden¹³⁹, H. McGlone⁵³, G. Mchedlidze^{51b},
R.A. McLaren²⁹, T. Mclaughlan¹⁷, S.J. McMahon¹²⁹,
R.A. McPherson^{169,i}, A. Meade⁸⁴, J. Mechnich¹⁰⁵,
M. Mechtel¹⁷⁴, M. Medinnis⁴¹, R. Meera-Lebbai¹¹¹,
T. Meguro¹¹⁶, R. Mehdiyev⁹³, S. Mehlhase³⁵,
A. Mehta⁷³, K. Meier^{58a}, B. Meirose⁷⁹,
C. Melachrinou³⁰, B.R. Mellado Garcia¹⁷²,
L. Mendoza Navas¹⁶², Z. Meng^{151,s},
A. Mengarelli^{19a,19b}, S. Menke⁹⁹, C. Menot²⁹,
E. Meoni¹¹, K.M. Mercurio⁵⁷, P. Mermod¹¹⁸,
L. Merola^{102a,102b}, C. Meroni^{89a}, F.S. Merritt³⁰,
A. Messina²⁹, J. Metcalfe¹⁰³, A.S. Mete⁶⁴, C. Meyer⁸¹,
C. Meyer³⁰, J.-P. Meyer¹³⁶, J. Meyer¹⁷³, J. Meyer⁵⁴,
T.C. Meyer²⁹, W.T. Meyer⁶⁴, J. Miao^{32d}, S. Michal²⁹,
L. Micu^{25a}, R.P. Middleton¹²⁹, P. Miele²⁹, S. Migas⁷³,
L. Mijović⁴¹, G. Mikenberg¹⁷¹, M. Mikestikova¹²⁵,
M. Mikuz⁷⁴, D.W. Miller³⁰, R.J. Miller⁸⁸, W.J. Mills¹⁶⁸,
C. Mills⁵⁷, A. Milov¹⁷¹, D.A. Milstead^{146a,146b},
D. Milstein¹⁷¹, A.A. Minaenko¹²⁸, M. Miñano¹⁶⁷,
I.A. Minashvili⁶⁵, A.I. Mincer¹⁰⁸, B. Mindur³⁷,
M. Mineev⁶⁵, Y. Ming¹³⁰, L.M. Mir¹¹, G. Mirabelli^{132a},
L. Miralles Verge¹¹, A. Misiejuk⁷⁶, J. Mitrevski¹³⁷,
G.Y. Mitrofanov¹²⁸, V.A. Mitsou¹⁶⁷, S. Mitsui⁶⁶,
P.S. Miyagawa¹³⁹, K. Miyazaki⁶⁷, J.U. Mjörnmark⁷⁹,
T. Moa^{146a,146b}, P. Mockett¹³⁸, S. Moed⁵⁷,
V. Moeller²⁷, K. Mönig⁴¹, N. Möser²⁰, S. Mohapatra¹⁴⁸,
W. Mohr⁴⁸, S. Mohr dieck-Möck⁹⁹, A.M. Moiseev^{128,*},

- R. Moles-Valls¹⁶⁷, J. Molina-Perez²⁹, J. Monk⁷⁷, E. Monnier⁸³, S. Montesano^{89a,89b}, F. Monticelli⁷⁰, S. Monzani^{19a,19b}, R.W. Moore², G.F. Moorhead⁸⁶, C. Mora Herrera⁴⁹, A. Moraes⁵³, N. Morange¹³⁶, J. Morel⁵⁴, G. Morello^{36a,36b}, D. Moreno⁸¹, M. Moreno Llácer¹⁶⁷, P. Moretini^{50a}, M. Morii⁵⁷, J. Morin⁷⁵, A.K. Morley²⁹, G. Mornacchi²⁹, S.V. Morozov⁹⁶, J.D. Morris⁷⁵, L. Morvaj¹⁰¹, H.G. Moser⁹⁹, M. Mosidze^{51b}, J. Moss¹⁰⁹, R. Mount¹⁴³, E. Mountricha¹³⁶, S.V. Mouraviev⁹⁴, E.J.W. Moyse⁸⁴, M. Mudrinic^{12b}, F. Mueller^{58a}, J. Mueller¹²³, K. Mueller²⁰, T.A. Müller⁹⁸, D. Muenstermann²⁹, A. Muir¹⁶⁸, Y. Munwes¹⁵³, W.J. Murray¹²⁹, I. Mussche¹⁰⁵, E. Musto^{102a,102b}, A.G. Myagkov¹²⁸, M. Myska¹²⁵, J. Nadal¹¹, K. Nagai¹⁶⁰, K. Nagano⁶⁶, Y. Nagasaka⁶⁰, A.M. Nairz²⁹, Y. Nakahama²⁹, K. Nakamura¹⁵⁵, T. Nakamura¹⁵⁵, I. Nakano¹¹⁰, G. Nanava²⁰, A. Napier¹⁶¹, M. Nash^{77,c}, N.R. Nation²¹, T. Nattermann²⁰, T. Naumann⁴¹, G. Navarro¹⁶², H.A. Neal⁸⁷, E. Nebot⁸⁰, P.Yu. Nechaeva⁹⁴, A. Negri^{119a,119b}, G. Negri²⁹, S. Nektarijevic⁴⁹, A. Nelson¹⁶³, S. Nelson¹⁴³, T.K. Nelson¹⁴³, S. Nemecek¹²⁵, P. Nemethy¹⁰⁸, A.A. Nepomuceno^{23a}, M. Nessi^{29,t}, M.S. Neubauer¹⁶⁵, A. Neusiedl⁸¹, R.M. Neves¹⁰⁸, P. Nevski²⁴, P.R. Newman¹⁷, V. Nguyen Thi Hong¹³⁶, R.B. Nickerson¹¹⁸, R. Nicolaidou¹³⁶, L. Nicolas¹³⁹, B. Nicquevert²⁹, F. Niedercorn¹¹⁵, J. Nielsen¹³⁷, T. Niimikoski²⁹, N. Nikiforou³⁴, A. Nikiforov¹⁵, V. Nikolaenko¹²⁸, K. Nikolaev⁶⁵, I. Nikolic-Audit⁷⁸, K. Nikolics⁴⁹, K. Nikolopoulos²⁴, H. Nilsen⁴⁸, P. Nilsson⁷, Y. Ninomiya¹⁵⁵, A. Nisati^{132a}, T. Nishiyama⁶⁷, R. Nisius⁹⁹, L. Nodulman⁵, M. Nomachi¹¹⁶, I. Nomidis¹⁵⁴, M. Nordberg²⁹, B. Nordkvist^{146a,146b}, P.R. Norton¹²⁹, J. Novakova¹²⁶, M. Nozaki⁶⁶, L. Nozka¹¹³, I.M. Nugent^{159a}, A.-E. Nuncio-Quiroz²⁰, G. Nunes Hanninger⁸⁶, T. Nunnemann⁹⁸, E. Nurse⁷⁷, T. Nyman²⁹, B.J. O'Brien⁴⁵, S.W. O'Neale^{17,*}, D.C. O'Neil¹⁴², V. O'Shea⁵³, F.G. Oakham^{28,d}, H. Oberlack⁹⁹, J. Ocariz⁷⁸, A. Ochi⁶⁷, S. Oda¹⁵⁵, S. Odaka⁶⁶, J. Odier⁸³, H. Ogren⁶¹, A. Oh⁸², S.H. Oh⁴⁴, C.C. Ohm^{146a,146b}, T. Ohshima¹⁰¹, H. Ohshita¹⁴⁰, T. Ohsugi⁵⁹, S. Okada⁶⁷, H. Okawa¹⁶³, Y. Okumura¹⁰¹, T. Okuyama¹⁵⁵, A. Olariu^{25a}, M. Olcese^{50a}, A.G. Olchevski⁶⁵, M. Oliveira^{124a,g}, D. Oliveira Damazio²⁴, E. Oliver Garcia¹⁶⁷, D. Olivito¹²⁰, A. Olszewski³⁸, J. Olszowska³⁸, C. Omachi⁶⁷, A. Onofre^{124a,u}, P.U.E. Onyisi³⁰, C.J. Oram^{159a}, M.J. Oreglia³⁰, Y. Oren¹⁵³, D. Orestano^{134a,134b}, I. Orlov¹⁰⁷, C. Oropeza Barrera⁵³, R.S. Orr¹⁵⁸, B. Osculati^{50a,50b}, R. Ospanov¹²⁰, C. Osuna¹¹, G. Otero y Garzon²⁶, J.P. Ottersbach¹⁰⁵, M. Ouchrif^{135d}, F. Ould-Saada¹¹⁷, A. Ouraou¹³⁶, Q. Ouyang^{32a}, M. Owen⁸², S. Owen¹³⁹, V.E. Ozcan^{18a}, N. Ozturk⁷, A. Pacheco Pages¹¹, C. Padilla Aranda¹¹, S. Pagan Griso¹⁴, E. Paganis¹³⁹, F. Paige²⁴, P. Pais⁸⁴, K. Pajchel¹¹⁷, G. Palacino^{159b}, C.P. Paleari⁶, S. Palestini²⁹, D. Pallin³³, A. Palma^{124a,b}, J.D. Palmer¹⁷, Y.B. Pan¹⁷², E. Panagiotopoulou⁹, B. Panes^{31a}, N. Panikashvili⁸⁷, S. Panitkin²⁴, D. Pantea^{25a}, M. Panuskova¹²⁵, V. Paolone¹²³, A. Papadelis^{146a}, Th.D. Papadopoulou⁹, A. Paramonov⁵, W. Park^{24,v}, M.A. Parker²⁷, F. Parodi^{50a,50b}, J.A. Parsons³⁴, U. Parzefall⁴⁸, E. Pasqualucci^{132a}, A. Passeri^{134a}, F. Pastore^{134a,134b}, Fr. Pastore⁷⁶, G. Pásztor^{49,w}, S. Patarraia¹⁷⁴, N. Patel¹⁵⁰, J.R. Pater⁸², S. Patricelli^{102a,102b}, T. Pauly²⁹, M. Pecsny^{144a}, M.I. Pedraza Morales¹⁷², S.V. Peleganchuk¹⁰⁷, H. Peng^{32b}, R. Pengo²⁹, A. Penson³⁴, J. Penwell⁶¹, M. Perantoni^{23a}, K. Perez^{34,x}, T. Perez Cavalcanti⁴¹, E. Perez Codina¹¹, M.T. Pérez García-Estañ¹⁶⁷, V. Perez Reale³⁴, L. Perini^{89a,89b}, H. Pernegger²⁹, R. Perrino^{72a}, P. Perrodo⁴, S. Perseme^{3a}, V.D. Peshekhonov⁶⁵, B.A. Petersen²⁹, J. Petersen²⁹, T.C. Petersen³⁵, E. Petit⁸³, A. Petridis¹⁵⁴, C. Petridou¹⁵⁴, E. Petrolo^{132a}, F. Petrucci^{134a,134b}, D. Petschull⁴¹, M. Petteni¹⁴², R. Pezoa^{31b}, A. Phan⁸⁶, A.W. Phillips²⁷, P.W. Phillips¹²⁹, G. Piacquadio²⁹, E. Piccaro⁷⁵, M. Piccinini^{19a,19b}, S.M. Piec⁴¹, R. Piegai²⁶, J.E. Pilcher³⁰, A.D. Pilkington⁸², J. Pina^{124a,b}, M. Pinamonti^{164a,164c}, A. Pinder¹¹⁸, J.L. Pinfold², J. Ping^{32c}, B. Pinto^{124a,b}, O. Pirotte²⁹, C. Pizio^{89a,89b}, R. Placakyte⁴¹, M. Plamondon¹⁶⁹, M.-A. Pleier²⁴, A.V. Pleskach¹²⁸, A. Poblaguev²⁴, S. Poddar^{58a}, F. Podlyski³³, L. Poggioli¹¹⁵, T. Poghosyan²⁰, M. Pohl⁴⁹, F. Polci⁵⁵, G. Polesello^{119a}, A. Policicchio¹³⁸, A. Polini^{19a}, J. Poll⁷⁵, V. Polychronakos²⁴, D.M. Pomarede¹³⁶, D. Pomeroy²², K. Pommès²⁹, L. Pontecorvo^{132a}, B.G. Pope⁸⁸, G.A. Popeneciu^{25a}, D.S. Popovic^{12a}, A. Poppleton²⁹, X. Portell Bueso²⁹, C. Posch²¹, G.E. Pospelov⁹⁹, S. Pospisil¹²⁷, I.N. Potrap⁹⁹, C.J. Potter¹⁴⁹, C.T. Potter¹¹⁴, G. Poulard²⁹, J. Poveda¹⁷², R. Prabhu⁷⁷, P. Pralavorio⁸³, A. Pranko¹⁴, S. Prasad⁵⁷, R. Pravahan⁷, S. Prell⁶⁴, K. Pretzl¹⁶, L. Pribyl²⁹, D. Price⁶¹, L.E. Price⁵, M.J. Price²⁹, D. Prieur¹²³, M. Primavera^{72a}, K. Prokofiev¹⁰⁸, F. Prokoshin^{31b}, S. Protopopescu²⁴, J. Proudfoot⁵, X. Prudent⁴³, H. Przysieznik⁴, S. Psoroula²⁰, E. Ptacek¹¹⁴, E. Pueschel⁸⁴, J. Purdham⁸⁷, M. Purohit^{24,v}, P. Puzo¹¹⁵, Y. Pylypchenko¹¹⁷, J. Qian⁸⁷, Z. Qian⁸³, Z. Qin⁴¹, A. Quadt⁵⁴, D.R. Quarrie¹⁴, W.B. Quayle¹⁷², F. Quinonez^{31a}, M. Raas¹⁰⁴, V. Radescu^{58b}, B. Radics²⁰, T. Rador^{18a}, F. Ragusa^{89a,89b}, G. Rahal¹⁷⁷, A.M. Rahimi¹⁰⁹, D. Rahm²⁴, S. Rajagopalan²⁴, M. Rammensee⁴⁸, M. Rammes¹⁴¹, M. Ramstedt^{146a,146b}, A.S. Randle-Conde³⁹, K. Randrianarivony²⁸, P.N. Ratoff⁷¹, F. Rauscher⁹⁸, M. Raymond²⁹, A.L. Read¹¹⁷, D.M. Rebuffi^{119a,119b}, A. Redelbach¹⁷³, G. Redlinger²⁴, R. Reece¹²⁰, K. Reeves⁴⁰, A. Reichold¹⁰⁵, E. Reinherz-Aronis¹⁵³, A. Reinsch¹¹⁴, I. Reisinger⁴², D. Reljic^{12a}, C. Rembser²⁹, Z.L. Ren¹⁵¹, A. Renaud¹¹⁵, P. Renkel³⁹, M. Rescigno^{132a}, S. Resconi^{89a}, B. Resende¹³⁶, P. Reznicek⁹⁸, R. Rezvani¹⁵⁸, A. Richards⁷⁷,

- R. Richter⁹⁹, E. Richter-Was^{4,y}, M. Ridel⁷⁸,
M. Rijpstra¹⁰⁵, M. Rijssenbeek¹⁴⁸, A. Rimoldi^{119a,119b},
L. Rinaldi^{19a}, R.R. Rios³⁹, I. Riu¹¹, G. Rivoltella^{89a,89b},
F. Rizatdinova¹¹², E. Rizvi⁷⁵, S.H. Robertson^{85,i},
A. Robichaud-Veronneau¹¹⁸, D. Robinson²⁷,
J.E.M. Robinson⁷⁷, M. Robinson¹¹⁴, A. Robson⁵³,
J.G. Rocha de Lima¹⁰⁶, C. Roda^{122a,122b},
D. Roda Dos Santos²⁹, S. Rodier⁸⁰, D. Rodriguez¹⁶²,
A. Roe⁵⁴, S. Roe²⁹, O. Røhne¹¹⁷, V. Rojo¹, S. Rolli¹⁶¹,
A. Romaniouk⁹⁶, M. Romano^{19a,19b}, V.M. Romanov⁶⁵,
G. Romeo²⁶, L. Roos⁷⁸, E. Ros¹⁶⁷, S. Rosati^{132a,132b},
K. Rosbach⁴⁹, A. Rose¹⁴⁹, M. Rose⁷⁶,
G.A. Rosenbaum¹⁵⁸, E.I. Rosenberg⁶⁴,
P.L. Rosendahl¹³, O. Rosenthal¹⁴¹, L. Rosselet⁴⁹,
V. Rossetti¹¹, E. Rossi^{132a,132b}, L.P. Rossi^{50a},
M. Rotaru^{25a}, I. Roth¹⁷¹, J. Rothberg¹³⁸,
D. Rousseau¹¹⁵, C.R. Royon¹³⁶, A. Rozanov⁸³,
Y. Rozen¹⁵², X. Ruan¹¹⁵, I. Rubinskiy⁴¹, B. Ruckert⁹⁸,
N. Ruckstuhl¹⁰⁵, V.I. Rud⁹⁷, C. Rudolph⁴³,
G. Rudolph⁶², F. Rühr⁶, F. Ruggieri^{134a,134b},
A. Ruiz-Martinez⁶⁴, V. Rumiantsev^{91,*},
L. Romyantsev⁶⁵, K. Runge⁴⁸, O. Runolfsson²⁰,
Z. Rurikova⁴⁸, N.A. Ruskovich⁶⁵, D.R. Rust⁶¹,
J.P. Rutherford⁶, C. Ruwiedel¹⁴, P. Ruzicka¹²⁵,
Y.F. Ryabov¹²¹, V. Ryadovikov¹²⁸, P. Ryan⁸⁸,
M. Rybar¹²⁶, G. Rybkin¹¹⁵, N.C. Ryder¹¹⁸, S. Rzaeva¹⁰,
A.F. Saavedra¹⁵⁰, I. Sadeh¹⁵³, H.F-W. Sadrozinski¹³⁷,
R. Sadykov⁶⁵, F. Safai Tehrani^{132a,132b},
H. Sakamoto¹⁵⁵, G. Salamanna⁷⁵, A. Salamon^{133a},
M. Saleem¹¹¹, D. Salihagic⁹⁹, A. Salnikov¹⁴³, J. Salt¹⁶⁷,
B.M. Salvachua Ferrando⁵, D. Salvatore^{36a,36b},
F. Salvatore¹⁴⁹, A. Salvucci¹⁰⁴, A. Salzburger²⁹,
D. Sampsonidis¹⁵⁴, B.H. Samset¹¹⁷, A. Sanchez^{102a,102b},
H. Sandaker¹³, H.G. Sander⁸¹, M.P. Sanders⁹⁸,
M. Sandhoff¹⁷⁴, T. Sandoval²⁷, C. Sandoval¹⁶²,
R. Sandstroem⁹⁹, S. Sandvoss¹⁷⁴, D.P.C. Sankey¹²⁹,
A. Sansoni⁴⁷, C. Santamarina Rios⁸⁵, C. Santoni³³,
R. Santonico^{133a,133b}, H. Santos^{124a}, J.G. Saraiva^{124a,b},
T. Sarangi¹⁷², E. Sarkisyan-Grinbaum⁷,
F. Sarri^{122a,122b}, G. Sartisohn¹⁷⁴, O. Sasaki⁶⁶,
T. Sasaki⁶⁶, N. Sasao⁶⁸, I. Satsounkevitch⁹⁰,
G. Sauvage⁴, E. Sauvan⁴, J.B. Sauvan¹¹⁵,
P. Savard^{158,d}, V. Savinov¹²³, D.O. Savu²⁹,
L. Sawyer^{24,k}, D.H. Saxon⁵³, L.P. SAYS³³, C. Sbarra^{19a},
A. Sbrizzi^{19a,19b}, O. Scallan⁹³, D.A. Scannicchio¹⁶³,
J. Schaarschmidt¹¹⁵, P. Schacht⁹⁹, U. Schäfer⁸¹,
S. Schaepe²⁰, S. Schaezel^{58b}, A.C. Schaffer¹¹⁵,
D. Schaile⁹⁸, R.D. Schamberger¹⁴⁸, A.G. Schamov¹⁰⁷,
V. Scharf^{58a}, V.A. Schegelsky¹²¹, D. Scheirich⁸⁷,
M. Schernau¹⁶³, M.I. Scherzer¹⁴, C. Schiavi^{50a,50b},
J. Schieck⁹⁸, M. Schioppa^{36a,36b}, S. Schlenker²⁹,
J.L. Schlereth⁵, E. Schmidt⁴⁸, K. Schmieden²⁰,
C. Schmitt⁸¹, S. Schmitt^{58b}, M. Schmitz²⁰,
A. Schöning^{58b}, M. Schott²⁹, D. Schouten^{159a},
J. Schovancova¹²⁵, M. Schram⁸⁵, C. Schroeder⁸¹,
N. Schroer^{58c}, S. Schuh²⁹, G. Schuler²⁹, J. Schultes¹⁷⁴,
H.-C. Schultz-Coulon^{58a}, H. Schulz¹⁵,
J.W. Schumacher²⁰, M. Schumacher⁴⁸,
B.A. Schumm¹³⁷, Ph. Schune¹³⁶, C. Schwanenberger⁸²,
A. Schwartzman¹⁴³, Ph. Schwemling⁷⁸,
R. Schwienhorst⁸⁸, R. Schwierz⁴³, J. Schwindling¹³⁶,
T. Schwindt²⁰, W.G. Scott¹²⁹, J. Searcy¹¹⁴, G. Sedov⁴¹,
E. Sedykh¹²¹, E. Segura¹¹, S.C. Seidel¹⁰³, A. Seiden¹³⁷,
F. Seifert⁴³, J.M. Seixas^{23a}, G. Sekhniaidze^{102a},
D.M. Seliverstov¹²¹, B. Sellden^{146a}, G. Sellers⁷³,
M. Seman^{144b}, N. Semprini-Cesari^{19a,19b}, C. Serfon⁹⁸,
L. Serin¹¹⁵, R. Seuster⁹⁹, H. Severini¹¹¹, M.E. Seviror⁸⁶,
A. Sfyrila²⁹, E. Shabalina⁵⁴, M. Shamim¹¹⁴,
L.Y. Shan^{32a}, J.T. Shank²¹, Q.T. Shao⁸⁶, M. Shapiro¹⁴,
P.B. Shatalov⁹⁵, L. Shaver⁶, K. Shaw^{164a,164c},
D. Sherman¹⁷⁵, P. Sherwood⁷⁷, A. Shibata¹⁰⁸,
H. Shichi¹⁰¹, S. Shimizu²⁹, M. Shimojima¹⁰⁰, T. Shin⁵⁶,
M. Shiyakova⁶⁵, A. Shmeleva⁹⁴, M.J. Shochet³⁰,
D. Short¹¹⁸, S. Shrestha⁶⁴, M.A. Shupe⁶, P. Sicho¹²⁵,
A. Sidoti^{132a,132b}, A. Siebel¹⁷⁴, F. Siegert⁴⁸,
Dj. Sijacki^{12a}, O. Silbert¹⁷¹, J. Silva^{124a,b}, Y. Silver¹⁵³,
D. Silverstein¹⁴³, S.B. Silverstein^{146a}, V. Simak¹²⁷,
O. Simard¹³⁶, Lj. Simic^{12a}, S. Simion¹¹⁵, B. Simmons⁷⁷,
M. Simonyan³⁵, P. Sinervo¹⁵⁸, N.B. Sinev¹¹⁴,
V. Sipica¹⁴¹, G. Siragusa¹⁷³, A. Sircar²⁴,
A.N. Sisakyan⁶⁵, S.Yu. Sivoklokov⁹⁷, J. Sjölin^{146a,146b},
T.B. Skjursen¹³, L.A. Skinnari¹⁴, H.P. Skottowe⁵⁷,
K. Skovpen¹⁰⁷, P. Skubic¹¹¹, N. Skvorodnev²²,
M. Slater¹⁷, T. Slavicek¹²⁷, K. Sliwa¹⁶¹, J. Sloper²⁹,
V. Smakhtin¹⁷¹, S.Yu. Smirnov⁹⁶, L.N. Smirnova⁹⁷,
O. Smirnova⁷⁹, B.C. Smith⁵⁷, D. Smith¹⁴³,
K.M. Smith⁵³, M. Smizanska⁷¹, K. Smolek¹²⁷,
A.A. Snesarev⁹⁴, S.W. Snow⁸², J. Snow¹¹¹,
J. Snuverink¹⁰⁵, S. Snyder²⁴, M. Soares^{124a},
R. Sobie^{169,i}, J. Sodomka¹²⁷, A. Soffer¹⁵³,
C.A. Solans¹⁶⁷, M. Solar¹²⁷, J. Solc¹²⁷, E. Soldatov⁹⁶,
U. Soldevila¹⁶⁷, E. Solfaroli Camillocci^{132a,132b},
A.A. Solodkov¹²⁸, O.V. Solovyanov¹²⁸, J. Sondericker²⁴,
N. Soni², V. Sopko¹²⁷, B. Sopko¹²⁷, M. Sosebee⁷,
R. Soualah^{164a,164c}, A. Soukharev¹⁰⁷,
S. Spagnolo^{72a,72b}, F. Spanò⁷⁶, R. Spighi^{19a}, G. Spigo²⁹,
F. Spila^{132a,132b}, R. Spiwoks²⁹, M. Spousta¹²⁶,
T. Spreitzer¹⁵⁸, B. Spurlock⁷, R.D. St. Denis⁵³,
T. Stahl¹⁴¹, J. Stahlman¹²⁰, R. Stamen^{58a},
E. Stanecka³⁸, R.W. Stanek⁵, C. Stanescu^{134a},
S. Stapnes¹¹⁷, E.A. Starchenko¹²⁸, J. Stark⁵⁵,
P. Staroba¹²⁵, P. Starovoitov⁹¹, A. Staude⁹⁸,
P. Stavina^{144a}, G. Stavropoulos¹⁴, G. Steele⁵³,
P. Steinbach⁴³, P. Steinberg²⁴, I. Stekl¹²⁷, B. Stelzer¹⁴²,
H.J. Stelzer⁸⁸, O. Stelzer-Chilton^{159a}, H. Stenzel⁵²,
K. Stevenson⁷⁵, G.A. Stewart²⁹, J.A. Stillings²⁰,
M.C. Stockton²⁹, K. Stoerig⁴⁸, G. Stoica^{25a},
S. Stonjek⁹⁹, P. Strachota¹²⁶, A.R. Stradling⁷,
A. Straessner⁴³, J. Strandberg¹⁴⁷,
S. Strandberg^{146a,146b}, A. Strandlie¹¹⁷, M. Strang¹⁰⁹,
E. Strauss¹⁴³, M. Strauss¹¹¹, P. Strizenec^{144b},
R. Ströhmer¹⁷³, D.M. Strom¹¹⁴, J.A. Strong^{76,*},
R. Stroynowski³⁹, J. Strube¹²⁹, B. Stugu¹³,
I. Stumer^{24,*}, J. Stupak¹⁴⁸, P. Sturm¹⁷⁴, D.A. Soh^{151,q},
D. Su¹⁴³, H.S. Subramania², A. Succurro¹¹,
Y. Sugaya¹¹⁶, T. Sugimoto¹⁰¹, C. Suhr¹⁰⁶, K. Suita⁶⁷,

- M. Suk¹²⁶, V.V. Sulin⁹⁴, S. Sultansoy^{3d}, T. Sumida²⁹,
X. Sun⁵⁵, J.E. Sundermann⁴⁸, K. Suruliz¹³⁹,
S. Sushkov¹¹, G. Susinno^{36a,36b}, M.R. Sutton¹⁴⁹,
Y. Suzuki⁶⁶, Y. Suzuki⁶⁷, M. Svatos¹²⁵,
Yu.M. Sviridov¹²⁸, S. Swedish¹⁶⁸, I. Sykora^{144a},
T. Sykora¹²⁶, B. Szeless²⁹, J. Sánchez¹⁶⁷, D. Ta¹⁰⁵,
K. Tackmann⁴¹, A. Taffard¹⁶³, R. Tafirout^{159a},
N. Taiblum¹⁵³, Y. Takahashi¹⁰¹, H. Takai²⁴,
R. Takashima⁶⁹, H. Takeda⁶⁷, T. Takeshita¹⁴⁰,
M. Talby⁸³, A. Talyshev¹⁰⁷, M.C. Tamsett²⁴,
J. Tanaka¹⁵⁵, R. Tanaka¹¹⁵, S. Tanaka¹³¹, S. Tanaka⁶⁶,
Y. Tanaka¹⁰⁰, K. Tani⁶⁷, N. Tannoury⁸³,
G.P. Tappern²⁹, S. Tapprogge⁸¹, D. Tardif¹⁵⁸,
S. Tarem¹⁵², F. Tarrade²⁸, G.F. Tartarelli^{89a}, P. Tas¹²⁶,
M. Tasevsky¹²⁵, E. Tassi^{36a,36b}, M. Tatarkhanov¹⁴,
Y. Tayalati^{135d}, C. Taylor⁷⁷, F.E. Taylor⁹²,
G.N. Taylor⁸⁶, W. Taylor^{159b}, M. Teinturier¹¹⁵,
M. Teixeira Dias Castanheira⁷⁵, P. Teixeira-Dias⁷⁶,
K.K. Temming⁴⁸, H. Ten Kate²⁹, P.K. Teng¹⁵¹,
S. Terada⁶⁶, K. Terashi¹⁵⁵, J. Terron⁸⁰, M. Terwort^{41,n},
M. Testa⁴⁷, R.J. Teuscher^{158,i}, J. Thadome¹⁷⁴,
J. Therhaag²⁰, T. Thevenaux-Pelzer⁷⁸, M. Thioye¹⁷⁵,
S. Thoma⁴⁸, J.P. Thomas¹⁷, E.N. Thompson³⁴,
P.D. Thompson¹⁷, P.D. Thompson¹⁵⁸,
A.S. Thompson⁵³, E. Thomson¹²⁰, M. Thomson²⁷,
R.P. Thun⁸⁷, F. Tian³⁴, T. Tic¹²⁵, V.O. Tikhomirov⁹⁴,
Y.A. Tikhonov¹⁰⁷, P. Tipton¹⁷⁵,
F.J. Tique Aires Viegas²⁹, S. Tisserant⁸³, J. Tobias⁴⁸,
B. Toczek³⁷, T. Todorov⁴, S. Todorova-Nova¹⁶¹,
B. Toggerson¹⁶³, J. Tojo⁶⁶, S. Tokár^{144a},
K. Tokunaga⁶⁷, K. Tokushuku⁶⁶, K. Tollefson⁸⁸,
M. Tomoto¹⁰¹, L. Tompkins³⁰, K. Toms¹⁰³, G. Tong^{32a},
A. Tonoyan¹³, C. Topfel¹⁶, N.D. Topilin⁶⁵,
I. Torchiani²⁹, E. Torrence¹¹⁴, H. Torres⁷⁸, E. Torró
Pastor¹⁶⁷, J. Toth^{83,w}, F. Touchard⁸³, D.R. Tovey¹³⁹,
D. Traynor⁷⁵, T. Trefzger¹⁷³, L. Tremblet²⁹,
A. Tricoli²⁹, I.M. Trigger^{159a}, S. Trincaz-Duvoid⁷⁸,
T.N. Trinh⁷⁸, M.F. Tripiana⁷⁰, W. Trischuk¹⁵⁸,
A. Trivedi^{24,v}, B. Trocmé⁵⁵, C. Troncon^{89a},
M. Trottier-McDonald¹⁴², M. Trzebinski³⁸,
A. Trzupek³⁸, C. Tsarouchas²⁹, J.C.-L. Tseng¹¹⁸,
M. Tsiakiris¹⁰⁵, P.V. Tsiareshka⁹⁰, D. Tsionou⁴,
G. Tsipolitis⁹, V. Tsiskaridze⁴⁸, E.G. Tskhadadze^{51a},
I.I. Tsukerman⁹⁵, V. Tsulaia¹⁴, J.-W. Tsung²⁰,
S. Tsuno⁶⁶, D. Tsybychev¹⁴⁸, A. Tua¹³⁹,
A. Tudorache^{25a}, V. Tudorache^{25a}, J.M. Tuggle³⁰,
M. Turala³⁸, D. Turecek¹²⁷, I. Turk Cakir^{3e},
E. Turlay¹⁰⁵, R. Turra^{89a,89b}, P.M. Tuts³⁴,
A. Tykhonov⁷⁴, M. Tylmad^{146a,146b}, M. Tyndel¹²⁹,
H. Tyrvaainen²⁹, G. Tzanakos⁸, K. Uchida²⁰, I. Ueda¹⁵⁵,
R. Ueno²⁸, M. Ugland¹³, M. Uhlenbrock²⁰,
M. Uhrmacher⁵⁴, F. Ukegawa¹⁶⁰, G. Unal²⁹,
D.G. Underwood⁵, A. Undrus²⁴, G. Unel¹⁶³, Y. Unno⁶⁶,
D. Urbaniec³⁴, E. Urkovsky¹⁵³, G. Usai⁷,
M. Uslenghi^{119a,119b}, L. Vacavant⁸³, V. Vacek¹²⁷,
B. Vachon⁸⁵, S. Vahsen¹⁴, J. Valenta¹²⁵, P. Valente^{132a},
S. Valentinetti^{19a,19b}, S. Valkar¹²⁶,
E. Valladolid Gallego¹⁶⁷, S. Vallecorsa¹⁵²,
J.A. Valls Ferrer¹⁶⁷, H. van der Graaf¹⁰⁵,
E. van der Kraaij¹⁰⁵, R. Van Der Leeuw¹⁰⁵,
E. van der Poel¹⁰⁵, D. van der Ster²⁹, N. van Eldik⁸⁴,
P. van Gemmeren⁵, Z. van Kesteren¹⁰⁵,
I. van Vulpen¹⁰⁵, M. Vanadia⁹⁹, W. Vandelli²⁹,
G. Vandoni²⁹, A. Vaniachine⁵, P. Vankov⁴¹,
F. Vannucci⁷⁸, F. Varela Rodriguez²⁹, R. Vari^{132a},
D. Varouchas¹⁴, A. Vartapetian⁷, K.E. Varvell¹⁵⁰,
V.I. Vassilakopoulos⁵⁶, F. Vazeille³³, G. Vegni^{89a,89b},
J.J. Veillet¹¹⁵, C. Vellidis⁸, F. Veloso^{124a}, R. Veness²⁹,
S. Veneziano^{132a}, A. Ventura^{72a,72b}, D. Ventura¹³⁸,
M. Venturi⁴⁸, N. Venturi¹⁶, V. Vercesi^{119a},
M. Verducci¹³⁸, W. Verkerke¹⁰⁵, J.C. Vermeulen¹⁰⁵,
A. Vest⁴³, M.C. Vetterli^{142,d}, I. Vichou¹⁶⁵,
T. Vickey^{145b,z}, O.E. Vickey Boeriu^{145b},
G.H.A. Viehhauser¹¹⁸, S. Viel¹⁶⁸, M. Villa^{19a,19b},
M. Villaplana Perez¹⁶⁷, E. Vilucchi⁴⁷, M.G. Vinciter²⁸,
E. Vinek²⁹, V.B. Vinogradov⁶⁵, M. Virchaux^{136,*},
J. Virzi¹⁴, O. Vitells¹⁷¹, M. Viti⁴¹, I. Vivarelli⁴⁸,
F. Vives Vaque², S. Vlachos⁹, D. Vladoiu⁹⁸,
M. Vlasak¹²⁷, N. Vlasov²⁰, A. Vogel²⁰, P. Vokac¹²⁷,
G. Volpi⁴⁷, M. Volpi⁸⁶, G. Volpini^{89a},
H. von der Schmitt⁹⁹, J. von Loeben⁹⁹,
H. von Radziewski⁴⁸, E. von Toerne²⁰, V. Vorobel¹²⁶,
A.P. Vorobiev¹²⁸, V. Vorwerk¹¹, M. Vos¹⁶⁷, R. Voss²⁹,
T.T. Voss¹⁷⁴, J.H. Vossebeld⁷³, N. Vranjes^{12a},
M. Vranjes Milosavljevic¹⁰⁵, V. Vrba¹²⁵,
M. Vreeswijk¹⁰⁵, T. Vu Anh⁸¹, R. Vuillermet²⁹,
I. Vukotic¹¹⁵, W. Wagner¹⁷⁴, P. Wagner¹²⁰,
H. Wahlen¹⁷⁴, J. Wakabayashi¹⁰¹, J. Walbersloh⁴²,
S. Walch⁸⁷, J. Walder⁷¹, R. Walker⁹⁸, W. Walkowiak¹⁴¹,
R. Wall¹⁷⁵, P. Waller⁷³, C. Wang⁴⁴, H. Wang¹⁷²,
H. Wang^{32b,aa}, J. Wang¹⁵¹, J. Wang^{32d}, J.C. Wang¹³⁸,
R. Wang¹⁰³, S.M. Wang¹⁵¹, A. Warburton⁸⁵,
C.P. Ward²⁷, M. Warsinsky⁴⁸, P.M. Watkins¹⁷,
A.T. Watson¹⁷, M.F. Watson¹⁷, G. Watts¹³⁸,
S. Watts⁸², A.T. Waugh¹⁵⁰, B.M. Waugh⁷⁷, J. Weber⁴²,
M. Weber¹²⁹, M.S. Weber¹⁶, P. Weber⁵⁴,
A.R. Weidberg¹¹⁸, P. Weigell⁹⁹, J. Weingarten⁵⁴,
C. Weiser⁴⁸, H. Wellenstein²², P.S. Wells²⁹, M. Wen⁴⁷,
T. Wenaus²⁴, S. Wendler¹²³, Z. Weng^{151,q},
T. Wengler²⁹, S. Wenig²⁹, N. Wermes²⁰, M. Werner⁴⁸,
P. Werner²⁹, M. Werth¹⁶³, M. Wessels^{58a}, C. Weydert⁵⁵,
K. Whalen²⁸, S.J. Wheeler-Ellis¹⁶³, S.P. Whitaker²¹,
A. White⁷, M.J. White⁸⁶, S.R. Whitehead¹¹⁸,
D. Whiteson¹⁶³, D. Whittington⁶¹, D. Wicke¹⁷⁴,
F.J. Wickens¹²⁹, W. Wiedenmann¹⁷², M. Wielers¹²⁹,
P. Wienemann²⁰, C. Wiglesworth⁷⁵, L.A.M. Wiik⁴⁸,
P.A. Wijeratne⁷⁷, A. Wildauer¹⁶⁷, M.A. Wildt^{41,n},
I. Wilhelm¹²⁶, H.G. Wilkens²⁹, J.Z. Will⁹⁸,
E. Williams³⁴, H.H. Williams¹²⁰, W. Willis³⁴,
S. Willocq⁸⁴, J.A. Wilson¹⁷, M.G. Wilson¹⁴³,
A. Wilson⁸⁷, I. Wingerter-Seez⁴, S. Winkelmann⁴⁸,
F. Winklmeier²⁹, M. Wittgen¹⁴³, M.W. Wolter³⁸,
H. Wolters^{124a,g}, W.C. Wong⁴⁰, G. Wooden⁸⁷,
B.K. Wosiek³⁸, J. Wotschack²⁹, M.J. Woudstra⁸⁴,
K. Wraight⁵³, C. Wright⁵³, M. Wright⁵³, B. Wrona⁷³,
S.L. Wu¹⁷², X. Wu⁴⁹, Y. Wu^{32b,ab}, E. Wulf³⁴,

R. Wunstorff⁴², B.M. Wynne⁴⁵, S. Xella³⁵, M. Xiao¹³⁶,
 S. Xie⁴⁸, Y. Xie^{32a}, C. Xu^{32b,ac}, D. Xu¹³⁹, G. Xu^{32a},
 B. Yabsley¹⁵⁰, S. Yacoub^{145b}, M. Yamada⁶⁶,
 H. Yamaguchi¹⁵⁵, A. Yamamoto⁶⁶, K. Yamamoto⁶⁴,
 S. Yamamoto¹⁵⁵, T. Yamamura¹⁵⁵, T. Yamanaka¹⁵⁵,
 J. Yamaoka⁴⁴, T. Yamazaki¹⁵⁵, Y. Yamazaki⁶⁷,
 Z. Yan²¹, H. Yang⁸⁷, U.K. Yang⁸², Y. Yang⁶¹,
 Y. Yang^{32a}, Z. Yang^{146a,146b}, S. Yanush⁹¹, Y. Yasu⁶⁶,
 G.V. Ybeles Smit¹³⁰, J. Ye³⁹, S. Ye²⁴, M. Yilmaz^{3c},
 R. Yoosofmiya¹²³, K. Yorita¹⁷⁰, R. Yoshida⁵,
 C. Young¹⁴³, S. Youssef²¹, D. Yu²⁴, J. Yu⁷, J. Yu¹¹²,
 L. Yuan^{32a,ad}, A. Yurkewicz¹⁰⁶, V.G. Zaets¹²⁸,
 R. Zaidan⁶³, A.M. Zaitsev¹²⁸, Z. Zajacova²⁹,
 Yo.K. Zalite¹²¹, L. Zanello^{132a,132b}, P. Zarzhitsky³⁹,
 A. Zaytsev¹⁰⁷, C. Zeitnitz¹⁷⁴, M. Zeller¹⁷⁵,
 M. Zeman¹²⁵, A. Zemla³⁸, C. Zender²⁰, O. Zenin¹²⁸,
 T. Ženiš^{144a}, Z. Zenonos^{122a,122b}, S. Zenz¹⁴,
 D. Zerwas¹¹⁵, G. Zevi della Porta⁵⁷, Z. Zhan^{32d},
 D. Zhang^{32b,aa}, H. Zhang⁸⁸, J. Zhang⁵, X. Zhang^{32d},
 Z. Zhang¹¹⁵, L. Zhao¹⁰⁸, T. Zhao¹³⁸, Z. Zhao^{32b},
 A. Zhemchugov⁶⁵, S. Zheng^{32a}, J. Zhong¹¹⁸, B. Zhou⁸⁷,
 N. Zhou¹⁶³, Y. Zhou¹⁵¹, C.G. Zhu^{32d}, H. Zhu⁴¹,
 J. Zhu⁸⁷, Y. Zhu^{32b}, X. Zhuang⁹⁸, V. Zhuravlov⁹⁹,
 D. Zieminska⁶¹, R. Zimmermann²⁰, S. Zimmermann²⁰,
 S. Zimmermann⁴⁸, M. Ziolkowski¹⁴¹, R. Zitoun⁴,
 L. Živković³⁴, V.V. Zmouchko^{128,*}, G. Zobernig¹⁷²,
 A. Zoccoli^{19a,19b}, Y. Zolnierowski⁴, A. Zsenei²⁹,
 M. zur Nedden¹⁵, V. Zutshi¹⁰⁶, L. Zwalinski²⁹.

¹ University at Albany, Albany NY, United States of America

² Department of Physics, University of Alberta, Edmonton AB, Canada

³ (a)Department of Physics, Ankara University, Ankara; (b)Department of Physics, Dumlupinar University, Kutahya; (c)Department of Physics, Gazi University, Ankara; (d)Division of Physics, TOBB University of Economics and Technology, Ankara; (e)Turkish Atomic Energy Authority, Ankara, Turkey

⁴ LAPP, CNRS/IN2P3 and Université de Savoie, Annecy-le-Vieux, France

⁵ High Energy Physics Division, Argonne National Laboratory, Argonne IL, United States of America

⁶ Department of Physics, University of Arizona, Tucson AZ, United States of America

⁷ Department of Physics, The University of Texas at Arlington, Arlington TX, United States of America

⁸ Physics Department, University of Athens, Athens, Greece

⁹ Physics Department, National Technical University of Athens, Zografou, Greece

¹⁰ Institute of Physics, Azerbaijan Academy of Sciences, Baku, Azerbaijan

¹¹ Institut de Física d'Altes Energies and Departament de Física de la Universitat Autònoma de Barcelona and ICREA, Barcelona, Spain

¹² (a)Institute of Physics, University of Belgrade, Belgrade; (b)Vinca Institute of Nuclear Sciences,

Belgrade, Serbia

¹³ Department for Physics and Technology, University of Bergen, Bergen, Norway

¹⁴ Physics Division, Lawrence Berkeley National Laboratory and University of California, Berkeley CA, United States of America

¹⁵ Department of Physics, Humboldt University, Berlin, Germany

¹⁶ Albert Einstein Center for Fundamental Physics and Laboratory for High Energy Physics, University of Bern, Bern, Switzerland

¹⁷ School of Physics and Astronomy, University of Birmingham, Birmingham, United Kingdom

¹⁸ (a)Department of Physics, Bogazici University, Istanbul; (b)Division of Physics, Dogus University, Istanbul; (c)Department of Physics Engineering, Gaziantep University, Gaziantep; (d)Department of Physics, Istanbul Technical University, Istanbul, Turkey

¹⁹ (a)INFN Sezione di Bologna; (b)Dipartimento di Fisica, Università di Bologna, Bologna, Italy

²⁰ Physikalisches Institut, University of Bonn, Bonn, Germany

²¹ Department of Physics, Boston University, Boston MA, United States of America

²² Department of Physics, Brandeis University, Waltham MA, United States of America

²³ (a)Universidade Federal do Rio De Janeiro COPPE/EE/IF, Rio de Janeiro; (b)Federal University of Juiz de Fora (UFJF), Juiz de Fora; (c)Federal University of Sao Joao del Rei (UFSJ), Sao Joao del Rei; (d)Instituto de Fisica, Universidade de Sao Paulo, Sao Paulo, Brazil

²⁴ Physics Department, Brookhaven National Laboratory, Upton NY, United States of America

²⁵ (a)National Institute of Physics and Nuclear Engineering, Bucharest; (b)University Politehnica Bucharest, Bucharest; (c)West University in Timisoara, Timisoara, Romania

²⁶ Departamento de Física, Universidad de Buenos Aires, Buenos Aires, Argentina

²⁷ Cavendish Laboratory, University of Cambridge, Cambridge, United Kingdom

²⁸ Department of Physics, Carleton University, Ottawa ON, Canada

²⁹ CERN, Geneva, Switzerland

³⁰ Enrico Fermi Institute, University of Chicago, Chicago IL, United States of America

³¹ (a)Departamento de Física, Pontificia Universidad Católica de Chile, Santiago; (b)Departamento de Física, Universidad Técnica Federico Santa María, Valparaíso, Chile

³² (a)Institute of High Energy Physics, Chinese Academy of Sciences, Beijing; (b)Department of Modern Physics, University of Science and Technology of China, Anhui; (c)Department of Physics, Nanjing University, Jiangsu; (d)High Energy Physics Group, Shandong University, Shandong, China

³³ Laboratoire de Physique Corpusculaire, Clermont

Université and Université Blaise Pascal and CNRS/IN2P3, Aubiere Cedex, France

³⁴ Nevis Laboratory, Columbia University, Irvington NY, United States of America

³⁵ Niels Bohr Institute, University of Copenhagen, Kobenhavn, Denmark

³⁶ ^(a)INFN Gruppo Collegato di Cosenza;

^(b)Dipartimento di Fisica, Università della Calabria, Arcavata di Rende, Italy

³⁷ Faculty of Physics and Applied Computer Science, AGH-University of Science and Technology, Krakow, Poland

³⁸ The Henryk Niewodniczanski Institute of Nuclear Physics, Polish Academy of Sciences, Krakow, Poland

³⁹ Physics Department, Southern Methodist University, Dallas TX, United States of America

⁴⁰ Physics Department, University of Texas at Dallas, Richardson TX, United States of America

⁴¹ DESY, Hamburg and Zeuthen, Germany

⁴² Institut für Experimentelle Physik IV, Technische Universität Dortmund, Dortmund, Germany

⁴³ Institut für Kern- und Teilchenphysik, Technical University Dresden, Dresden, Germany

⁴⁴ Department of Physics, Duke University, Durham NC, United States of America

⁴⁵ SUPA - School of Physics and Astronomy, University of Edinburgh, Edinburgh, United Kingdom

⁴⁶ Fachhochschule Wiener Neustadt, Johannes Gutenbergstrasse 3, 2700 Wiener Neustadt, Austria

⁴⁷ INFN Laboratori Nazionali di Frascati, Frascati, Italy

⁴⁸ Fakultät für Mathematik und Physik, Albert-Ludwigs-Universität, Freiburg i.Br., Germany

⁴⁹ Section de Physique, Université de Genève, Geneva, Switzerland

⁵⁰ ^(a)INFN Sezione di Genova; ^(b)Dipartimento di Fisica, Università di Genova, Genova, Italy

⁵¹ ^(a)E.Andronikashvili Institute of Physics, Georgian Academy of Sciences, Tbilisi; ^(b)High Energy Physics Institute, Tbilisi State University, Tbilisi, Georgia

⁵² II Physikalisches Institut, Justus-Liebig-Universität Giessen, Giessen, Germany

⁵³ SUPA - School of Physics and Astronomy, University of Glasgow, Glasgow, United Kingdom

⁵⁴ II Physikalisches Institut, Georg-August-Universität, Göttingen, Germany

⁵⁵ Laboratoire de Physique Subatomique et de Cosmologie, Université Joseph Fourier and CNRS/IN2P3 and Institut National Polytechnique de Grenoble, Grenoble, France

⁵⁶ Department of Physics, Hampton University, Hampton VA, United States of America

⁵⁷ Laboratory for Particle Physics and Cosmology, Harvard University, Cambridge MA, United States of America

⁵⁸ ^(a)Kirchhoff-Institut für Physik, Ruprecht-Karls-Universität Heidelberg, Heidelberg; ^(b)Physikalisches Institut, Ruprecht-Karls-Universität Heidelberg, Heidelberg; ^(c)ZITI Institut für technische

Informatik, Ruprecht-Karls-Universität Heidelberg, Mannheim, Germany

⁵⁹ Faculty of Science, Hiroshima University, Hiroshima, Japan

⁶⁰ Faculty of Applied Information Science, Hiroshima Institute of Technology, Hiroshima, Japan

⁶¹ Department of Physics, Indiana University, Bloomington IN, United States of America

⁶² Institut für Astro- und Teilchenphysik, Leopold-Franzens-Universität, Innsbruck, Austria

⁶³ University of Iowa, Iowa City IA, United States of America

⁶⁴ Department of Physics and Astronomy, Iowa State University, Ames IA, United States of America

⁶⁵ Joint Institute for Nuclear Research, JINR Dubna, Dubna, Russia

⁶⁶ KEK, High Energy Accelerator Research Organization, Tsukuba, Japan

⁶⁷ Graduate School of Science, Kobe University, Kobe, Japan

⁶⁸ Faculty of Science, Kyoto University, Kyoto, Japan

⁶⁹ Kyoto University of Education, Kyoto, Japan

⁷⁰ Instituto de Física La Plata, Universidad Nacional de La Plata and CONICET, La Plata, Argentina

⁷¹ Physics Department, Lancaster University, Lancaster, United Kingdom

⁷² ^(a)INFN Sezione di Lecce; ^(b)Dipartimento di Fisica, Università del Salento, Lecce, Italy

⁷³ Oliver Lodge Laboratory, University of Liverpool, Liverpool, United Kingdom

⁷⁴ Department of Physics, Jožef Stefan Institute and University of Ljubljana, Ljubljana, Slovenia

⁷⁵ Department of Physics, Queen Mary University of London, London, United Kingdom

⁷⁶ Department of Physics, Royal Holloway University of London, Surrey, United Kingdom

⁷⁷ Department of Physics and Astronomy, University College London, London, United Kingdom

⁷⁸ Laboratoire de Physique Nucléaire et de Hautes Energies, UPMC and Université Paris-Diderot and CNRS/IN2P3, Paris, France

⁷⁹ Fysiska institutionen, Lunds universitet, Lund, Sweden

⁸⁰ Departamento de Física Teórica C-15, Universidad Autónoma de Madrid, Madrid, Spain

⁸¹ Institut für Physik, Universität Mainz, Mainz, Germany

⁸² School of Physics and Astronomy, University of Manchester, Manchester, United Kingdom

⁸³ CPPM, Aix-Marseille Université and CNRS/IN2P3, Marseille, France

⁸⁴ Department of Physics, University of Massachusetts, Amherst MA, United States of America

⁸⁵ Department of Physics, McGill University, Montreal QC, Canada

⁸⁶ School of Physics, University of Melbourne, Victoria, Australia

⁸⁷ Department of Physics, The University of Michigan,

Ann Arbor MI, United States of America

⁸⁸ Department of Physics and Astronomy, Michigan State University, East Lansing MI, United States of America

⁸⁹ ^(a)INFN Sezione di Milano; ^(b)Dipartimento di Fisica, Università di Milano, Milano, Italy

⁹⁰ B.I. Stepanov Institute of Physics, National Academy of Sciences of Belarus, Minsk, Republic of Belarus

⁹¹ National Scientific and Educational Centre for Particle and High Energy Physics, Minsk, Republic of Belarus

⁹² Department of Physics, Massachusetts Institute of Technology, Cambridge MA, United States of America

⁹³ Group of Particle Physics, University of Montreal, Montreal QC, Canada

⁹⁴ P.N. Lebedev Institute of Physics, Academy of Sciences, Moscow, Russia

⁹⁵ Institute for Theoretical and Experimental Physics (ITEP), Moscow, Russia

⁹⁶ Moscow Engineering and Physics Institute (MEPhI), Moscow, Russia

⁹⁷ Skobel'syn Institute of Nuclear Physics, Lomonosov Moscow State University, Moscow, Russia

⁹⁸ Fakultät für Physik, Ludwig-Maximilians-Universität München, München, Germany

⁹⁹ Max-Planck-Institut für Physik (Werner-Heisenberg-Institut), München, Germany

¹⁰⁰ Nagasaki Institute of Applied Science, Nagasaki, Japan

¹⁰¹ Graduate School of Science, Nagoya University, Nagoya, Japan

¹⁰² ^(a)INFN Sezione di Napoli; ^(b)Dipartimento di Scienze Fisiche, Università di Napoli, Napoli, Italy

¹⁰³ Department of Physics and Astronomy, University of New Mexico, Albuquerque NM, United States of America

¹⁰⁴ Institute for Mathematics, Astrophysics and Particle Physics, Radboud University Nijmegen/Nikhef, Nijmegen, Netherlands

¹⁰⁵ Nikhef National Institute for Subatomic Physics and University of Amsterdam, Amsterdam, Netherlands

¹⁰⁶ Department of Physics, Northern Illinois University, DeKalb IL, United States of America

¹⁰⁷ Budker Institute of Nuclear Physics (BINP), Novosibirsk, Russia

¹⁰⁸ Department of Physics, New York University, New York NY, United States of America

¹⁰⁹ Ohio State University, Columbus OH, United States of America

¹¹⁰ Faculty of Science, Okayama University, Okayama, Japan

¹¹¹ Homer L. Dodge Department of Physics and Astronomy, University of Oklahoma, Norman OK, United States of America

¹¹² Department of Physics, Oklahoma State University, Stillwater OK, United States of America

¹¹³ Palacký University, RCPTM, Olomouc, Czech Republic

¹¹⁴ Center for High Energy Physics, University of Oregon, Eugene OR, United States of America

¹¹⁵ LAL, Univ. Paris-Sud and CNRS/IN2P3, Orsay, France

¹¹⁶ Graduate School of Science, Osaka University, Osaka, Japan

¹¹⁷ Department of Physics, University of Oslo, Oslo, Norway

¹¹⁸ Department of Physics, Oxford University, Oxford, United Kingdom

¹¹⁹ ^(a)INFN Sezione di Pavia; ^(b)Dipartimento di Fisica Nucleare e Teorica, Università di Pavia, Pavia, Italy

¹²⁰ Department of Physics, University of Pennsylvania, Philadelphia PA, United States of America

¹²¹ Petersburg Nuclear Physics Institute, Gatchina, Russia

¹²² ^(a)INFN Sezione di Pisa; ^(b)Dipartimento di Fisica E. Fermi, Università di Pisa, Pisa, Italy

¹²³ Department of Physics and Astronomy, University of Pittsburgh, Pittsburgh PA, United States of America

¹²⁴ ^(a)Laboratorio de Instrumentacao e Fisica

Experimental de Partículas - LIP, Lisboa, Portugal;

^(b)Departamento de Fisica Teorica y del Cosmos and CAFPE, Universidad de Granada, Granada, Spain

¹²⁵ Institute of Physics, Academy of Sciences of the Czech Republic, Praha, Czech Republic

¹²⁶ Faculty of Mathematics and Physics, Charles University in Prague, Praha, Czech Republic

¹²⁷ Czech Technical University in Prague, Praha, Czech Republic

¹²⁸ State Research Center Institute for High Energy Physics, Protvino, Russia

¹²⁹ Particle Physics Department, Rutherford Appleton Laboratory, Didcot, United Kingdom

¹³⁰ Physics Department, University of Regina, Regina SK, Canada

¹³¹ Ritsumeikan University, Kusatsu, Shiga, Japan

¹³² ^(a)INFN Sezione di Roma I; ^(b)Dipartimento di Fisica, Università La Sapienza, Roma, Italy

¹³³ ^(a)INFN Sezione di Roma Tor Vergata;

^(b)Dipartimento di Fisica, Università di Roma Tor Vergata, Roma, Italy

¹³⁴ ^(a)INFN Sezione di Roma Tre; ^(b)Dipartimento di Fisica, Università Roma Tre, Roma, Italy

¹³⁵ ^(a)Faculté des Sciences Ain Chock, Réseau

Universitaire de Physique des Hautes Energies - Université Hassan II, Casablanca; ^(b)Centre National de

l'Energie des Sciences Techniques Nucleaires, Rabat;

^(c)Université Cadi Ayyad, Faculté des sciences Semlalia Département de Physique, B.P. 2390 Marrakech 40000;

^(d)Faculté des Sciences, Université Mohamed Premier and LPTPM, Oujda; ^(e)Faculté des Sciences, Université Mohammed V, Rabat, Morocco

¹³⁶ DSM/IRFU (Institut de Recherches sur les Lois Fondamentales de l'Univers), CEA Saclay

(Commissariat a l'Energie Atomique), Gif-sur-Yvette, France

¹³⁷ Santa Cruz Institute for Particle Physics, University

- of California Santa Cruz, Santa Cruz CA, United States of America
- ¹³⁸ Department of Physics, University of Washington, Seattle WA, United States of America
- ¹³⁹ Department of Physics and Astronomy, University of Sheffield, Sheffield, United Kingdom
- ¹⁴⁰ Department of Physics, Shinshu University, Nagano, Japan
- ¹⁴¹ Fachbereich Physik, Universität Siegen, Siegen, Germany
- ¹⁴² Department of Physics, Simon Fraser University, Burnaby BC, Canada
- ¹⁴³ SLAC National Accelerator Laboratory, Stanford CA, United States of America
- ¹⁴⁴ ^(a) Faculty of Mathematics, Physics & Informatics, Comenius University, Bratislava; ^(b) Department of Subnuclear Physics, Institute of Experimental Physics of the Slovak Academy of Sciences, Kosice, Slovak Republic
- ¹⁴⁵ ^(a) Department of Physics, University of Johannesburg, Johannesburg; ^(b) School of Physics, University of the Witwatersrand, Johannesburg, South Africa
- ¹⁴⁶ ^(a) Department of Physics, Stockholm University; ^(b) The Oskar Klein Centre, Stockholm, Sweden
- ¹⁴⁷ Physics Department, Royal Institute of Technology, Stockholm, Sweden
- ¹⁴⁸ Department of Physics and Astronomy, Stony Brook University, Stony Brook NY, United States of America
- ¹⁴⁹ Department of Physics and Astronomy, University of Sussex, Brighton, United Kingdom
- ¹⁵⁰ School of Physics, University of Sydney, Sydney, Australia
- ¹⁵¹ Institute of Physics, Academia Sinica, Taipei, Taiwan
- ¹⁵² Department of Physics, Technion: Israel Inst. of Technology, Haifa, Israel
- ¹⁵³ Raymond and Beverly Sackler School of Physics and Astronomy, Tel Aviv University, Tel Aviv, Israel
- ¹⁵⁴ Department of Physics, Aristotle University of Thessaloniki, Thessaloniki, Greece
- ¹⁵⁵ International Center for Elementary Particle Physics and Department of Physics, The University of Tokyo, Tokyo, Japan
- ¹⁵⁶ Graduate School of Science and Technology, Tokyo Metropolitan University, Tokyo, Japan
- ¹⁵⁷ Department of Physics, Tokyo Institute of Technology, Tokyo, Japan
- ¹⁵⁸ Department of Physics, University of Toronto, Toronto ON, Canada
- ¹⁵⁹ ^(a) TRIUMF, Vancouver BC; ^(b) Department of Physics and Astronomy, York University, Toronto ON, Canada
- ¹⁶⁰ Institute of Pure and Applied Sciences, University of Tsukuba, Ibaraki, Japan
- ¹⁶¹ Science and Technology Center, Tufts University, Medford MA, United States of America
- ¹⁶² Centro de Investigaciones, Universidad Antonio Narino, Bogota, Colombia
- ¹⁶³ Department of Physics and Astronomy, University of California Irvine, Irvine CA, United States of America
- ¹⁶⁴ ^(a) INFN Gruppo Collegato di Udine; ^(b) ICTP, Trieste; ^(c) Dipartimento di Chimica, Fisica e Ambiente, Università di Udine, Udine, Italy
- ¹⁶⁵ Department of Physics, University of Illinois, Urbana IL, United States of America
- ¹⁶⁶ Department of Physics and Astronomy, University of Uppsala, Uppsala, Sweden
- ¹⁶⁷ Instituto de Física Corpuscular (IFIC) and Departamento de Física Atómica, Molecular y Nuclear and Departamento de Ingeniería Electrónica and Instituto de Microelectrónica de Barcelona (IMB-CNM), University of Valencia and CSIC, Valencia, Spain
- ¹⁶⁸ Department of Physics, University of British Columbia, Vancouver BC, Canada
- ¹⁶⁹ Department of Physics and Astronomy, University of Victoria, Victoria BC, Canada
- ¹⁷⁰ Waseda University, Tokyo, Japan
- ¹⁷¹ Department of Particle Physics, The Weizmann Institute of Science, Rehovot, Israel
- ¹⁷² Department of Physics, University of Wisconsin, Madison WI, United States of America
- ¹⁷³ Fakultät für Physik und Astronomie, Julius-Maximilians-Universität, Würzburg, Germany
- ¹⁷⁴ Fachbereich C Physik, Bergische Universität Wuppertal, Wuppertal, Germany
- ¹⁷⁵ Department of Physics, Yale University, New Haven CT, United States of America
- ¹⁷⁶ Yerevan Physics Institute, Yerevan, Armenia
- ¹⁷⁷ Domaine scientifique de la Doua, Centre de Calcul CNRS/IN2P3, Villeurbanne Cedex, France
- ^a Also at Laboratório de Instrumentação e Física Experimental de Partículas - LIP, Lisboa, Portugal
- ^b Also at Faculdade de Ciências and CFNUL, Universidade de Lisboa, Lisboa, Portugal
- ^c Also at Particle Physics Department, Rutherford Appleton Laboratory, Didcot, United Kingdom
- ^d Also at TRIUMF, Vancouver BC, Canada
- ^e Also at Department of Physics, California State University, Fresno CA, United States of America
- ^f Also at Fermilab, Batavia IL, United States of America
- ^g Also at Department of Physics, University of Coimbra, Coimbra, Portugal
- ^h Also at Università di Napoli Parthenope, Napoli, Italy
- ⁱ Also at Institute of Particle Physics (IPP), Canada
- ^j Also at Department of Physics, Middle East Technical University, Ankara, Turkey
- ^k Also at Louisiana Tech University, Ruston LA, United States of America
- ^l Also at Group of Particle Physics, University of Montreal, Montreal QC, Canada
- ^m Also at Institute of Physics, Azerbaijan Academy of Sciences, Baku, Azerbaijan
- ⁿ Also at Institut für Experimentalphysik, Universität Hamburg, Hamburg, Germany

^o Also at Manhattan College, New York NY, United States of America

^p Also at CPPM, Aix-Marseille Université and CNRS/IN2P3, Marseille, France

^q Also at School of Physics and Engineering, Sun Yat-sen University, Guanzhou, China

^r Also at Academia Sinica Grid Computing, Institute of Physics, Academia Sinica, Taipei, Taiwan

^s Also at High Energy Physics Group, Shandong University, Shandong, China

^t Also at Section de Physique, Université de Genève, Geneva, Switzerland

^u Also at Departamento de Fisica, Universidade de Minho, Braga, Portugal

^v Also at Department of Physics and Astronomy, University of South Carolina, Columbia SC, United States of America

^w Also at KFKI Research Institute for Particle and

Nuclear Physics, Budapest, Hungary

^x Also at California Institute of Technology, Pasadena CA, United States of America

^y Also at Institute of Physics, Jagiellonian University, Krakow, Poland

^z Also at Department of Physics, Oxford University, Oxford, United Kingdom

^{aa} Also at Institute of Physics, Academia Sinica, Taipei, Taiwan

^{ab} Also at Department of Physics, The University of Michigan, Ann Arbor MI, United States of America

^{ac} Also at DSM/IRFU (Institut de Recherches sur les Lois Fondamentales de l'Univers), CEA Saclay (Commissariat a l'Energie Atomique), Gif-sur-Yvette, France

^{ad} Also at Laboratoire de Physique Nucléaire et de Hautes Energies, UPMC and Université Paris-Diderot and CNRS/IN2P3, Paris, France

* Deceased